JUSTUS-LIEBIG-UNIVERSITÄT GIESSEN

RUNOFF SOURCES AND FLOWPATH DYNAMICS IN THE ANDEAN PÁRAMO

ALICIA BEATRIZ CORREA BARAHONA

From the Institute of Natural Science at the Department of Landscape, Water and Biogeochemical Cycles of the Justus-Liebig University Giessen
Dissertation from M.Sc. Alicia Beatriz Correa Barahona for the degree Doctor of Natural Science (Dr. rer. nat.)

Referees from the Justus-Liebig-University Gießen:

Prof. Dr. Lutz Breuer (1st Supervisor)
Prof. Dr. Jan Siemens (2nd Supervisor)
Prof. Dr. Andreas Gattinger
Prof. Dr. Jürg Luterbacher

Submitted: 16th October 2017

ABSTRACT

As a consequence of the remote location of the Andean Páramo, knowledge on their hydrologic functioning is, despite their importance as local water towers, still limited. To improve our understanding, we identified hydrological informative periods, defined dominant water sources as well as flow paths and analyzed their spatio-temporal dynamics throughout the year and during events. We therefore collected hydro-metrical (2010 - 2014) and hydro-chemical (2012 - 2014) information within a tropical headwater catchment (7.53 km^2) in the Ecuadorian Andes. Our results showed that rainfall-runoff events and continues data sets reveal similar information and that a single event in the wet season can provide the same insights than continuous monitoring, indicating that the hydrological processes at that time are almost stationary. Further, we identified that water from the riparian zone represented the dominant contributing source to streamflow year-round and connectivity with hillslopes was particularly important during the wet season. During rainfall-runoff events, different patterns in the upper compared to the lower catchment suggested a fast reaction of fresh water and water from the riparian zone, respectively. This study demonstrated that catchments with almost stable hydrological conditions can still be characterized by varying inter-annual source contributions, related to topography and soil types occurring in the catchment.

TABLE OF CONTENTS

LIST OF FIGURES

LIST OF TABLES

1 SYNOPSIS

1.1 INTRODUCTION

Understanding the runoff generation and water source dynamics of headwater catchments is a central issue for scientific and management goals. The conceptualization of high variable involved processes is challenging due to the complexity of catchments' heterogeneity, large variability of hydrological conditions, and spatio-temporal data-scarcity, especially in remote areas such as the Andean mountains (Bendix, 2000; Célleri et al., 2009). Additionally, the influence of the Pacific Ocean and the Amazon Rainforest affects the climatology and behavior of these natural systems (Josse et al., 2009), further complicating the conceptualization of hydrological processes that dominate runoff generation. Head water catchments in the Andean mountains are considered sentinels for climate change (Dangles et al., 2017) and deliver more freshwater to the ocean per square kilometer land area than any other region in the world (Harden, 2006).

The Páramo is a high-altitude grassland-dominated ecosystem with scarce patches of woodlands (i.e. Polylepis species) and intermittent wetlands and ponds in the Andean mountains. This perennial humid ecosystem typically occurs between the upper parts of tropical mountains forest (3000 to 3500 m a.s.l.) to the snow line (Célleri et al., 2009; Josse et al., 2009). Constant rainfall, low temperatures, high inter-daily temperature variation, and large water-holding capacities (Buytaert et al., 2006) are some of its most representative features. They provide a variety of important ecosystem services in countries such as Venezuela, Colombia, Ecuador, and Peru. These services include, for example, biodiversity conservation (Vuille, 2013) and carbon stocks (Gibbon et al., 2010; Harden et al., 2013), as well as hydrological regulation, high-quality water for human consumption, industrial uses, hydropower generation, and irrigation in the lowlands (Buytaert et al., 2006).

Regardless its key role in the provisioning of water-related services, knowledge about hydrological processes occurring in these ecosystems is limited, and views are often contradictory (Buytaert et al., 2010a; Célleri and Feyen, 2009). The lack of knowledge restricts effective management of the natural and unnatural impacts, which negatively change the dynamics of water resources in terms of quality and quantity in catchment systems (Erwin,

2009; Neal et al., 2001). There is physical evidence of environmental change due land use changes on a global scale, e.g., Scanlon et al. (2007) and, particularly, in Andean ecosystems on the local to regional scale, where decision-makers applied pragmatic conservation strategies that were not suitably assessed, resulting in loss of local species and a reduction of total water yield (Buytaert et al., 2007). Unfortunately, until today effective strategies can hardly be defined, due the lack of reliable hydrological knowledge to support decision-making processes (Célleri et al., 2009).

In recent decades, research in the in Páramo ecosystems has increased (Correa et al., 2016; Crespo et al., 2011; Mosquera et al., 2016a; Ochoa-Tocachi et al., 2016), generating a partial understanding of hydrological processes. However, monitoring for research purposes in the Andes has up to now almost always been limited to individual and isolated small-funded projects (Célleri and Feyen, 2009). As a result, the available data for Páramo catchments is frequently limited to shorter time periods (<1 year) and rarely contains sufficient or any costly tracer data suitable to apply tracer based methods. This, together with inadequate or non-existing soil and land maps, jeopardizes the full picture and suitable understanding of hydrological process in this ecosystem. Data-scarcity also hinders the ability to extrapolate hydrological understanding from gauged to ungauged catchments (Crespo et al., 2011).

Although data-scarcity is a frequently-referred problem in the region (Buytaert and Beven, 2011; Crespo et al., 2011), limited effort has been put into optimizing the use of available hydro-metric information. Buytaert and Beven (2011) applied several hydrological models in the Andean Páramo with different complexities to understand the flow generation and the ecosystem's functionality at the catchment scale. They concluded that complex models are likely underutilized in this ecosystem as a result of the scarcity of data, irregular topography, and extreme spatial variability in meteorological boundary conditions.

The urgent requirement of data enhances the optimized use of hydrologic information and the establishment of guidelines for monitoring ungauged catchments with limited efforts and resources. It can greatly increase the amount of spatial data to improve our understanding of catchment hydrology and ecosystems management (Beven, 2007; McIntyre et al., 2014; Wagener and Montanari, 2011).

Various approaches have been tested to determine the necessary amount of information that a sub-set of rainfall-runoff measurements should contain in comparison with continuous time series for different hydrological systems (Perrin et al., 2007; Seibert and Beven, 2009; Seibert and McDonnell, 2015). Results of those studies often show that a small amount of data can provide almost as much information as a continuous time series (McIntyre et al., 2005). Perrin et al. (2007) explained that 2.5% of data available, randomly extracted from a full time series, might contain similar information as the full data record. Similarly, Juston et al. (2009) showed that using only 5% of information based on rainfall-runoff events can help gain a similar level of knowledge. After testing several subsets of a larger data set, McIntyre et al. (2005) concluded that event-based monitoring has the greatest potential to reduce effort required for monitoring. Approaches for evaluating the content of hydrological information contained in any given subset of the original data are well-established, and the results are satisfactory, but so far, no comparison has been conducted for Andean ecosystems.

Once the methods have been established to identify the optimum balance between the number of samples to be collected and the hydrological information within those samples, additional knowledge about the spatial distribution of dominant water sources and temporal dynamics of water-release mechanisms is needed to represent an integrated response of catchment behavior. Such knowledge can be gained using tracers-based studies, in which conservative tracers are well-established tools to define spatio-temporal dynamics of runoff sources, flow paths, and the mixing and release of water variable processes over a range of scales (Katsuyama et al., 2009; Kirchner et al., 2010).

End Member Mixing Analysis (EMMA) (Hooper, 2003; Liu et al., 2004) is one prominent example for the application of hydrochemical tracers used to estimate the main sources contributing to geographical runoff and the areas contributing to streamflow. Using the EMMA approach, the composition of stream water is assumed to be an integrated mixture of hydrochemical signatures of end-members (sources) (Christophersen et al., 1990). It thereby relies on the conservative behavior of tracers and linear mixing process (Hooper, 2001). The remarkable feature of this methodology is that it takes the variability of multi-tracer data sets into account, thus enhancing the probability to identify sources and reducing the risk of false conclusions about catchment functioning (Barthold et al., 2011, 2017). End-members are defined as source solutions that have more extreme chemical concentrations than the stream water (Christophersen and Hooper, 1992). They represent functional units of catchments that

only physically mix during travel time to the stream channel (James and Roulet, 2006). Key end-members typically include precipitation, throughfall, litter leachate, shallow and deep groundwater, and soil water from hillslopes and riparian zones (Inamdar et al., 2013). Preferably, end-members should be monitored individually and independently, across the entire range of hydrologic conditions of the catchment (Levia et al., 2011) , and not derived from stream chemistry information. In recent years, several authors (Barthold et al., 2017; Inamdar et al., 2013) suggested that a better understanding of catchment runoff response can be reached by investigating the stream chemistry evolution throughout the different storm hydrograph stages (rising limb, falling limb, and recession). Special attention must be addressed to analyze their hysteresis patterns, shapes, directional shifts, and relative position with respect to the end-members. In this context, hydro-chemical data is particularly valuable when used in conjunction with independently-measured hydro-metric data (Buttle, 1994; Inamdar et al., 2013). Authors use hydro-metrical data to separate, for example, seasons or rainfall-runoff events, where end-members and their relative contributions can be analyzed with a multi-criteria approach (Ali et al., 2010; Correa et al., 2017; Morel et al., 2009).

Time-domain tracers, such as stable isotopes, have enhanced the characterization of flow paths, water age, transit time distributions, mean transit time, and can evaluate the streamflow contribution of event and pre-event water (Buttle, 1994; Klaus and McDonnell, 2013; McDonnell, 2003). Their natural fractionations in the water cycle allow researchers to track their fate and study, for instance, hydrological processes involved in their change (Gibson et al., 2005; Luz et al., 2009). Water age has traditionally been evaluated in lumped convolution models, assessing mean transit times (MTT) and travel time distributions (Maloszewski and Zuber, 1982; McGuire and McDonnell, 2006).This approach assumes a travel time that mimics the mean over the entire period under consideration, nevertheless, its application presents limitations based on the length of data records required, aggregation errors (Kirchner, 2016a, 2016b), and implicitly presumes stationarity. Inter-annual fluctuations and conditions outside the assumed stationary zones (e.g., during discharge events) are not considered by the MTT. Tetzlaff et al. (2009) proposed an alternative measure (Inverse transit time proxies (ITTPs)) to represent the relative water ages and assess the inter-annual variability based on a simple measure of tracer damping. ITTPs are the ratio of standard deviations between the input and output isotope time series and are reported as a dampening factor of the isotope signatures rather than an actual time. ITTPs are inversely proportional to

MTT and can be considered a rough proxy of the water ages (Seeger and Weiler, 2014; Tetzlaff et al., 2009). More recent work has also integrated water-stable isotopes as soft data into conceptual models (Fenicia et al., 2008; Seibert and McDonnell, 2002; Weiler et al., 2003).

In Andean ecosystems, very few tracer-based studies have been conducted. Some studies used hydro-chemical tracers to identify the major catchment factors controlling stream water chemistry (Bücker et al., 2010), and others used performed isotopic hydrograph separation to evaluate the effect of land use change on rainfall-runoff response (Blume et al., 2007; Roa-García et al., 2011). MTT was evaluated in order to understand catchment dynamics (Mosquera et al., 2016b; Muñoz-Villers and McDonnell, 2012; Roa and Weiler, 2010; Timbe et al., 2014).

The uncertainty that underlies different methodologies is often discussed, and efforts are concentrated on quantifying the uncertainty of individual methods to increase the confidence in the results (e.g., selection and number of end-members (Barthold et al., 2011; Delsman et al., 2013) and estimate of MTTs (Timbe et al., 2014)). Besides that, different methodologies provide hydrological insight from diverse perspectives and should ideally complement each other to depict the same hydrological processes; however, such methods are rarely combined. An ensemble of methods allows researchers to gain a more comprehensive and deep knowledge about hydrological system functioning, investigate structural differences between methodologies, and reduce the epistemic uncertainty from inaccurate knowledge of the system.

1.2 GENERAL OBJECTIVE

The overall objective of this study was to obtain knowledge about the spatio-temporally-distributed hydrological processes and the water source dynamics of headwater catchments in different time scales. This work uses a multi-method approach based on hydro-metric and large hydro-chemical data sets. Hydro-metric data analysis was used to identify storm events as the most hydrologically-informative periods, and in combination with a lot of hydro-chemical data, dominant water sources, flow paths, and relative age were identified. Rainfall-runoff processes and the dynamics of water sources were analyzed during different weather seasons and during storm events.

1.3 STUDY AREA

The study was conducted in the Zhurucay River Ecohydrological Observatory (Fig. 1.1), a fourth-order headwater catchment (7.53 km^2) in Southern Ecuador (3°4′38″S, 79°15′30″O), situated in the perennially-humid Páramo region (Josse et al., 2009). The observatory is located in the divide between the waters draining into the Pacific and Atlantic Oceans in the Western and Eastern Andean Cordillera, respectively. It ultimately drains into the Pacific Ocean and is mainly influenced by the climate in this region (Vuille et al., 2000).

The annual rainfall sum in the study area is 1345 mm (Padrón et al., 2015) on average at 3780 m a.s.l., with higher values from December to February. Rainfall generally falls with low intensities (rarely exceeding 5 mm h^{-1}), with the most commonly-recorded intensity of 0.061 mm h^{-1}. Drizzle is very common and poorly measured in the region (Buytaert et al., 2006; Padrón et al., 2015), resulting in an underestimation of the annual rainfall by nearly 15% (Padrón et al., 2015).

The average annual discharge is 864 mm yr^{-1}, with an average runoff coefficient (RC) of 0.68 (Mosquera et al., 2015). This coefficient increases up to 0.80 for isolated storms (Correa et al., 2016), indicating that an even higher proportion of water in the active catchment storages is quickly released during storm events. Runoff events are characterized by peaks that range from 50 to 700 l s^{-1} km^{-2}, most of which fall between 150 and 400 l s^{-1} km^{-2}. Flow records presented 10% high flows, 55% moderate, and 35% low during the study period (Q90 = 45 l s^{-1} km^{-2} and Q35 = 10 l s^{-1} km^{-2} were used as thresholds). The low flows were mainly observed in two periods: July-October 2012 and October-December 2013.

The annual reference evapotranspiration is 723 mm (Córdova et al., 2015), and mean air temperature is 6°C. Temperatures below 0°C rarely occur and only for a few of hours, preventing any freezing processes and the average relative humidity is 91%. According to Padrón et al. (2015), a cloudy sky is very common, but when it is clear, solar radiation is extremely high. Wind speeds vary seasonally, showing higher values between May and September. The wind blew predominantly from the east or northeast (65%).

The elevation varies between 3,505 and 3,900 m a.s.l., but a majority of the area is concentrated between 3750 and 3850 m a.s.l. The glacial-formed valley presented wide valleys

at the catchment bottom, and the average hillslope is 17%, in some places reaching 40%; however, most of the land surface exhibits slopes between 0% and 20%.

The geology of the catchment corresponds to deposits of volcanic and volcanoclastic rocks compacted during the last ice age (Coltorti and Ollier, 2000). The Quimsacocha Formation is the dominant in the catchment (56%), consisting of basalt flows with plagioclase, feldspar, and andesitic pyroclastic deposits (Pratt et al., 1997). According to IAMGOLD (2006) as cited by Crespo et al. (2011), the age of the deposits is not defined, and the formation is hydraulically nearly impermeable, with low density of fissures in the shallow layer. Turi formation (31%), located mainly in the central valley of the catchment, consists of an accumulation of a thick sequence of conglomerates, clays, tuffs and volcanic breccia, and horizontally-stratified sands (Coltorti and Ollier, 2000). Both formations belong to the late Miocene geological period (Pratt et al., 1997). The remaining 13% is covered by Quaternary deposits (glacial moraines), generally located in escarpments and steep slope areas, which are typically 5–7 meters deep.

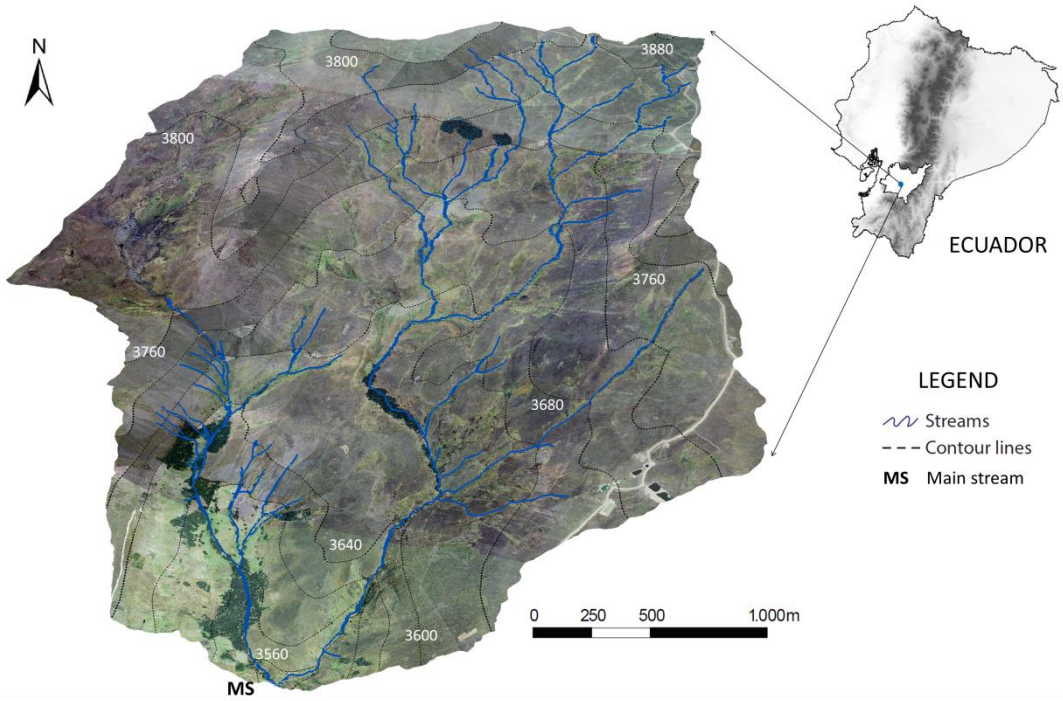

Figure 1-1. The Zhurucay River Ecohydrological Observatory located in southern Ecuador.

The black and humic Páramo soils are important regulators of headwater hydrology (Harden, 2006). In the study area, these soils arise from the volcanic ash of the Sangay and Tungurahua volcanoes (Quichimbo et al., 2012). The cold-humid climate and the low atmospheric pressure,

in combination with the geomorphology of the zone, have favored volcanic formation. Histosols (24%) and Andosols (72%) (IUSS Working Group WRB, 2015) are the dominant soils in the study catchment. Both are extremely porous and present high infiltration capacities, high organic matter content, and exceptional water retention properties.

Histosols are mainly located at the foot of the hillslopes and in the valley bottoms and present nearly-saturated conditions year-round (Buytaert and Beven, 2011; Mosquera et al., 2015). This soil presents an organic matter content of approximately 440 g kg^{-1} and high water retention between saturation and field capacity (Crespo et al., 2011). A high fraction of non-decomposed plant fibers is presented in the superficial horizon (Beck et al., 2008). Histosols in the study area typically present a histic horizon (*H*) in the upper 33 cm. Chemically, soils are very strong acids (pH = 4.8), with an exchangeable acidity of 2.54 $cmol_c$ dm^{-3}, a cation exchange capacity of 16 $cmol_c$ per kilogram of soil, and an effective base saturation of 52.4%. Andosols are generally characterized by less-developed horizons and they mainly cover hillslopes. The organic layer consists of short-range-order minerals and organo-metallic complexes and is characterized as an *Ah* horizon. The soils present an organic matter content of approximately 310 g kg^{-1}, an average pH of 4.7, an exchangeable acidity of 5.27 $cmol_c$ dm^{-3}, a cation exchange capacity of 46 $cmol_c$ per kilogram of soil, and an effective base saturation of 36%. Both soils overlay an organic-mineral interface horizon classified as the *C* horizon. The saturated hydraulic conductivity inversely related to bulk density (Mosquera et al., 2016a), and it is higher in the Histosols than in the Andosols, decreasing from shallow to deep horizons in both cases (Histosols 1.55 cm h^{-1} to 0.72 cm h^{-1} and Andosols 0.89 cm h^{-1} to 0.28 cmh^{-1}). The remaining catchment area is covered by shallow organic Leptosols (4%) soils, which are typically located on steep valley slopes lying directly on the bedrock.

The land cover is relatively undisturbed with species, like tussock grass (72% of the catchment area) and cushion plants (24%), in the central and northeastern part of the catchment, riparian forests species, (e.g. *Polylepis incana Kunth* and *Polylepis reticulata Kunth*) covering 2% of the basin, and the remaining 2% are intermittent plots planted with pine trees. The intermittent pine plots negatively affect the water retention capacity of the underlying soil, as a consequence of the reduction in moisture content at saturation and field capacity (Quichimbo et al., 2012). Land uses are limited to extensive grazing with low animal density. An overview of the study area is presented in the Figure 1.2.

1.4 THESIS OUTLINE

The thesis document is structured around chapters (2 to 4), which present and synthesize the major findings of this doctoral project. Three interlinked papers describe the main spatio-temporally-distributed hydrological processes controlling rainfall-runoff generation in tropical mountain catchments.

Chapter 1 presents a brief introduction to the topics of this thesis: general objectives, description of the study site, outline, main findings, and a description of unresolved issues and possible future research directions. The three following chapters (2, 3, and 4) are presented in a format for scientific journals and can be read independently. All are based on information from the Zhurucay River Ecohydrological Observatory, located in the Ecuadorian Andes.

Chapter 2 addresses the hydro-metric analysis of precipitation and specific discharge time series of a densely-monitored nested catchment system (0.20 - 7.53 km^2). Hydrological indices, derived from a subset of 34 rainfall-runoff events, were compared with indices derived from a continuous monitoring scheme. The richness of information extracted from a subset of isolated events allowed us to define the extreme significance of soils for runoff generation. The rapid infiltration of precipitation thought the porous soils raises the water table to near the surface and in consequence the contribution from the valley bottom area increases. Additionally, guidelines for the monitoring of previously-ungauged catchments with similar environmental settings and comparable catchment characteristics to the sample basin can be found in this chapter.

As previously mentioned, the incorporation of environmental hydro-chemical tracers (water stable isotopes and geochemical tracers) can strongly improve hydrological knowledge about the spatial and temporal dynamics of water provenances and flow paths. Especially when the variability of multi-tracer data sets is taken into account, the probability of an incomplete conceptualization of catchment functioning is reduced. Therefore, chapter 3 assesses the temporal dynamics in source areas, flow paths, and relative water age by combining End Member Mixing Analysis (EMMA), hydrograph separation, and Inverse Transit Time Proxies (ITTPs). Analyses were based on twenty-two solutes, stable isotopes, pH, and electrical conductivity from a stream and twelve potential sources. Once again, the importance of water from soils was highlighted, especially from the riparian zone. In this section, the

quantification of contribution percentages during different weather seasons (wetter and drier) was performed. Likewise, contributions from shallow groundwater were only possible to identify due the novelty of using multi-tracer data sets. Previously, contributions from this type of source were mostly considered negligible in Páramo catchments. Connectivity processes with the hillslopes were evident based on the increases of contribution to stream of water from this source in wetter conditions. The application of an ensemble of methods enabled us to closely study the importance of flow processes and water source dynamics from an inter-annual perspective and reduce the epistemic uncertainty from our imprecise knowledge of the system.

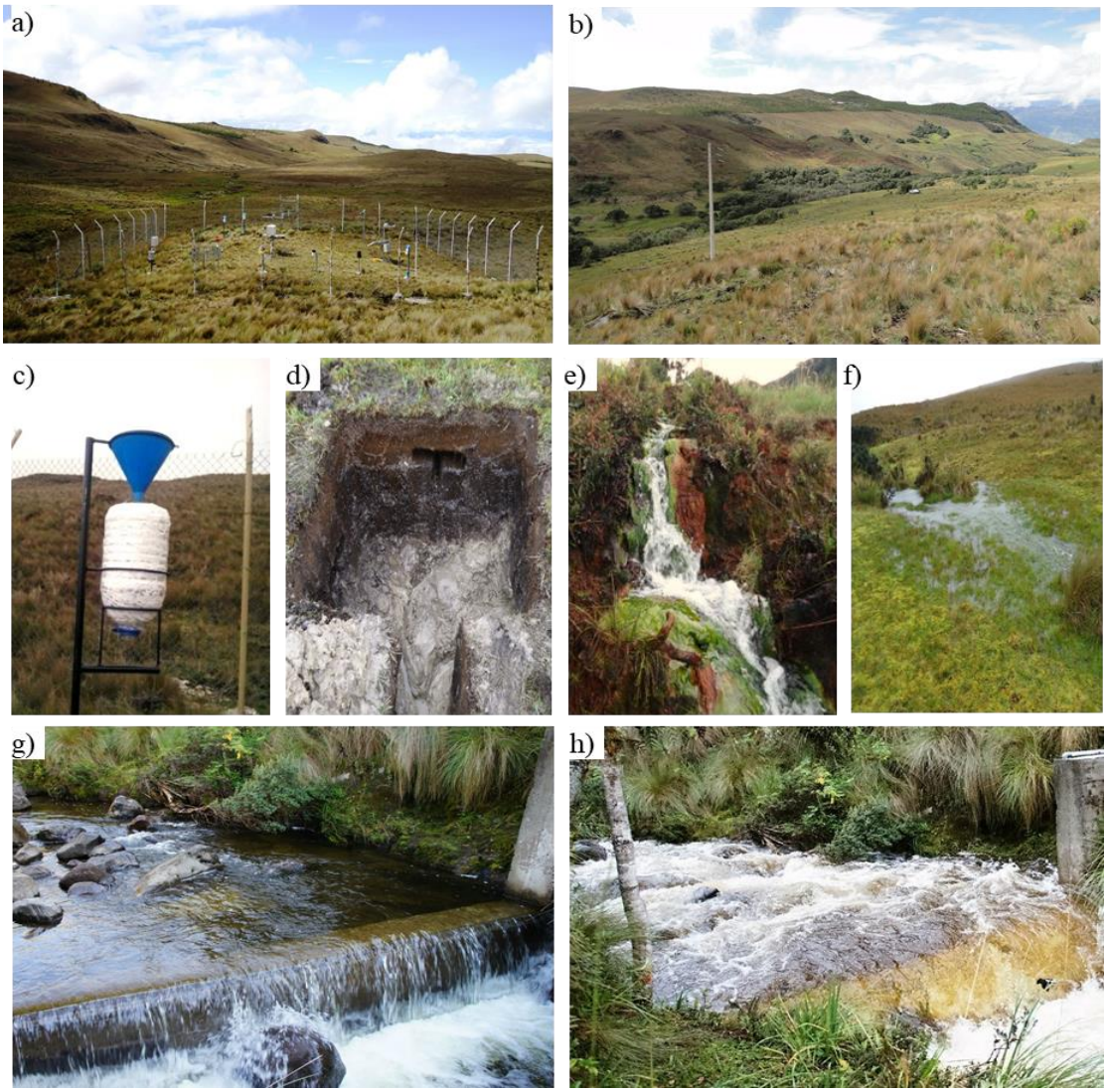

Figure 1-2. View across the study area. a) Overview from the upper catchment showing hydro-climatic instrumentation and b) landscape overview. The following images present the potential end members: c) rainfall collector; d) Histosols, prior installation of wick samplers; e) spring water point; f) overland flow during storm events. The main stream in: g) drier and h) wetter seasons.

Finally, Chapter 4 demonstrated the feasibility of including event-resolution hydro-chemical tracers in conjunction with hydro-metrical information to enhance knowledge of how water is released in the nested catchments system. The first two methods provide a detailed insight into spatially-distributed hydrological processes and the evolution of storm events in Páramo catchments. The chapter showed that internal stream hydro-chemical information is necessary to avoid false conclusions about the hydrological functioning. Additionally, different hydrological behavior in the upper sub-catchments (compared to the lower sub-catchments) became evident. Information on the spatio-temporal runoff-generation process is very helpful to conceptualize the catchment functioning in different time scales and for evaluating process-based hydrological models on these water towers of the remote Andes.

1.5 SUMMARY OF RESULTS

The objective of this doctoral research was to gain insight into the spatio-temporally distributed hydrological processes in a tropical mountain head water catchment in the Ecuadorian Andes. Findings in all chapters were in good agreement and strengthened our interpretation of the general results of this research.

To improve our understanding, we identified the main hydrological processes based on the most informative periods (events), defined dominant water sources as well as flow paths, and analyzed their dynamics and contributions throughout the year and during events. Results presented in this dissertation make use of multiple methodologies and detailed analysis of hydro-chemical data collected data for this research in a remote Páramo catchment with a nested sub-catchments approach. A cascade of flow processes was identified, resulting from the presence of organic porous soils (extremely important for runoff generation), high infiltration capacity, high frequency of precipitation, and the dynamic of the contributing area in the valley bottom. The expansion of contributing area connects the adjacent hillslopes to the channel network mainly during wetter conditions and storm events. This research developed catchment-functioning knowledge and provided guidelines for the hydrological monitoring of ungauged headwater catchments. Additionally, this study demonstrated that tropical mountain catchments with perennially humid climates still have varying inter-annual source contributions and different hydrological behavior within the nested system, which was frequently neglected or underestimated in the past.

Chapter 2 explores precipitation and specific discharge time series from the main outlet and tributaries. Eleven hydrological indices from a subset of 34 rainfall-runoff events were compared with monthly values derived from a continuous monitoring scheme from December 2010 to November 2013. The aim of this study was to quantify the amount of samples required to reach sufficient knowledge about the hydrological processes (based on Monte Carlo model framework) using a subset of selected events compared with continuously measured data. The main questions were: (1) can event sampling provide similar information in comparison to continuous monitoring, particularly with regard to the influence of land cover and physiographic descriptors on the hydrological response in Andean páramo ecosystem, and (2) if so, how many events are needed to achieve a conceptual insight of the rainfall-runoff response for the given region? A stepwise approach was applied to select independent events, and only events that simultaneously occurred in all sub-catchments were retained. Hydrological indices were correlated with land cover and physiographic characteristics from the correspondent sub-catchment, and significant correlations form both schemes were compared by using asymmetric bean plots. The correlation analysis from both time schemes indicates that total flow volume and the RC are strongly correlated with the percent distribution of the soils. The slow flow (baseflow + interflow) correlates to soil distribution significantly, but to a lesser extent than the total flow volume and RC. Furthermore, the previously-mentioned index (total flow, RC and slow flow) presents correlations with the distribution of geological formations. The value of the correlation coefficient increases with the areal fraction of Histosols, and decreases with Andosols, thus showing that runoff is controlled by the soil and land cover in undisturbed catchments in most cases. The positive relation of the above-mentioned index with Histosols (mainly located in the valley bottom) is likely driven by the available storage water capacity of these soils, the dynamically recharge by the higher, situated Andosols on the hillside, and discharge constantly to the creeks and water channel network. The rainfall-runoff response of the valley bottoms is, to a certain extent, controlled by the variable source area concept. Expansion during the rainy periods accounted for the flashy response of streamflow. Lower correlations values to the geological layers suggest little dependency on these descriptors. The determination of the comparability between monitoring schemes is based on correlation, associated p-values, and the analysis of correlation coefficient distributions via bean plots. Results from both schemes point in the same direction, showing that, despite some distinct differences between event and continuous sampling, both data sets reveal similar information

(in particular for total flow and RC). For those indexes, the monitoring of a single event in the rainy season can offer the same information as continuous monitoring, while during the dry season several (in our case ten) events should to be monitored. Event information provides sufficient information for the reconstruction of the relations with the areal extent of soils. By monitoring events, the greatest potential to reduce the monitoring effort gaining the maximum insight to hydrological information is possible. Here, we present guidelines that the sample used in this study for the monitoring of similar ungauged catchments.

In the Chapter 3, understand the catchment response and related hydrological processes with a more integrated approach is proposed. A large hydro-chemical dataset collected over two years was included in our research (see scheme in Fig. 1.3). A distinction was made between the less rainy months, from July to October, and the rainy months, between November and June. We refer to these periods hereinafter as the drier and wetter seasons, respectively. The following specific objectives were stated: (1) identify the dominant water sources of runoff generation; and (2) assess the temporal response of the water sources, the dynamic of the flow paths, and the water ages. The data was used to perform End Member Mixing Analysis (EMMA). With this analysis, we identify and quantify the runoff-contributing water sources (objective 1). The hydro-chemical mixing of end-members tries to mimic the hydro-chemical composition of the stream. It therefore relies on the assumption of conservative behavior of tracers and linear mixing processes (Hooper, 2001). The application of the EMMA method includes (1) the identification of conservative tracers, (2) a principal component analysis (PCA) and residual error analyses to determine the dimensionality of the hydrologic system, and (3) the identification of the best fit end-members. From the initial set of tracers (twenty-two solutes, stable isotopes, electrical conductivity (EC), and pH), fourteen were identified as conservatives (Na, Mg, Al, Si, K, Ca, Rb, Sr, Ba, Ce, V, Y, Nd, and EC) and used in future analyses. PCA and residual errors analyses suggested that a third mixing space dimension should be considered, and therefore four end-members are required to acceptably represent the hydrological catchment system. Analyzing four or higher end-member systems is more mathematically challenging, but this approach presents a more complete conceptualization of the mixing processes. Based on the foregoing, we developed a mathematical methodology to project stream observations that lie outside the domain that is defined by the selected end-members in a third dimensional space. Our findings are particularly interesting, because they

show the feasibility of the EMMA approach beyond the classical three end-member applications.

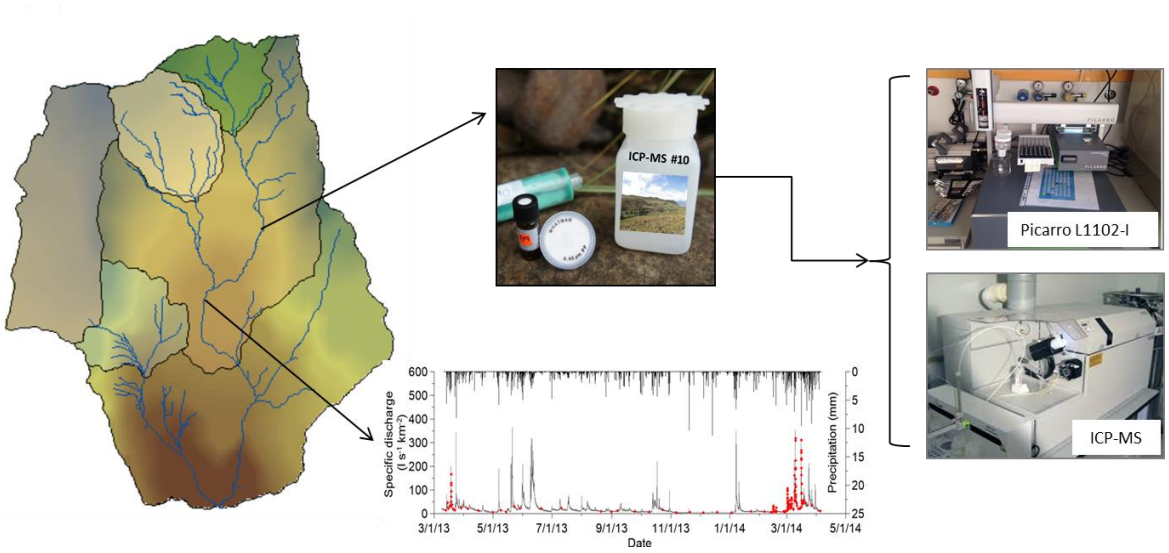

Figure 1-3. Scheme from field to laboratory. Hydro-chemical and hydro-metrical collected data sets. Red dots represent collected water samples.

Our results suggest that the most suitable set of end-members consisted of rainfall, spring water, and water from the bottom horizons of two different soil types: Histosols and Andosols. Most of the stream water observations fell into the domain that was defined by the selected end-members. A satisfactory quality was found for the end-members, with Pearson coefficients between the observed and predicted stream concentrations, between 0.98 and 0.78 ($p<0.01$). As the fresh water that enters a system, rainfall is an important source of runoff generation (22%–30%), suggesting direct channel precipitation and some shallow flow from the riparian area. The nearly-saturated conditions of the riparian zone cause the storage capacity in these soils to be limited to the top centimeters of the upper soil horizon; consequently, only a small fraction of rainfall can infiltrate the top layer. This new water flows horizontally above the saturated zone in the Histosols and feeds the stream. Implementation of multi-tracer techniques enabled us to pinpoint the influence of groundwater on stream generation that was traditionally described as nearly absent in Páramo ecosystems. As the chemical richest end-member (showing higher solute concentrations than other sources), spring water revealed the importance of shallow groundwater sources and the weathering of the mineral layers in our study area. The water from the Andosols underlined the importance of hillslopes in runoff generation due its imperative interaction with riparian zones. Based on our analysis, water from the Andosols contributed to runoff primarily via the

deeper soil horizons. Rainwater infiltrated through the upper porous horizon of the Andosols, percolated through the soil profile, thus obtaining its chemical fingerprint. Histosols representing water from the foot of the hillslopes, and the riparian zone seemed to be the most significant influence on stream generation, as suggested by plotting close to the stream water in the mixing subspace. An ensemble approach to EMMA, hydrograph separation, and ITTPs showed that rainfall presented low variations in its contribution to runoff. Water from Histosols was the main contributor to stream water year-round, matching a hydrological system that is dominated by pre-event water and is even more important during the drier season, when 45% of the stream water was estimated to originate from this source. As expected, spring water contributions also played a considerable role during the drier season; stream water became enriched in solutes with higher contributions from this source. During the wetter season, the contributing area expanded, thus increasing the connectivity with lateral flow from hillslopes and therefore its contribution to the channel network. Based on the isotope two-component hydrograph separation, the studied headwater catchment is dominated by pre-event water during both wetter and drier seasons. This is consistent with the broadly-accepted concept that stored water primarily controls runoff generation. The pre-event component is slightly reduced during wetter periods, given the higher contribution of water from hillslopes and RF. Figure 1.4 depicts the conceptualization of our findings.

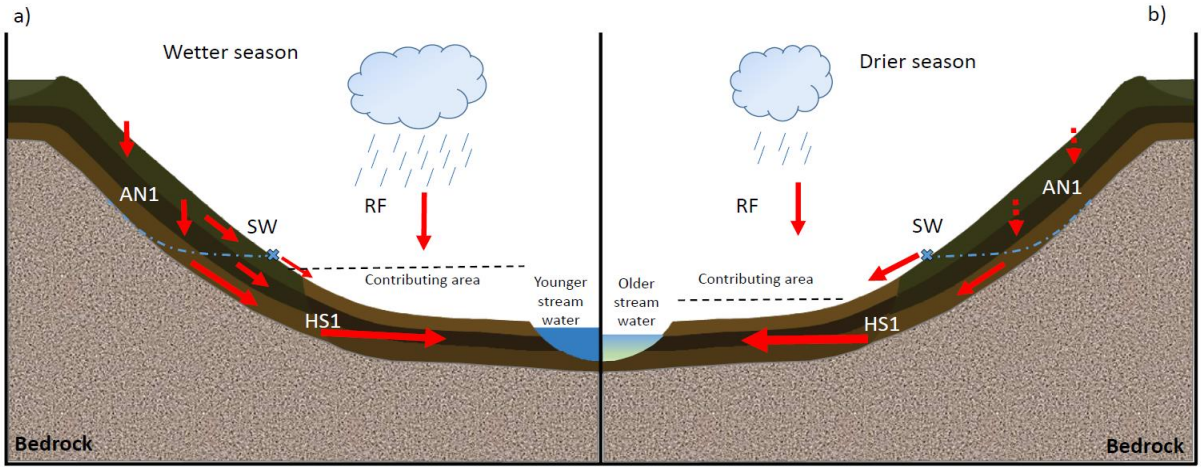

Figure 1-4. Scheme of a conceptual model showing the relative contributions of the main water sources of runoff generation during the wetter season and drier season. Red arrows, proportional contribution of each source to stream.

Our findings from ITTPs revealed older stream water during drier periods and younger stream water during wetter periods, thus providing a reference for the movement of water through the

landscape in different seasons. During the wettest periods, stream water was influenced by all the Andosol horizons, confirming a high connection with the hillslopes. During the drier season, only the deepest Andosol horizon seemed to contribute to Histosols and thus push stored water into streams, which correlates to previous findings for the Páramo ecosystems. The generally younger ITTP signatures of the superficial horizons were caused by the low antecedent soil moisture and high porosity of Andosols. The new water that entered the upper soil horizons rapidly drained towards the bottom without extensive mixing with the stored water. In contrast, this mixing occurred during the wetter season and was reflected by an increase in relative water age. During drier periods, the older stream water plotted close to the Histosols, indicating a longer retention time and the overall regulation capacity of the catchment. Applying ITTPs provided satisfactory results and presented strong potential for isotope data applications beyond the scope of classical MTT estimates, reporting only the average transit time for multi-year datasets. This study is the first to use this multi-method approach to conceptualize the inter-annual temporal dynamics of the dominant water sources and flow paths in high mountain tropical catchments, explaining how flow processes change during drier and wetter seasons.

Based on the findings presented in Chapter 2 and 3, the new research questions have surfaced: Are the defined end-members (rainfall, spring water, water from Andosols and Histosols) for the main outlet suitable for the tributaries? And how do the end-members interact with each other during the most hydrologically- informative periods (storm events)? Here, we overcome previous limitations by taking a more spatially-distributed EMMA into account and, specifically, analyzing the water provenance in a short time scale. The specific objectives were: (1) assess the consistency of stream chemistry from tributaries with the stream outlet (site comparison); and (2) calculate the end-member contributions and stream evolution during storm events. From March 2013 to April 2014, stream and end-member water samples were collected biweekly and during two field campaigns in a higher temporal resolution for selected events from the nested headwater catchments and the end-members in (March 2013 and March 2014). Conservative solutes and EC were used as set of tracers to perform analyses in this section. The novel three-dimensional EMMA model, generated with stream chemistry of the main stream, was used as the reference site, and the upstream sub-catchments were projected into this space. Residuals errors for each sub-catchment were computed, and the corresponding RBias and RRMSE as scalar measures were calculated. The RBias and

RRMSE values of the upstream sub-catchments can be compared to the main outlet. Based on the RBias and RMMSEs values, the EMMA model represents the nearby lower sub-catchments more successfully. Upstream in the northwestern catchment, large RBias and RMMSEs were found, suggesting a different composition of stream chemistry than in the other sub-catchments. This sub-catchment is also likely influenced by water from a pounded wetland in the hilltop and the nearby shallower soils. RRMSEs and RBias are small for the upper sub-catchments, indicating that the main stream EMMA model is able to represent these tributaries well. Following these findings, the main stream mixing model largely explained the hydro-chemical behavior of the tributaries (except for the northwestern catchment). Our results suggest that internal stream chemical information is necessary to avoid false conclusions about the hydrological functioning when compared to the findings considering only a fixed set of end-members for the entire catchment.

During storm events, connectivity processes between riparian areas and hillslopes can be identified. Histosols and Andosols, are the main contributors to runoff across the nested system. Water from the hillslopes plays an essential role being, in general, the most important source for tributaries; on the other hand, the main outlet, is dominated by water from the riparian area. The small storm event with less wet catchment conditions (1-2 March 2014) presented, in most of the cases, a high influence of Histosols, stressing that antecedent catchment conditions and storm event characteristics affect the relative contributions of end-members, although only minimally.

Hysteresis patterns of stream chemistry in the EMMA subspace across the nested system reveals that stream water during storm events generally starts out near end-members with higher solute concentrations. During the rising limb of the specific discharge hydrographs, they move to less-imprinted end-members (an area between soils and rainfall). Afterwards, during times of falling limbs and recessions, they return to the area where they began.

In general, hysteresis loops of the upper sub-catchments show a clockwise direction (except for E1 in S1, U1-U3 mixing space). For this part of the catchment, the rising limb and peak of the hydrograph are dominated by rainfall and soil water from the hillslopes, whereas during the falling limb and recession periods, soil water from the riparian zone and shallow groundwater (in very small proportions) take over. This behavior is likely due to the presence of temporal tributaries and lateral flow in near-surface flow paths of saturated soils during wet

conditions. Contrarily, storm events in lower sub-catchments exhibit counter-clockwise hysteresis, and therefore, a different arrangement of the end-members. The conceptualization for these sub-catchments includes an early influence of Histosols, suggesting that water stored in the riparian zone is pushed by soil water from the hillslopes. Nevertheless, the wet catchment conditions made the "new water" end-members (Andosols and rainfall) act immediately thereafter. The lower catchments have wider valley bottoms and thus a large share of Histosols compared to the upper catchments. The propagation times for RF and water from the hillslopes (Andosols) seem to be longer than the required times to start impacting the rising limb of the hydrograph during storm events, during which water from the riparian zone (Histosols) plays an important role. This study confirmed the usefulness of multi-tracer sets with event data resolution to provide insights into the complex, spatio-temporal, distributed hydrological processes in mountain ecosystems.

1.6 FUTURE RESEARCH

This doctoral dissertation presented detailed insights on spatially-distributed hydrological processes controlling runoff generation during different weather seasons, and for identified informative periods (storm events). Future research challenges that became apparent during this work are summarized below.

Transferability and testing of the new hydrological process understanding

The inclusion of tracers in hydrological models (Objective 1) has been shown to improve model calibration and evaluation, contributing to build a realistic processes representation of the catchment functioning (Fenicia et al., 2008; Seibert and McDonnell, 2002). An acceptable model performance for tracer and hydro-metrical observations promises correct results for the right reasons (McDonnell and Beven, 2014). There is a critical need for high-frequency and high-quality data sets, as well as new observational methods, to evaluate models more rigorously than in the past. The large data set of tracers and advanced catchment knowledge has the potential to be used during the calibration process of hydrological models. The identified dominant water sources and their conceptualized dynamics revealed by this thesis should be included to setup a more realistic model structure. For model evaluation, simulated results can be compared with the empirically derived contribution of flow sources investigated in this doctoral research, to accept or reject model hypotheses about system

functioning. Once an acceptable model structure and model outputs are found, it can be tested in a nearby Páramo area, as for example Quinuas, a medium-scale catchment (91.4 km^2) with similar landscape and hydrological conditions.

A way forward for hydrological monitoring in remote and data scarce regions

As previously described in our findings (Chapter 2), a smart-planned monitoring campaign reduces efforts and maximizes insights on hydrological information (Correa et al., 2016; Juston et al., 2009; Perrin et al., 2007). The task at hand now is to test the proposed monitoring scheme at various other hydrological systems and catchments. Finding from previously ungauged catchments will show how valuable the new routines are for future hydrological studies.

The newly developed ITTPs approach presents a strong potential for isotope data applications with shorter time series (inter-annual) than MTT (requiring typically >2 years of data). It allows for a faster and less expensive collection of samples to estimate relative water ages. Research in poorly or ungauged catchments will benefit the most from our approach to gain insights on the dynamics, connectivity and mixing processes.

EMMA improvements

Despite its benefits the EMMA approach still has some limitations, such as the large degree of subjectivity in the selection of end-members (Hooper, 2003; James and Roulet, 2006). To our knowledge only a few EMMA studies so far presented an uncertainty assessment for the selection of sets of end-members (Delsman et al., 2013), whereas a rigorous method to assess the individual uncertainties in the calculation of contribution to stream or to different end-members has yet to be developed.

Although methods have been developed in the past to identify the number of end-members (Hooper, 2003) and tracers (Barthold et al., 2011) to be used in an EMMA, standardized criteria to define the optimum number of samples per end-member should be developed. Our guidelines to optimize the monitoring of hydro-metrical data is a first step in this direction, but further efforts are required to translate our findings in concrete guidelines for EMMA applications. This task is tightly linked to the need for answers about the following questions (a) how far is too far for the chemical footprint of an endmember to be used in an EMMA?,

(b) should endmembers located outside the study area be used in an EMMA at all?, and (c) what is the maximum distance allowed to project outlining samples back into the mixing space of an EMMA? Again our large hydro-chemical dataset, can be used to seek answers to this kind of questions, by e.g. the inclusion/exclusion of samples or end-members.

Finally, to facilitate multi-dimensional EMMA applications using three or more end-members in the future, ready-to-use software packages and public licenses (e.g. as R or Python packages) should be developed. For example the 3D-EMMA application for projecting stream observations developed in our research (Correa et al., 2017), could be part of such an package.

2 CONTINUOUS VERSUS EVENT-BASED SAMPLING: HOW MANY SAMPLES ARE REQUIRED FOR DERIVING GENERAL HYDROLOGICAL UNDERSTANDING ON ECUADOR'S PÁRAMO REGION?

Abstract

As a consequence of the remote location of the Andean páramo, knowledge on their hydrologic functioning is limited; notwithstanding, these alpine tundra ecosystems acts as water towers for a large fraction of the society. Given the harsh environmental conditions in this region, year-round monitoring is cumbersome, and it would be beneficial if the monitoring needed for the understanding of the rainfall–runoff response could be limited in time. To identify the hydrological response and the effect of temporal monitoring, a nested (n = 7) hydrological monitoring network was set up in the Zhurucay catchment (7.53 km^2), south Ecuador. The research questions were as follows: (1) Can event sampling provide similar information in comparison with continuous monitoring, and (2) if so, how many events are needed to achieve a similar degree of information? A subset of 34 rainfall–runoff events was compared with monthly values derived from a continuous monitoring scheme from December 2010 to November 2013. Land cover and physiographic characteristics were correlated with 11 hydrological indices. Results show that despite some distinct differences between event and continuous sampling, both data sets reveal similar information; more in particular, the monitoring of a single event in the rainy season provides the same information as continuous monitoring, while during the dry season, ten events ought to be monitored.

Published in Hydrological Processes as:

Correa, A., D. Windhorst, P. Crespo, R. Celleri, J. Feyen, and L. Breuer (2016), Continuous *versus* event-based sampling: How many samples are required for deriving general hydrological understanding on Ecuador' s Páramo region?, Hydrol. Processes, 30, 4059‑4073, doi:10.1002/hyp.10975.

2.1 INTRODUCCION

The páramo is tundra-like, a grassland dominated ecosystem with scarce patches of woodlands (e.g, *Polylepis* species*)* and intermittent wetlands and ponds, located in the upper part of the Andean mountains. Depending on the local geographical and climate conditions, páramo normally occurs at altitudes higher than 3,500 m a.s.l (Buytaert et al., 2006), exceptionally at elevations down to 2,800 m a.s.l. (Mena and Hofstede, 2006). The páramo is a fragile ecosystem, and it is to be expected that climate change and anthropogenic impacts will increasingly alter its dynamics, negatively affecting species and habitat diversity and their functional capacity (Erwin, 2009). The páramo covers approximately 10% of Ecuador's land area and provides essential ecosystem services such as the delivery of water resources for other ecosystems, the generation of hydropower, as well as water for irrigation, human and industrial uses (Buytaert et al., 2006; Célleri and Feyen, 2009). Several large cities in the Andes like Quito and Bogotá are almost completely dependent on water from these landscapes (Buytaert et al., 2006). Regardless of this key role in the provisioning of water related services, knowledge about the rainfall-runoff response and the water balance of páramo is limited and views are often contradictory (Buytaert et al., 2010b; Célleri and Feyen, 2009). The foregoing is partly due to the scanty availability of long-term time series of coherent hydrological and related data (Crespo et al., 2011), and the large variability in biophysical and hydrological conditions (Bendix, 2000; Célleri et al., 2009; Ochoa-Tocachi, 2014; Vuille et al., 2000).

Quite an extensive volume of literature exists relating the hydrological response of basins to land cover, climate and physiographic descriptors in different ecosystems. Several researchers studied the effect of landscape characteristics on the hydrological response at the level of a single basin (Le Tellier et al., 2009; Mosquera et al., 2015; Roa-García et al., 2011). Others concentrated on the use of landscape characteristics as a basis for the regionalization of the rainfall-runoff response (Berger and Entekhabi, 2001; Buytaert and Beven, 2009; Post and Jakeman, 1999; Sefton and Howarth, 1998; Yadav et al., 2007). Models and multivariate algorithms are applied to link physiographic parameters and hydrological responses with satisfactory results at different scales (Acreman and Sinclair, 1986; Karalis et al., 2014; Sajikumar and Remya, 2015). In the páramo region of southern Ecuador, Buytaert and Beven (2011) applied several hydrological models to understand surface and baseflow generation with valuable results, concluding that complex models are likely underutilized in this

ecosystem due to the scarcity of data and the non-stationary vegetation conditions. In their efforts to define the factors controlling catchment response in the tropical Ecuadorian Andes, Crespo et al. (2011) studied 13 intensively monitored micro-catchments. They identified that the annual rainfall depth and the physical soil properties are the main controls, suggesting that streamflow generation is dominated by the subsurface flow component and emphasized the importance of this component for streamflow generation.

The concept of deriving hydrological information based on catchment response using event-based information has been used since the early 1970s (Mosley, 1979), whereby rainfall-runoff characteristics are analyzed and related with catchment characteristics and conditions. Several authors have tested the amount of information that a subset of data contains in comparison to a continuously measured streamflow series and the impact this has on the derived hydrological information (Juston et al., 2009; McIntyre et al., 2005; Perrin et al., 2007; Seibert and Beven, 2009; Seibert and McDonnell, 2015). Surprisingly, results often show that a small portion of data can provide almost as much information as long time series (McIntyre et al., 2005). Even though methods for evaluating the information content of a given subset of the original data are well established, a comparison so far has not been conducted for Andean ecosystems with their unique properties (e.g. thick organic soil layer, extreme climatic conditions).

We therefore established a new approach based on Monte Carlo sampling to quantify the amount of samples required to reach a certain degree of information with a subset of selected events compared to continuously measured data. The main questions we aimed to answer in this research were: (1) Can event sampling provide similar information in comparison to continuous monitoring, particular with regard to the influence of land cover and physiographic descriptors on the hydrological response in Andean páramo ecosystem?, and (2) if so, how many events are needed to achieve for the given region a conceptual insight of the rainfall-runoff response?

2.2 SITE DESCRIPTION AND DATA

2.2.1 SITE DESCRIPTION

The study was conducted in the Zhurucay River Ecohydrological Observatory of the University of Cuenca, which is located in Southern Ecuador (85 km southwest of the city of Cuenca). The observatory encompasses a headwater catchment of the Río Zhurucay, with a drainage area of 7.53 km^2, which drains into the Pacific Ocean, and covers elevations between 3,505 and 3,900 m a.s.l. Within this catchment, seven micro-catchments (0.20-7.53 km^2) were established and equipped with measuring instruments (Fig. 2.1a). Fog and drizzle are very common in the region (Buytaert et al., 2006) and the majority of the rain falls with low intensities. The measured average annual rainfall for the study period was 1200 mm. As estimated by Padrón et al. (2015) an additional amount of 15% of precipitation is fog water. The seasonal variation during the year is rather low with a rainy season from December to May (62% of annual rainfall) and a drier period from June to November (38% of annual rainfall).

Histosols and Andosols (IUSS Working Group WRB, 2015) are the dominant soils in the basin (Quichimbo et al., 2012), covering respectively 72 and 24% of the basin area. Whereas the Histosols are mainly situated on plateaus and wet bottoms of the valleys, the Andosols are primarily located on the slopes. The remaining area is covered by Leptosols (4%) which are shallow organic soils preferentially situated on steep valley slopes lying directly on the bedrock. The mechanical strength of the soils is low, but they possess a high water retention capacity.

The geology of the basin mainly belongs to the Quimsacocha formation (basalt flows with plagioclase, feldspar and andesitic pyroclastic) (Pratt et al., 1997) and the Turi formation (accumulation of a thick sequence of conglomerates, fluvial sands, clays, tuffs and volcanic breccias) (Coltorti and Ollier, 2000). Quaternary formations were deposited during the glacial activity of the last ice age. Detailed geological information of the study area is available in Mosquera et al. (2015).

The land cover is characterized by tussock grass (72% of the catchment area) and cushion plants (24%) in the central and northeastern part of the catchment, well adapted to the overall

low temperature, constant rainfall and high wind speed. Forest species (*Polylepis incana* Kunth and *Polylepis reticulata* Kunth) cover the ridges of the basin (2%). The remaining 2% consists of intermittent plots of pine trees and pastures. Land cover and physiographic descriptors of the sub-catchments are presented in Table 2.1.

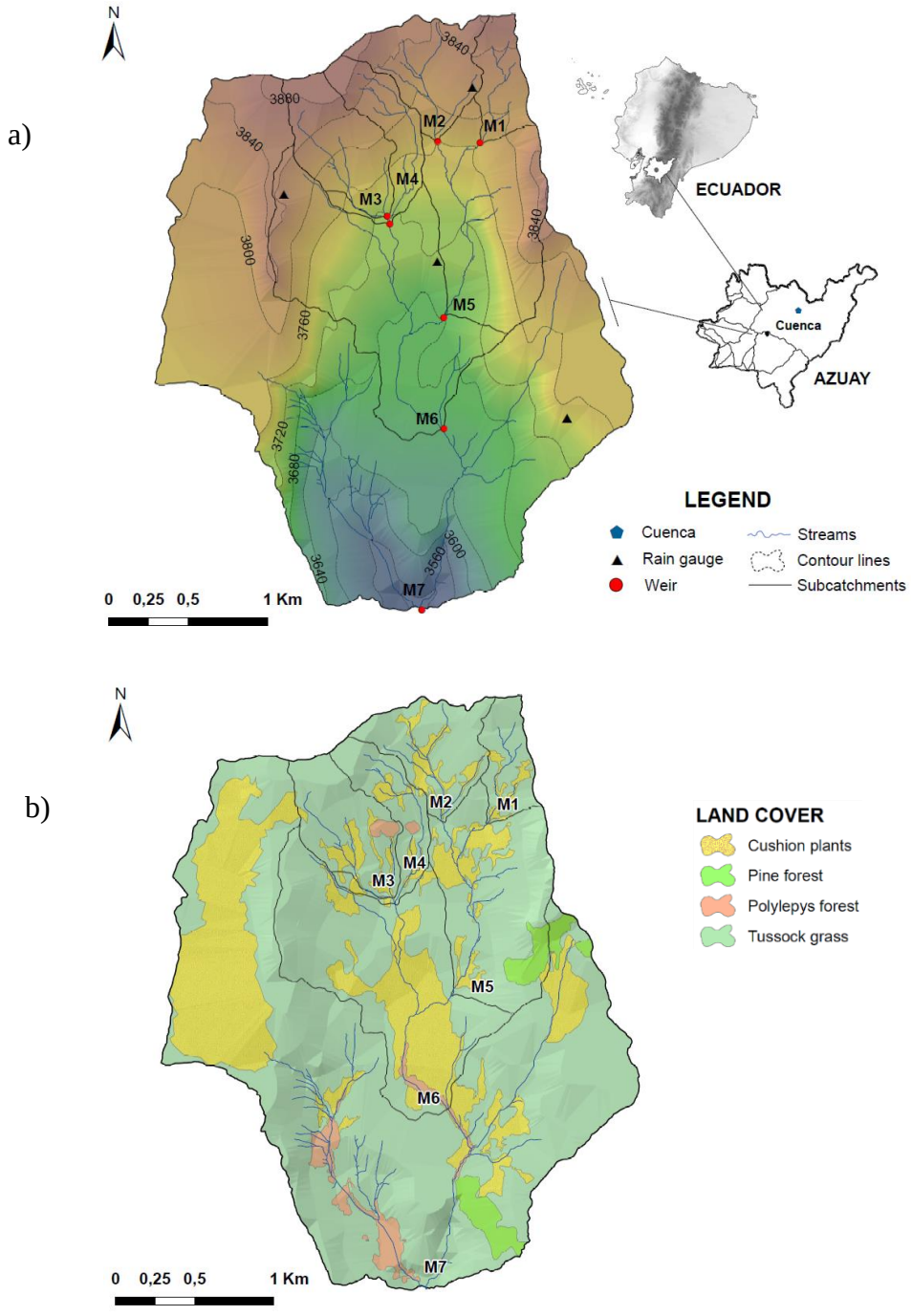

Figure 2-1. The Zhurucay River Ecohydrological Observatory located in southern Ecuador (a) the even nested micro-catchments and (b) the land cover vegetation types.

2.2.2 HYDROLOGICAL MONITORING

Rainfall and runoff data used in this study were monitored from December 2010 to November 2013. Streamflow in the six micro-catchments (M1 to M6) was measured with a V-notch weir, and with a rectangular weir at the main outlet of the basin (M7). Each discharge gauging station (Fig. 2.1a) was equipped with a Schlumberger Diver water level sensor (precision ±5 mm) measuring the water level at 5-minute intervals. The theoretical Kindsvater-Shen equation (USDI Bureau of Reclamation, 2001) adjusted with manual discharge measurements was used to convert the water level to streamflow. Data gaps, 2% for M1 and M2 as well as 4% for M7 were filled via linear correlation with discharge data of the highest correlated gauge. The precipitation network consists of four fully automatic tipping-bucket rain gauges (0.2 mm resolution, RG3-M Onset, Bourne, USA), installed 1 m above soil surface. The average areal precipitation was calculated applying the Thiessen polygon method, yielding for the outlet M7 1,282 mm in 2011, 1,255 mm in 2012 and 1,070 mm in 2013.

Table 2-1. Catchment characteristics of the nested sub-catchments (TWI = topographic wetness index)

Catchment	Area	Perimeter	Altitude (m a.s.l.)		Slope (%)		Mainstream length	Drainage density	Drainage slope	TWI
	(km^2)	(km)	Range	Avg	Range	Avg	(km)	(km/km^2)	(%)	(-)
M1	0.21	2.26	3777 - 3900	3838.5	0 - 33.33	14	0.9	6.71	1.87	9.63
M2	0.38	3.06	3770 - 3900	3835	0 - 30.73	24	0.79	6.92	1.9	12.75
M3	0.38	2.78	3723 - 3850	3786.5	0 - 34.71	19	0.99	4.77	2.04	9.4
M4	0.65	3.23	3715 - 3850	3782.5	0 - 25.35	18	1.28	6.76	2	12.46
M5	1.4	5.97	3680 - 3900	3790	0 - 45.8	20	2.47	4.49	1.89	11.77
M6	3.28	8.09	3676 - 3900	3788	0 - 45.8	18	3.29	4.21	1.79	8.23
M7	7.53	12.09	3505 - 3900	3702.5	0 - 45.8	17	4.63	3.26	1.86	16.72

Catchment	Distribution of soil types (%)			Geology (%)			Land cover (%)			
	Andosols	Histosols	Leptosols	Quarternay deposits	Turi	Quimsacocha	Tussock grass	Cushion plants	Polylepis forest	Pine forest
M1	85	13	2	0	0	100	85	15	0	0
M2	83	15	2	33	1	66	87	13	0	0
M3	80	16	4	0	41	59	78	18	4	0
M4	76	20	4	1	48	51	79	18	3	0
M5	78	20	2	29	1	70	79	17	0	4
M6	74	22	4	20	30	50	73	24	1	2
M7	72	24	4	13	31	56	72	24	2	2

2.3 METHODS

2.3.1 EVENT RUNOFF SELECTION

A step-wise approach was applied for the selection of independent events using the Water Engineering Time Series PROcessing tool, WETSPRO (Willems, 2014). In a first step the flow components were separated using a numerical digital filter technique (Chapman, 1991). The concept of WETSPRO is based on a linear reservoir and the exponential shape of the recession of subflows. Baseflow was separated first, followed by the separation of interflow, and the remaining fraction was considered quick flow. Thereafter, we applied the Peak-Over-Threshold (POT) approach from WETSPRO to identify independent hydrological events by isolating independent flow periods (Kabubi et al., 2005; Willems, 2014). The POT selection was based on the following criteria: (i) two successive peaks can be considered independent when the time between the two peaks exceeds the recession constant for the considered subflow; (ii) the minimum discharge in between these two peaks is smaller than a fraction of the baseflow value; and (iii) application of a threshold value for flow, below which small peaks are not selected (Willems, 2014). This procedure was conducted in each of the seven sub-catchments considering specific discharge data. Only events that simultaneously occurred in all sub-catchments were retained. Peak values ranged between 50 to 1000 l s^{-1} km^{-2}, and were well distributed over time with at least one event in each month of the year. The rainfall information of the selected independent streamflow events were used to calculate the hydrological indices for each event. In total 34 rainfall-runoff events in each sub-catchment with a large variation in magnitude and duration were kept. These results are summarized in Figure 2.2, depicting boxplots for a selected range of hydrological indices, while Figure 2.3 presents the time series of discharge and precipitation in the main outlet for the study period and the selected events.

2.3.2 HYDROLOGICAL INDICES

The following hydrological indices were calculated for each event: total flow volume; runoff coefficient (RC); percentage of slow flow; normalized peak flow; peak discharge; the volume and duration of the high, medium and low flow conditions, using P90 and P35 as thresholds.

Total volume was calculated as the area below the hydrograph of the event and the RC as the ratio of discharge over precipitation. Given the problems encountered in separating interflow from baseflow both were combined and named slow flow. The slow flow component expressed as a percentage of total flow was defined using the subflow filtering module of WETSPRO and is represented by the light grey area in the hydrograph in Figure 2.4. The remaining flow, referred to as quickflow, can mostly be attributed to shallow sub-surface flow in the Histosols during discharge events. Normalized peak flow was calculated as the high flow event value divided by the annual median, and peak discharge as the high flow event value. The high, medium and low flow volumes were calculated as the area between the hydrograph and the thresholds previously established. Additionally, the duration for each flow component was estimated. A closer view of two events is given in Figure 2.4 (March 2011 and January 2013)

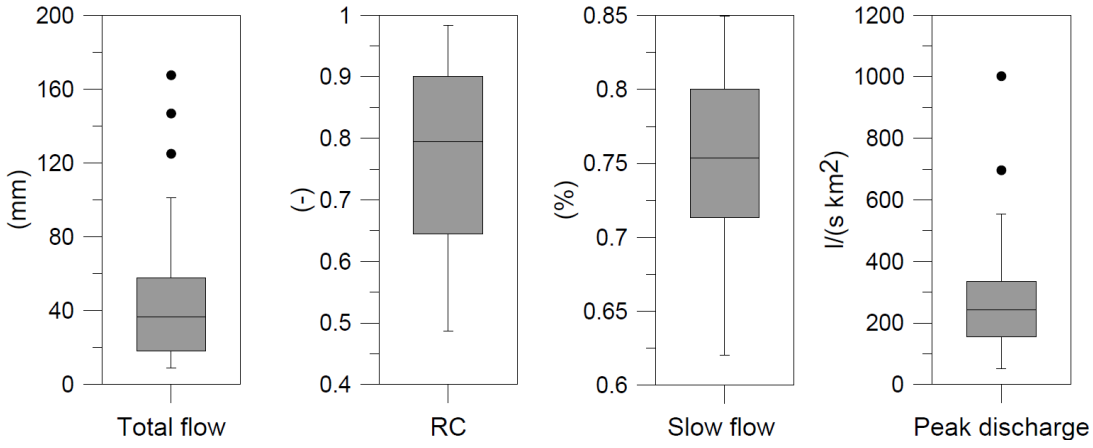

Figure 2-2. Box plots showing selected hydrological indices of the 34 rainfall-runoff events monitored at M7.

2.3.3 LAND COVER AND PHYSIOGRAPHIC CHARACTERISTICS

Data on catchment shape and land cover were obtained during a field survey, and tracked by using a handheld GPS. Distinction was made between four vegetation classes: tussock grass, cushion vegetation, Polylepis and Pine forest. Pine and Polylepis forest cover less than 5% of the total area (Fig. 2.1b). Due to their limited areal extent, they have not been further considered in the analysis. Per sub-catchment, ten physiographic and land cover descriptors were calculated (Table 2.1). These include catchment area (km^2), perimeter (km), average and range of the altitude (m a.s.l.), average and range of the slope (%), main stream length (km), drainage density (km km^{-2}), drainage slope (%), topographic wetness index (TWI),

distribution of Andosols, Histosols and Leptosols (%), distribution of the Quimsacocha and Turi formations and the Quaternary deposits (%). TWI was computed as: $TWI = \ln(A)/\tan\beta$ (Beven and Kirkby, 1979), where A = the specific contributing area, and β = the local slope angle. The descriptors present two general classes: (1) linear scale measurements, whereby geometrically analogues units of topography can be compared as to size; and (2) dimensionless numbers, usually angles or ratios of length/area measures, whereby the shape of analogous units can be compared irrespective of scale (Strahler, 1957). As stated by Karalis et al. (2014) the linear scale measurements and dimensionless numbers are most suited to correlate with the hydrological indices.

A redundancy analysis between land cover and physiographic characteristics was performed, although some authors mention that most catchment characteristics are relatively independent (Olden and Poff, 2003). For this, a Principal Component Analysis (PCA) was applied to explore and reduce the correlated and redundant variables (Sefton and Howarth, 1998), allowing to retain and identify the variables that best explain the variation.

2.3.4 COMPARISON OF THE MONITORING SCHEMES

We draw bi-plots and calculated the Pearson correlation coefficients between the physiographic descriptors and the hydrological indices derived from isolated rainfall-runoff events. After defining the strongly correlated indices, we conducted a similar analysis using the same indices for monthly values using the continuous rainfall-runoff datasets as input.

Using Pearson correlation, our methodology is based on a relative simple and well-known metric, and allows testing whether or not we can detect, a similar system response from two different sampling schemes recorded on different temporal scales (continuous vs. event-based sampling).

The first comparison between the two monitoring schemes consisted of a correlation of each descriptor with a hydrological index, using the data of both monitoring schemes and considering the average values in the spatial distribution of the nested system. After that, the behavior of the most significant relations between the descriptors and the hydrological indices were compared using asymmetric Beanplots (Kampstra, 2008). Beanplots are a combination of a 1d-scatter plot and a density trace. They are used as an alternative to the traditional

boxplot for visual comparison of univariate data between groups, in our case the univariate data refer to Pearson correlation values.

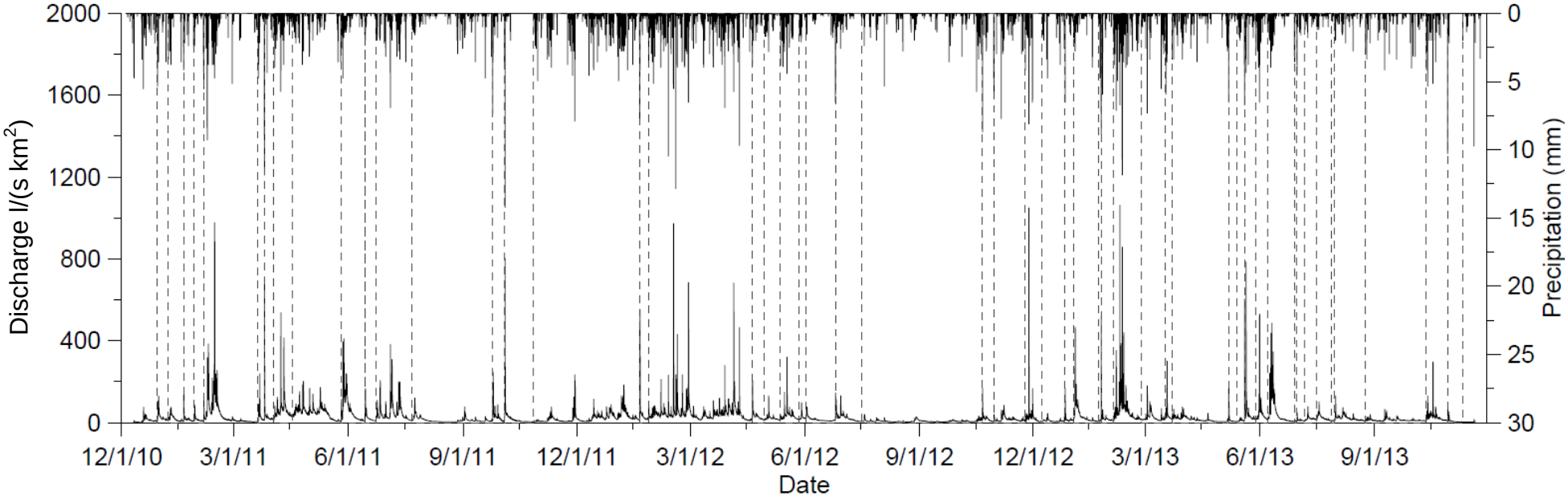

Figure 2-3. Time series of discharge and precipitation in the main outlet between December 2010 and November 2013. Dotted line separate the selected 34 rainfall-runoff events.

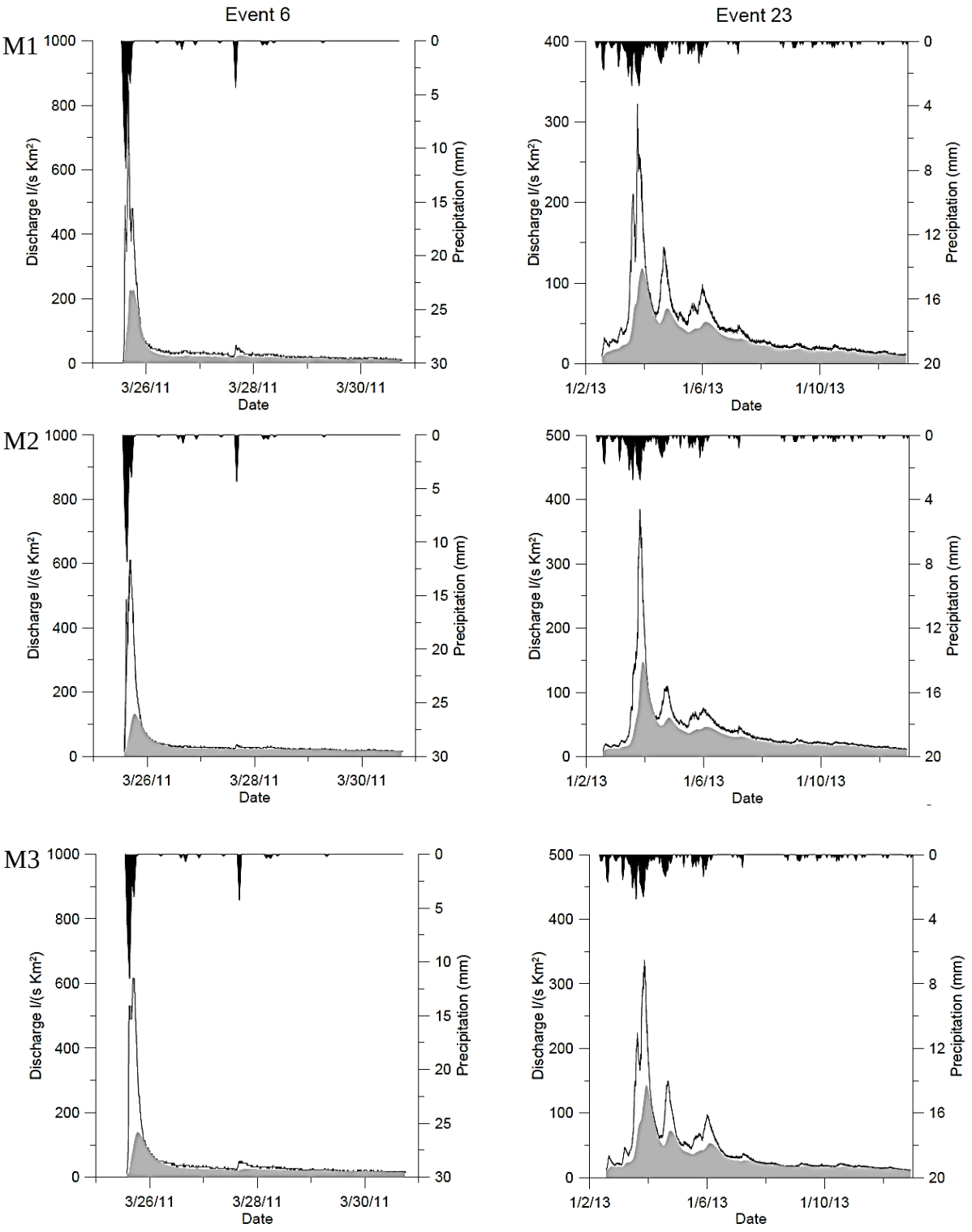
Event 6
Event 23
M1
M2
M3
Discharge l/(s Km²)
Precipitation (mm)
Date
3/26/11
3/28/11
3/30/11
1/2/13
1/6/13
1/10/13

M4

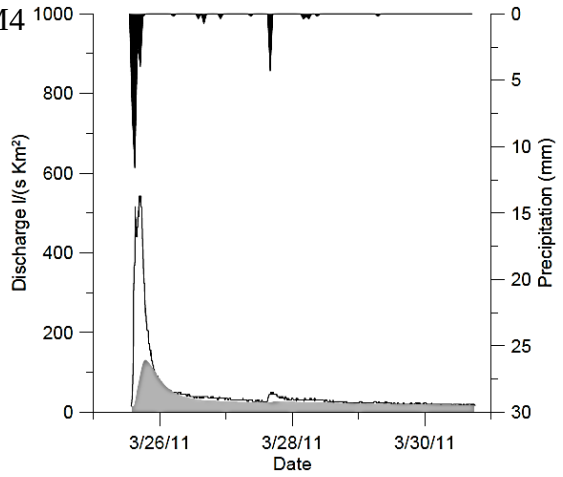
Discharge l/(s Km²)
Precipitation (mm)
3/26/11
3/28/11
3/30/11
Date

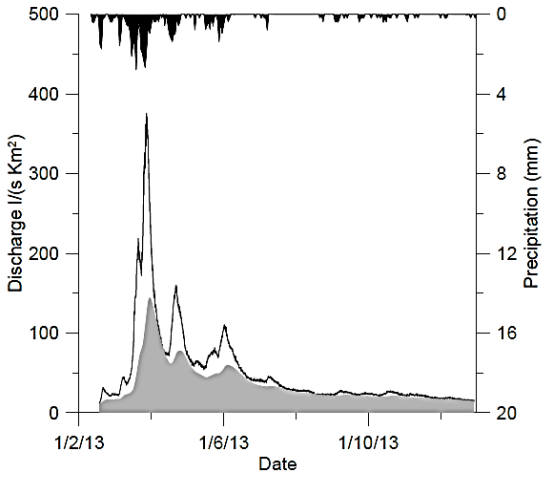
Discharge l/(s Km²)
Precipitation (mm)
1/2/13
1/6/13
1/10/13
Date

M5

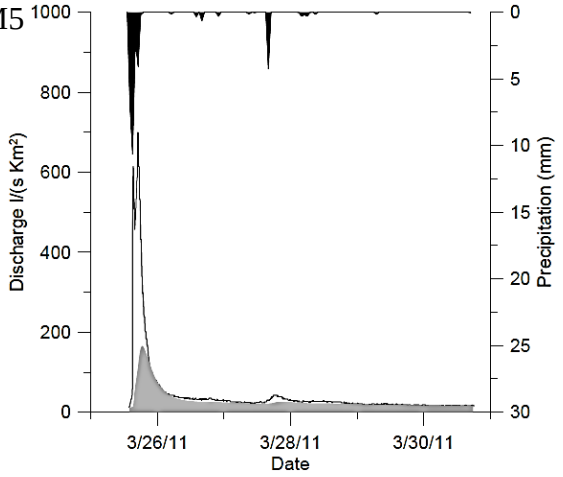
Discharge l/(s Km²)
Precipitation (mm)
3/26/11
3/28/11
3/30/11
Date

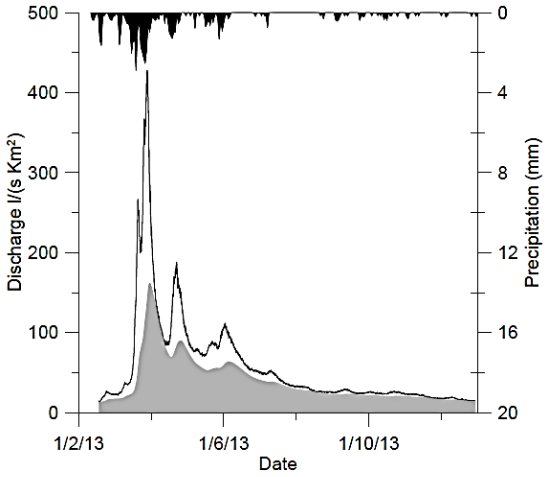
Discharge l/(s Km²)
Precipitation (mm)
1/2/13
1/6/13
1/10/13
Date

M6

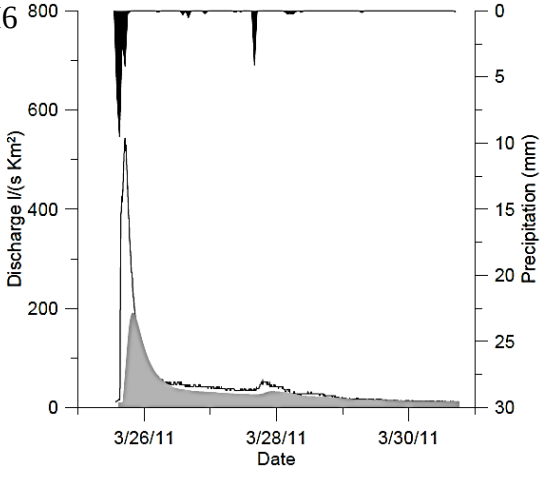
Discharge l/(s Km²)
Precipitation (mm)
3/26/11
3/28/11
3/30/11
Date

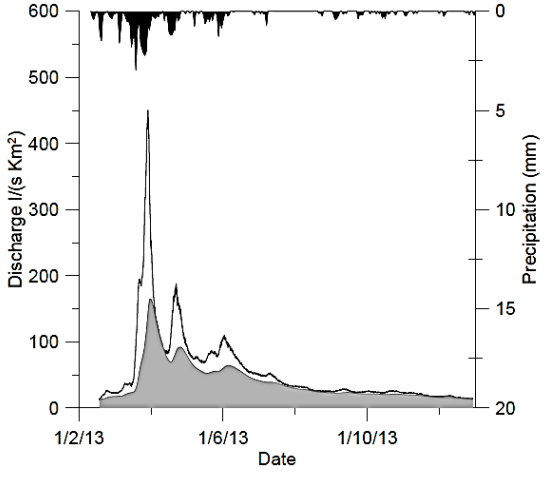
Discharge l/(s Km²)
Precipitation (mm)
1/2/13
1/6/13
1/10/13
Date

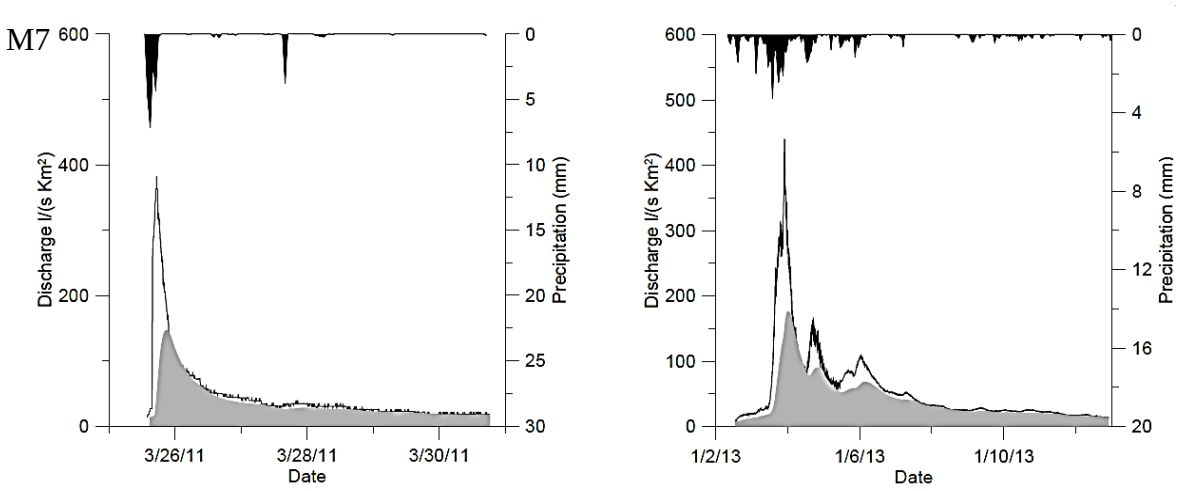

Figure 2-4. Rainfall-runoff events in the seven nested system during March 2011 and January 2013. Light grey represents the slow flow (baseflow + interflow) component in each event.

2.3.5 MINIMUM NUMBER OF EVENT SAMPLINGS

To define the minimum number of events to be monitored we followed a bootstrap sampling method (Efron, 1979) which is based on a Monte Carlo simulation. The main idea was the generation of a large number of random samples and definition of thresholds for drawing conclusions about the minimum number of observations and/or events required. The original data set consisted of correlation values $\{\rho_i\}_{i=1}^{34}$ between variables defined from hydrological indices and catchments physiographic descriptors. For the bootstrap technique a number n, in our study equal to 1000, Monte Carlo simulations were run. A simulation is built by randomly extracting a number of correlation values form the original set. This process was repeated with replacement of the correlation values. A sampling distribution S was then built, with S containing the proportion of the values with correlation equal or larger a threshold (0.9). The threshold denotes the probability that the number of members in S were higher than predefined correlation values (see, Table 2.4 in the results section). The condition for selecting a minimum number of necessary observations were defined by a 95% confidence value that the threshold is attained. The same process was repeated by extracting $\{ne_i\}_{i=1}^{34}$ correlation values, being *ne* number of events.

A twofold analysis was performed in order to compare results and understand the effect of including unusual conditions. In the first analysis, the correlation values of all samples were calculated, and in the second analysis only statistical significant correlations were retained.

2.3.6 SEASONAL SAMPLING

In order to determine monitoring strategies, we separated our event samples in two subsets based on observations during the period December-May and during June-November. We refer to these as *rainy* and *dry* period, respectively. The bootstrap sampling was conducted for each period. To this end, the analysis was repeated for 23 events in the rainy season and 11 events in the dry season.

2.4 RESULTS AND DISCUSSION

2.4.1 DELIMITATION OF RELEVANT CATCHMENT DESCRIPTORS

In a first step we identified the most relevant and uncorrelated descriptors of land cover and physiography. Table 2.2 lists the variables associated with the 1st and 2nd principal components after elimination of the strongly correlated variables and lower factor loadings. In total, they explain 54% and 27% of the total variance. The values clearly show that the variables with highest positive factor loading on PC1 are the area of Andosols (0.99) and the drainage density (0.81). On the other hand, the negative highest factor loadings correspond to the variables Histosol soils (-0.97) and catchment area (-0.84).

Measures such as stream slope, areal distribution of the geological formation Turi and Quaternary deposits with factor loadings of 0.85, 0.81 and -0,75 are most useful in explaining the 2nd principal component. In summary, the first two principal components explain 81% of the variance. The most relevant physiographic descriptors areal extent of soils and geologic layers clearly present a high load with bilateral symmetry.

Table 2-2. Loadings of physical descriptors to principal components PC1, PC2 and percent of explained variance by PC in the Zhurucay basin.

Variables	PC1 54%	PC2 27%
Area	-0.84	-0.28
Drainage density	0.81	0.21
Stream slope	0.27	0.85
Soil Andosol	0.99	-0.07
Soil Histosol	-0.97	-0.08
Geology Quarternary deposits	-0.12	-0.75
Geology Quimsacocha	0.77	-0.35
Geology Turi	-0.57	0.81

2.4.2 CORRELATION OF HYDROLOGICAL INDICES AND PHYSIOGRAPHIC DESCRIPTORS

Correlation analysis between the dominant physiographic descriptors and the hydrological indices indicates that only two of the eleven hydrological indices, namely the total flow volume and the RC, are strongly correlated with the percent distribution of the soils (as shown in Table S1 in the supplement). Ali et al. (2012a) using catchment information grouped by the affinity propagation algorithm presented an overall lack of correlations between hydrological and physiographic derived indices; this relation was slightly explained by soil properties, topographic characteristics and mean transit times.

The value of the correlation coefficient increases with the areal fraction of Histosols, and vice versa with Andosols. Similar findings are reported by authors as Blume et al. (2007); Guzha et al. (2015) and Mosquera et al. (2015) showing that runoff in most cases is controlled by the soil and land cover in undisturbed catchments. Meanwhile Ali et al. (2012a) found that soil drainability properties influenced the temporal variability of runoff pathways in catchments with analogous hydropedological characteristics in Scotland.

Results reveal that the total flow volume in 32 of the 34 runoff events (94%) and the RC in 31 of the 34 events (91%) (see Table S1) are statistically significant correlated with the soil distribution in the basin. It is to be expected that due to the low climate and seasonal variation the hydrological response of the nested system to rainfall-runoff events is mostly defined by catchment characteristics, in our study area by the areal distribution of the soils. Systems of

similar behavior were found in New Zealand where the low seasonal variation resulted in simple catchment responses (Seibert and McDonnell, 2015).

The correlation between total flow volume and the RC with the distribution of the geological formations present statistically significant values in lower than 41% of the cases. The slow flow, considered by Freeze (1972a), Freeze (1972b), Bazemore et al. (1994), Brown et al. (1999), Célleri (2007), Crespo et al. (2011) and Rodríguez-Blanco et al. (2012) as the dominant streamflow component, represented in our study on average 67% of the total flow and correlates significantly, but to a lesser extent than the total flow volume and RC, with the soil distribution. 59% and 29% of the correlations between percent of slow flow and the areal distribution of Histosols and Andosols are statistical significant, respectively positive and negative.

The positive relation of total flow volume, RC and slow flow percentage with Histosols is probably driven by the available storage water capacity of these soils. The Histosols, which are mainly situated in the depressions and lower parts of the basin, are recharged dynamically by the higher, on-the-hillside situated Andosols (Mosquera et al., 2012) and discharge constantly to the creeks and water channel network.

Our indices exhibit similar trends in relation with the geological layers Turi and Quaternary deposits, but low correlation values suggest that the selected indices are little dependent on these descriptors. The higher values of the correlations with the Quimsacocha formation are likely due to the correlation of this substrate with the distribution of Andosols.

2.4.3 COMPARISON OF EVENT VERSUS CONTINUOUS MONITORING

The determination of the comparability between monitoring schemes is based on a twofold analysis, Firstly, correlation and associated p-values based on the average values of continuously measured flows and the 34 event-based measurements in the seven sub-catchments were calculated. Total flow volume present in both cases strong negative correlation coefficients with Andosols, (r of -0.97 and -0.99), and highly significant p-values, ($p=4x10^{-4}$ and $p=1x10^{-5}$) (see Table 2.3). Runoff coefficient and percent of slow flow versus the soil distribution show similar tendencies, with the lowest correlation coefficient values presented for the percentage of slow flow (-0.86 for monthly and -0.76 for event data).

Figure 2.5 presents an example of the linear relationship between RCs and the percentages of Andosols for monthly and events based data. The overall high dependencies underline the important regulating role of the soils in the Zhurucay catchment. Our results are consistent with Juston et al. (2009), who stated that a reduced fraction of data extracted from a longer time series might contain similar information as the full data record, particularly for event-based samples. These authors used around 5% of the total data available while Perrin et al. (2007) explained that 2.5% of data, randomly extracted from a full time series, is sufficient for providing similar understanding.

Table 2-3. Correlation coefficients and p values between hydrological indices and percentage of soil cover and geological layers based on the average values of seven sub-catchments, 34 event-based and continuously measured.

Physiographic descriptors	Total flow volume		Runoff coefficient		Slow flow percentage	
	Event	Monthly	Event	Monthly	Event	Monthly
Andosols	**-0.99**	**-0.97**	**-0.99**	**-0.98**	**-0.76**	**-0.86**
	0.00	0.00	0.00	0.00	0.04	0.02
Histosols	**0.97**	**0.93**	**0.96**	**0.95**	**0.81**	**0.89**
	0.00	0.00	0.00	0.00	0.02	0.01
Quarternay deposits	0.08	0.01	0.04	0.10	0.62	0.54
	0.86	0.99	0.93	0.82	0.14	0.21
Quimsacocha	**-0.80**	**-0.85**	**-0.81**	**-0.84**	**-0.76**	-0.64
	0.03	0.02	0.03	0.02	0.05	0.12
Turi	0.61	0.71	0.65	0.64	0.22	0.17
	0.14	0.08	0.12	0.13	0.64	0.72

Values in bold are statistically significant in a level of (0.05)

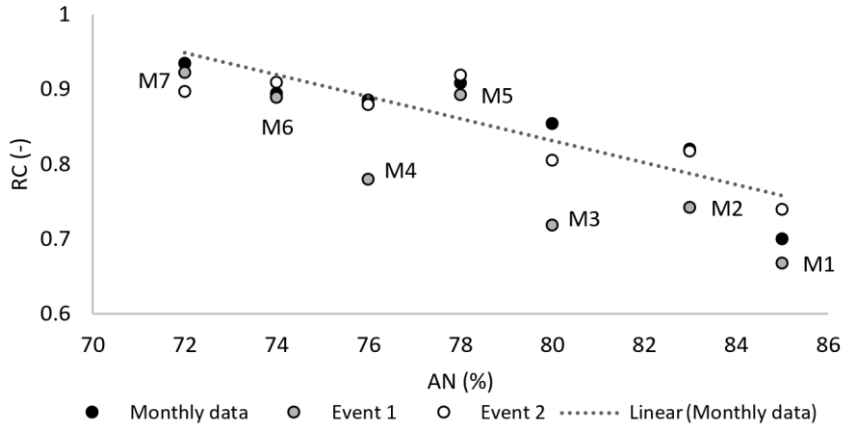

Figure 2-5. Runoff coefficient versus the percentage of Andosols for a specific month (Jun 2013) and two events during the same month. Monthly end event-based data for the seven nested micro-catchments.

Secondly, Figures 2.6a and 2.6b depict the similarity of distributions of correlation coefficients between the total flow (Fig. 2.6a), RC (Fig. 2.6b) and the percent distribution of soils and geological layers, for both data sets. The average correlation coefficients for soils are higher using event-based information compared to continuous data. The distributions of the correlation coefficients with the percent distribution of the geological substrates Quimsacocha and Turi are similar, with the absolute value of the averages slightly higher when using the continuous dataset as compared to the event data. Figure 2.6c shows the distribution of correlations between slow flow percentage and the physiographic descriptors. Again, high correlation values can be observed for both data sets. The average correlations for the distribution of soils are higher when using the continuous based data dataset. In no cases, a clear impact of the geology on the hydrological response could be distinguished.

Findings support the hypothesis that the rainfall-runoff response of the valley bottoms to a certain extend is controlled by the variable source area concept. In rainy periods precipitation fills up quickly the unsaturated zone of the Histosols in the valley bottom and the water draining from the Andosols on the slopes of the surrounding zone is responsible for the expansion of the saturated zone in the valley bottom. Both phenomena are accountable for the flashy response of stream flow during wet periods, seemingly a typical feature of páramo ecosystems. In fact, the flashy response of the hydrograph is the result of a combination of factors such as the highly vertical and lateral permeability of the Histosols, the near saturation conditions year-round of these soils, the variable extent of the saturated zone in the valley bottom, and the topographic gradient of the underlying rock formation.

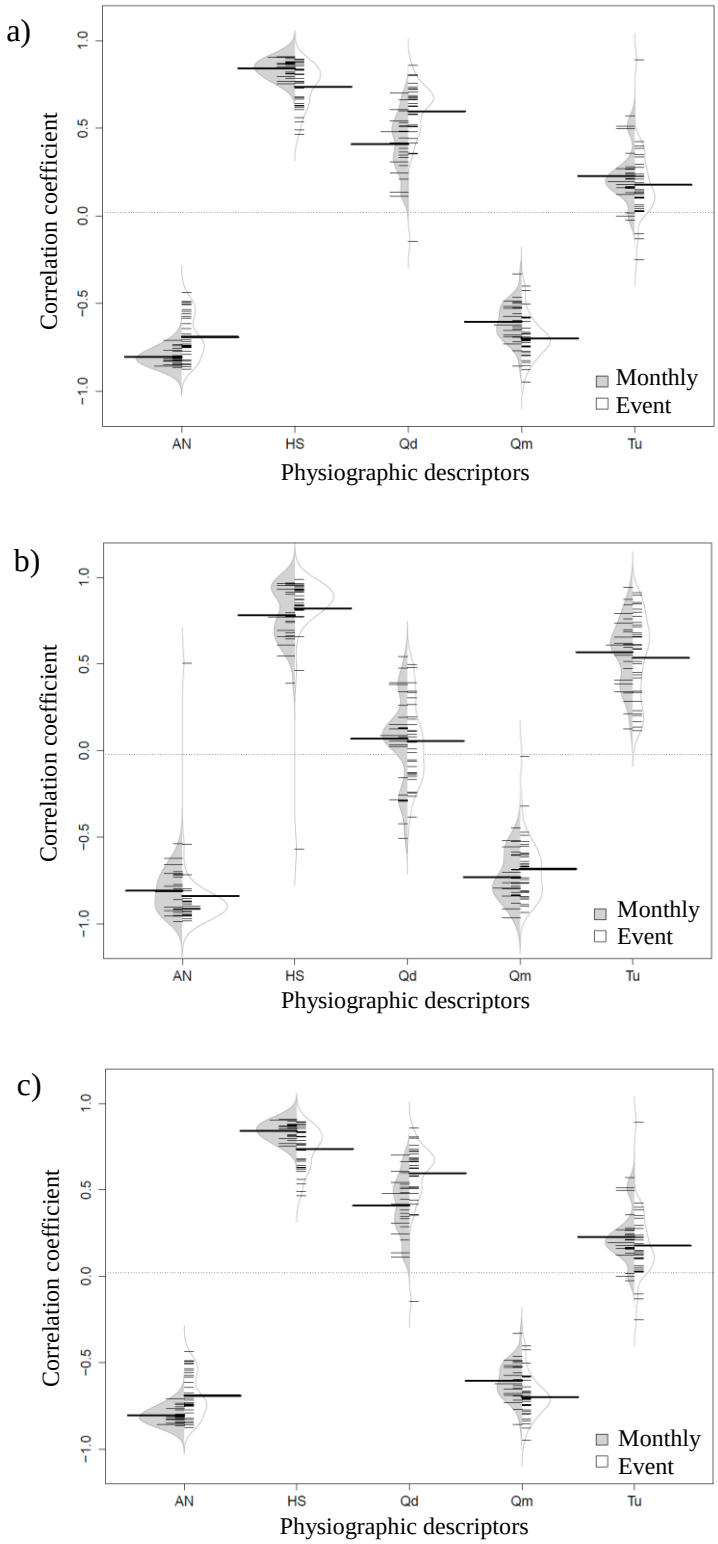

Figure 2-6. Asymmetric bean plots for comparison of monitoring schemes based on continuously measured monthly data and 34 event data. Beans represent correlation coefficients of a) total flow volume b) RC and c) slow flow percentage with physiographic descriptors. The horizontal linesshow the individual observations, while the curve shows the distribution; the bold lines represent the average value of each distribution. AN, Andosols; HS, Histosols; Qd, Quaternary deposits; Qm, Quimsacocha formation; Tu, Turi formation

2.4.4 MINIMUM SAMPLING REQUIRED

We applied a Monte Carlo model framework to all 34 events. Table 2.4 presents the minimum number of events to be monitored to approximate with 90% probability the same distribution of correlation values using the continuous time series. Accordingly, data of one single event provide sufficient information for the reconstruction of the relation between total flow and areal extent of the Histosols (with r = 0.60). Correlation values of 0.65 were obtained increasing the number of monitored events to eleven, and 0.80 when all 34 events are considered. A similar behavior was found for Andosols (r = 0.65). The same analysis considering the relation between the RC and the areal extent of Andosols and Histosols ends up in a correlation coefficient of 0.50 and 0.55, respectively, for just one event, and values around 0.60 when considering the information of twelve events. These findings are consistent with other studies in different environments, such as the Maimai catchment in New Zealand (Seibert and McDonnell, 2015). According to these authors, the monitoring of one up to ten observations in different flow conditions provide the same information as the information derived from continuous monitoring. McIntyre et al. (2005) concluded, after testing several subsets of a larger data set, that event-based monitoring offers the greatest potential in reducing the monitoring effort.

Whereas the latter is true for total flow and RC, the story is different to derive information on slow flows. Here, 30 and 12 events need to be monitored to obtain strong correlations with the distribution of Andosols and Histosols. With respect to slow flow information, we conclude that runoff needs to be monitored almost continuously over a long period. Reducing the number of monitored events will automatically reduce the value of the correlations and likely lead to misinterpretation of the processes that this index can explain in relation to physiographic basin descriptors.

By considering only statistical significant correlation coefficients the monitoring for the three hydrological indices (total flow, RC and percent of slow flow) can be reduced to a single event sampling, with even stronger correlations coefficients as high as 0.75 (Table 2.4).

However, even though this second analyses is statistically more sound and results in higher correlation coefficients with less measurements, we believe it is less operational. During field work one does not know beforehand whether an event results in statistical significant relations

or not. Hitherto, monitoring more often increases the chances to catch one statistical significant event.

Table 2-4. Minimum number of events to be monitored to approximate with 90% probability the same distribution of correlation coefficients using continuous time series.

Correlation value	Total flow volume				Runoff coefficient				Slow flow percentage			
	Andosol		Histosol		Andosol		Histosol		Andosol		Histosol	
α	*n=34*	*n=32*	*n=34*	*n=32*	*n=34*	*n=31*	*n=34*	*n=31*	*n=34*	*n=10*	*n=34*	*n=20*
0.5	1	1	1	1	1	1	1	1	30	1	12	1
0.55	1	1	1	1	12	1	1	1	34	1	30	1
0.6	1	1	1	1	12	1	12	1	34	1	34	1
0.65	1	1	11	1	12	1	12	1	34	1	34	1
0.7	12	1	12	1	12	1	30	1	34	1	34	1
0.75	12	1	12	1	30	1	30	1	34	1	34	1
0.8	34	14	34	32	34	1	34	31	34	10	34	20

Analyses based on all n=34 events and including only number of events (n) with statistical significant correlations. Grey fields indicate the lowest number of sampling possible with at the same time highest correlation value to be achieved.

2.4.5 SAMPLING PERIOD

Table 2.5 shows that for total flow it is sufficient to sample just one event in the rainy season to obtain a correlation value of 0.75 with the areal extent of Andosols and Histosols, respectively. Ten events need to be monitored in the dry season to obtain comparable results. Considering the RC one event ought to be monitored in the rainy season to obtain a correlation coefficient of 0.70 and 0.65 in respect to areal extent of soils. Similar to total flow, this increases up to ten events during the dry season. The percentage of slow flow was not considered in this analysis, since our results indicate that the percentage of slow flow must be monitored over a long period.

Our results indicate that the more homogeneous the sub-catchments are, the easier it is to derive common information on the hydrological functioning from a single event, preferentially during the rainy season. In particular, when funding is scarce, monitoring of a limited number of events might be even more valuable given the monitoring is scheduled in an intelligent way (Seibert and Beven, 2009), more in particular during the most informative periods (Wagener et al., 2003). To this end, our findings are helpful because they contradict the traditional believe that long time series of rainfall and runoff data are necessary for a correct understanding of the hydrological behavior of a basin.

Table 2-5. Minimum number of events to represent seasonal variability to approximate with 90% probability the same distribution of correlation coefficients using continuous time series.

Correlation value	Total flow volume				Runoff coefficient			
	Andosol		Histosol		Andosol		Histosol	
	Rainy	Dry	Rainy	Dry	Rainy	Dry	Rainy	Dry
A	*n=23*	*n=11*	*n=23*	*n=11*	*n=23*	*n=11*	*n=23*	*n=11*
0.50	1	10	1	10	1	1	1	1
0.55	1	10	1	10	1	10	1	1
0.60	1	10	1	10	1	10	1	10
0.65	1	10	1	10	1	10	1	10
0.70	1	10	1	10	1	10	20	10
0.75	1	10	1	10	20	10	20	10
0.80	23	10	23	10	23	10	23	10

Analyses based on all n=34 events. Grey fields indicate the lowest number of sampling possible with at the same time highest correlation value to be achieved.

2.5 CONCLUSIONS

The richness of information extracted from a subset of isolated events has hardly been investigated in Andean páramo catchments. The research presented herein is one of the first studies that verified if the monitoring of an event provides the same information as continuous monitoring. Findings are the result of the data gathered in a dense monitored nested catchment system. Runoff in the study area is mainly controlled by the areal distribution of the soils, considered the main physiographic descriptor, and slow flow is dominant over surface flow. During storm events, the rapid infiltration of precipitation raises the water table to near the surface and the saturated contributing area in the valley bottom expands. This in combination with the drainage water descending from the hillslopes enhances the lateral movement of excess water through the Histosols in the valley bottom and explains the flashy response of streamflow. The study also revealed that the monitoring of a single rainfall event in the wet season and of 10 events in the dry season provides the same amount of insight than continuous monitoring.

The study results offer guidelines for the monitoring of previously ungauged catchments, similar in environmental setting and comparable catchment characteristics as the sample basin used in this study. This is in particular interesting for the Andean region where the number of gauged catchments is limited and the high degree of similarities between headwater catchments allows applying a reduced and event-based monitoring scheme. If a monitoring

scheme is to be implemented, we recommend starting at the beginning of the dry season, and extended the sampling until the first events of the rainy season. According to our results, such a monitoring scheme is the best trade-off between reducing sampling effort and gaining the maximum insight to hydrological information.

Supporting information

Table S1 shows the correlation coefficients between the hydrological indices of 34 individual events and the percentage of soil cover of seven sub-catchments. Please contact the authors for access to the data used in this paper.

Acknowledgements

We thank the mining company N.V. METALS ECUADOR S.A. for providing the geologic map and the hydrographic and topographic data of the study area. This study was mainly funded by the Central Research Office (DIUC) of the Universidad de Cuenca through the project "Identificación de las relaciones entre las propiedades biofísicas y la respuesta hidrológica en cuencas de páramo húmedo". In addition, the authors are grateful to SENESCYT 112-2012 and DFG PAK 825/3 (BR2238/14-1) for their financial support.

3 TEMPORAL DYNAMICS IN DOMINANT RUNOFF SOURCES AND FLOW PATHS IN THE ANDEAN PÁRAMO

Abstract

The relative importance of catchment's water provenance and flow paths varies in space and time, complicating the conceptualization of the rainfall-runoff responses. We assessed the temporal dynamics in source areas, flow paths, and age by End Member Mixing Analysis (EMMA), hydrograph separation, and Inverse Transit Time Proxies (ITTPs) estimation within a headwater catchment in the Ecuadorian Andes. Twenty-two solutes, stable isotopes, pH, and electrical conductivity from a stream and 12 potential sources were analyzed. Four end-members were required to satisfactorily represent the hydrological system, i.e., rainfall, spring water, and water from the bottom layers of Histosols and Andosols. Water from Histosols in and near the riparian zone was the highest source contributor to runoff throughout the year (39% for the wetter season, 45% for the drier season), highlighting the importance of the water that is stored in the riparian zone. Spring water contributions to streamflow tripled during the drier season, as evidenced by geochemical signatures that are consistent with deeper flow paths rather than shallow interflow through Andosols. Rainfall exhibited low seasonal variation in this contribution. Hydrograph separation revealed that 94% and 84% is preevent water in the drier and wetter seasons, respectively. From low-flow to high-flow conditions, all the sources increased their contribution except spring water. The relative age of stream water decreased during wetter periods, when the contributing area of the riparian zone expands. The multimethod and multi-tracer approach enabled to closely study the interchanging importance of flow processes and water source dynamics from an inter-annual perspective.

Published in Water Resources Research as:

Correa, A., D. Windhorst, D. Tetzlaff, P. Crespo, R. Célleri, J. Feyen, and L. Breuer (2017), Temporal dynamics in dominant runoff sources and flow paths in the Andean Páramo, Water Resour. Res., 53, 5998–6017, doi:10.1002/2016WR020187.

3.1 INTRODUCTION

Knowledge of processes that control the rainfall-runoff behavior of high-elevation tropical mountain catchments is relevant because of the range of ecosystem services that these areas provide (Buytaert et al., 2006), especially in the Andean region, where surrounding communities mainly depend on the fresh water that is supplied by these ecosystems (Buytaert et al., 2006; Célleri and Feyen, 2009; Roa-García et al., 2011). Recent evidence revealed that changes in land use and land cover are major drivers of hydrological alteration in the tropical Andes (Ochoa-Tocachi et al., 2016), and wetlands greatly affect the generation of moderate and high flows, which directly affects the water yield (Mosquera et al., 2015). In previous research, Correa et al. (2016) noted that soils are the most relevant physiographic descriptor of the hydrological response and that the rainfall-runoff response is mainly controlled by a variable source area in the riparian zone. Another study showed that the stream water quality exhibits the greatest similarity to the water that is stored in the topsoil from the valley bottom and describes flow paths through the slopes and riparian area (Mosquera et al., 2016a). However, far too little attention has been paid to improving our understanding through an inter-annual approach.

Flow paths vary on temporal and spatial scales; so unraveling the dynamics of hydrological-hydrochemical responses is rather complex (Brown et al., 1999; Capell et al., 2012; Soulsby et al., 2006). Research in tracer hydrology has produced several applications to grasp this complexity, improve our understanding of the hydrological responses, and study, for example, the estimation of the main geographical runoff contributing sources (Hooper, 2003; Liu et al., 2004) and the tracking of flow paths (Klaus and McDonnell, 2013; McDonnell, 2003). In this context, hydrochemical tracers are mostly used to identify the geographical runoff sources and their contribution by End Member Mixing Analysis EMMA. In the EMMA approach, stream water is assumed to be an integrated mixture of different water sources, namely, end-members (Christophersen et al., 1990). Generally, precipitation, through-fall, litter leachate, shallow and deep groundwater and soil water from hillslopes and riparian zones are considered key geographical end-members (Inamdar et al., 2013)

Stable water isotopes are commonly used to evaluate the temporal dynamics of flow paths and the relative importance of pre-event and event water contributions (Buttle, 1994; Klaus and McDonnell, 2013). Water-age distributions are frequently evaluated by Mean Transit Time

(MTT) calculations based on lumped parameter models and adjusted Transit Time Distributions (McGuire and McDonnell, 2006), assuming that the resulting travel times reflect the mean over the entire period under consideration. Recent work proved that the MTT frequently exhibits aggregation errors (Kirchner, 2016a) and implicitly presumes stationarity. This assumption is often violated because every catchment in the real world exhibits nonstationary and heterogeneous behavior in some degree (Kirchner, 2016a, 2016b; McGuire and McDonnell, 2006). Inter-annual fluctuations and conditions outside the assumed stationary zones (e.g., during discharge events) are not considered by the MTT.

Kirchner (2016a, 2016b) introduced the concept of the fraction of young water (FYW) in streams as a metric of transit times, which is less sensitive to the spatial heterogeneity and non-stationarity compared to MTTs. FYW defines the fraction of water in the stream that is younger than a predefined age. For instance, Jasechko et al. (2016) recently used this metric to quantify the annual percentages of the FYW for several catchments around the globe. However, similar to the MTT, the FYW still requires relatively long datasets (> 1 year) and does not allow an assessment of the inter-annual variability.

Our analysis of relative water ages is based on Inverse Transit Time Proxies (ITTPs) (Tetzlaff et al., 2009) to overcome the limitations of MTTs and the FYW. Similar to the FYW and MTTs, ITTPs assess the temporal delay between an input signal (commonly rainfall) and the outgoing signal (commonly stream water). In contrast to the MTT, the temporal delay is reported as a dampening factor of the isotope signatures of those signals rather than an actual time. The simplicity of this approach enables to calculate ITTPs on a much shorter timespan than what is required for the FYW or MTT. ITTPs are therefore an alternative measure to represent the relative water ages and assess the inter-annual variability of water ages (Seeger and Weiler, 2014; Tetzlaff et al., 2009).

Generally, all these methods provide insight into the system from different perspectives and should ideally complement each other to depict the same hydrological processes; however, such methods are rarely combined with each other. This study combines several methods to elucidate the hydrological behavior of a Páramo covered catchment and analyze the temporal shift in the timing/response and the spatial shift in flow paths and source regions for different seasons and flow conditions. Several methods can support or contradict each other, thereby

strengthening the interpretation and improving our understanding or revealing flaws in the selected methods.

The methods in this research include: (1) geographical runoff source identification by End Member Mixing Analysis (EMMA) as part of the spatial domain (Christophersen and Hooper, 1992; Hooper, 2003); (2) two-component hydrograph separation (HS) by stable water isotopes (Klaus and McDonnell, 2013); and (3) the estimation of water ages by a simple measure of isotope signature damping with Inverse Transit Time Proxies (ITTPs) (Tetzlaff et al., 2009). Furthermore, MTT estimations that were derived by Mosquera et al. (2016b) for the same study area are used to test the applicability of the ITTPs.

Data that were collected from 2012 to 2014 in the high tropical mountain Zhurucay River Ecohydrological Observatory, which is situated in South Ecuador, are used to reach the following specific objectives: 1) to characterize our study area from hydro-climatic, hydro-chemical and isotopic perspective; 2) identify the dominant water sources of runoff generation; and 3) assess the temporal response of the water sources, the dynamics of the flow paths and the water ages.

3.2 STUDY SITE

The study was conducted in the Zhurucay River Ecohydrological Observatory, a small tropical headwater catchment (7.53 km^2) in South Ecuador, situated in the perennially humid Páramo region (Josse et al., 2009; Ochoa-Tocachi et al., 2016). The elevation within the catchment varies between 3,505 and 3,900 m a.s.l. (Fig. 3.1). The annual rainfall averages 1,345 mm (Padrón et al., 2015), and the annual reference evapotranspiration is 723 mm as estimated by Córdova et al. (2015).

The average annual discharge is 864 mm yr^{-1} with an average runoff coefficient (RC) of 0.68 (Mosquera et al., 2015). Correa et al. (2016) evaluated individual rainfall-runoff events in the same study area and derived from this information a median RC of 0.80, indicating that an even higher proportion of water in the active catchment storages is quickly released during rainfall events.

The geology of the basin belongs to the Quimsacocha (basalt flows with plagioclase, feldspat

and andesitic pyroclastic deposits) (Pratt et al., 1997) and Turi Formations (accumulation of a thick sequence of conglomerates, fluvial sands, clays, tuffs and volcanic breccia) (Coltorti and Ollier, 2000). (Table 3.1). Quaternary formations were deposited during the glacial activity of the last Ice Age and cover 13% of the catchment area.

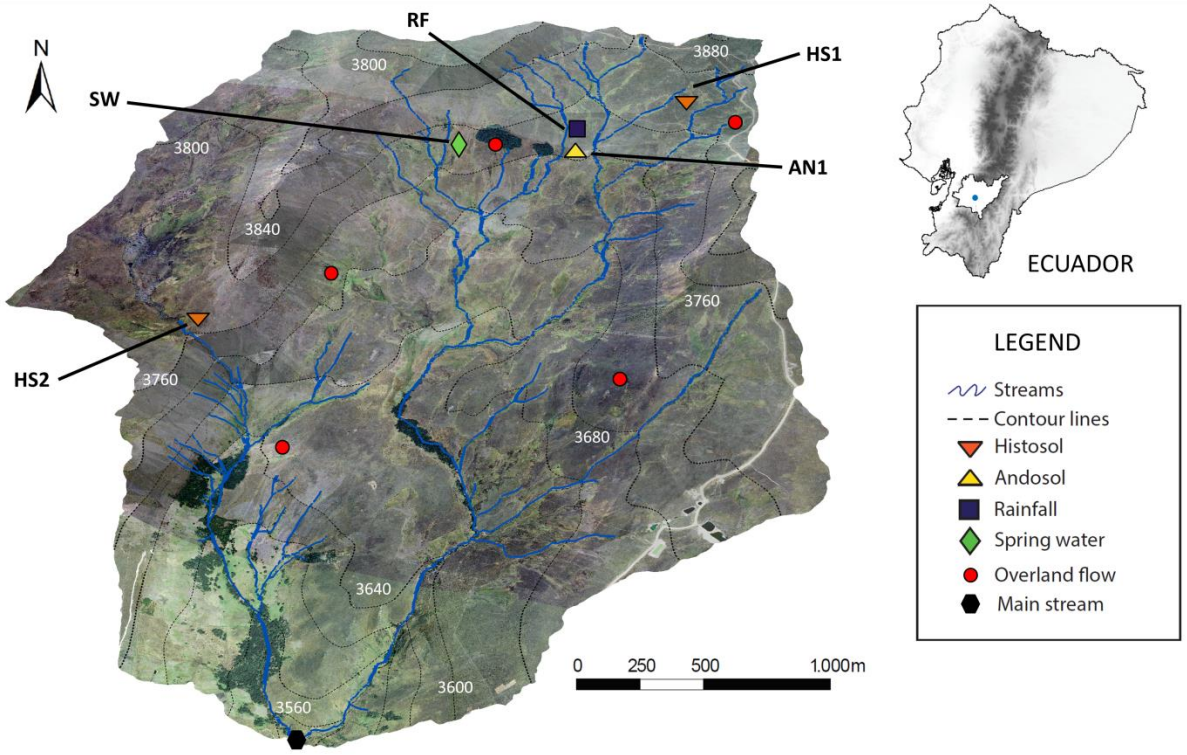

Figure 3-1. The Zhurucay River Ecohydrological Observatory located in southern Ecuador, showing the sites of water sampling:HS1 and HS2 represent the Histosol soil sampling sites; AN1 stands for the Andosol soil sampling site; RF represents rainfall measuring sites; SW stands for spring water, OF the overland flow and MS are the main stream monitoring sites. White numbers represent meters above the sea level.

Table 3-1. Physiographic characteristics of the catchment.

Physiographic characteristics	Unit	Value
Area	km²	7.6
Altitude avg.	m a.s.l	3,700
Slope avg.	%	17
Mainstream length	km	4.6
Drainage density	km km^{-2}	3.2
Drainage slope	%	1.9
Topographic wetness index (TWI)	-	16.7
Distribution of soil types	Andosols %	72
	Histosols %	24
	Leptosols %	4
Land cover	Tussock grass %	72
	Cushion plants %	24
	Polylepis forest %	2
	Pine forest %	2
Land use	Natural %	57
	Extensive grazed %	37
	Intensive grazed %	2
	Forest %	4
Geology	Quimsacocha %	56
	Turi %	31
	Quaternary deposits %	13

Histosols (24%) and Andosols (72%) are the dominant soils in the basin, which are characterized by low mechanical strength. These soils are strongly acidic with pH values around 4.8. The soils in the catchment are highly porous and possess a high retention capacity for water. The top layer of the Andosols averages 44 cm thick (Quichimbo et al., 2012). The top horizons of the Histosols are histic, containing a high fraction of non-decomposed plant fibers (Beck et al., 2008), and have an average depth of 33 cm (Quichimbo et al., 2012). The organic-rich Histosols are primarily located at the foot of the hillslopes and in the valley bottoms and are commonly covered by cushion plants and *Polylepis* trees. The more freely draining Andosols are situated on the hillslopes under a cover of tussock grass.

The land cover is relatively undisturbed with species such as tussock grass (72% of the catchment area) and cushion plants (24%) in the central and northeastern areas of the catchment. Riparian forests species such as *Polylepis incana* Kunth and *Polylepis reticulata* Kunth cover 2% of the basin. The remaining 2% are intermittent plots that are planted with pine trees.

3.3 DATA AND METHODS

3.3.1 HYDRO-CLIMATIC DATA

The discharge station was equipped with a Schlumberger Diver water-level sensor, which has a precision of ±5 mm and measures the water level at 5-min intervals. The theoretical Kindsvater-Shen equation, which was adjusted by manual discharge measurements, was used to convert the water level to streamflow. The discharge values of Q35 and Q90 (frequency of non-exceedance based on flow duration curves), which were determined by *Mosquera et al.* (2015), were used as thresholds for the classification of flow rates. Low flow rates were those below Q35, flow rates between Q35 and Q90 were classified as moderate, and high flow rates were runoff values above Q90.

The precipitation network consisted of four fully automatic tipping-bucket rain gauges (0.2 mm resolution) across the catchment. The measured precipitation time series were corrected by Padrón et al. (2015) to account for drizzles (+15 %). After this correction, the area-weighted precipitation for the entire catchment was calculated by applying the Thiessen polygon method, yielding an average annual value of 1300 mm for our study period. A summary of the hydro-climatic characteristics is shown in Table 3.2.

For the interpretation of the results a distinction was made between the less rainy months, from July to October (covering the 4 consecutive months with the lowest amount of rainfall, with mean rainfall rates of 52 mm per month in 2012 and 76 mm per month in 2013), and the rainy months between November and June (mean rainfall rates of 151 mm per month in 2012 and 110 mm per month in 2013). We refer to these periods as the *drier* and *wetter* seasons, respectively.

Table 3-2. Hydro-climatic characterization of the Zhurucay basin 2012-2014.

[a]Precipitation	[a]Total runoff	Runoff coefficient	[a]Specific discharge	[b]Average time to peak	[a]Relative humidity	[a]Temperature
(mm yr^{-1})	(mm yr^{-1})	(-)	(l s^{-1} km^{-2})	(hr)	(%)	(°C)
1300	828	0.64	26.2	6.6	92.7	6
		Flow rates, as frequency of non-exceedance (l s^{-1} km^{-2})				
Qmin	Q10	Q30	Q50	Q70	Q90	Qmax
2.2	5.6	9.0	13.0	20.9	44.9	695.7

[a]Average annual values.
[b]Time from the beginning of the rising limb to the occurrence of the peak discharge.

3.3.2 WATER SAMPLING DESIGN AND FIELD COLLECTION

The monitoring sites were selected to capture as much of the catchment's heterogeneity as possible (e.g., geology, geomorphology, soils or land-cover types) and the origins of flow components, as reflected in the signals of the environmental tracers (Barthold et al., 2011). Twelve potential sources and stream waters were monitored from April 2012 to April 2014, including the rainfall, soil water in an Andosol and two Histosols at three depths, spring water and overland flow (Fig. 3.1).

Rainwater samples were collected by using circular funnels (diameter = 16 cm) that were connected to polypropylene collectors to analyze the element concentrations. Similar collectors were used for stable isotopes, but these devices were covered with aluminum foil, a 0.5-cm layer of mineral oil was placed on top of the collected water, and plastic spheres were placed inside the funnels to prevent evaporation. An extensive description of the sample collection procedure is available in Mosquera et al. (2016a). Both collection devices were placed next to a tipping bucket gauge that recorded the rainfall (RF).

Soil water in an Andosol along a hillslope was collected at 0.25, 0.35 and 0.65 m below the surface (IDs = AN 1.1, AN1.2, AN1.3); the first two depths were at a horizon with high organic matter content and the third depth was at an organic mineral interface horizon. The soil water samples in the Histosol soil were collected at two sites: HS1 near the valley bottom and HS2 in a confined wetland on a flat hilltop in the northeast of the catchment. Water samples were collected at three depths, namely, 0.25, 0.45 and 0.75 m below the surface (IDs = HS1.1, HS1.2, HS1.3 and HS2.1, HS2.2, HS2.3). The slope at HS1 was slightly higher than that at HS2. Following the methodology of Boll et al. (1992), wick samplers were installed to collect soil water.

Spring water (SW, Figure 1) was included in the monitoring since April 2013 based on the distinct differences in the electrical conductivity with local stream, namely, 116 versus 63 µS cm^{-1}.

Overland flow (OF) rarely occurred but was observed at a few occasions after long and intense precipitation when the soils exceeded saturation. Three times OF samples were collected at five locations (Fig. 3.1) in April 2014 by using handmade devices that consisted of a 100-cm-long and 10-cm-diameter polypropylene container that was cut over a length of

approximately 3 cm (avoiding contamination from rain water), closed at one end and connected to bottles through funnels at the other end.

Stable water isotope samples were filtered *in situ* through 0.45-µm polypropylene membrane filters (Puradisc 25PP Whatman Inc., Clifton, NJ, USA) to minimize organic matter contamination. The isotope samples were stored in 2-ml amber glass bottles and sealed with screw caps with silicon septa. The bottles were covered with parafilm and placed in a dark container to avoid evaporative fractionation and the incidence of sunlight.

Samples for element analysis by inductively coupled plasma-mass spectrometry (ICP-MS) were filtered *in situ* (0.45-µm polypropylene membrane filters, Puradisc 25PP Whatman Inc., Clifton, NJ, USA), stored in acid-washed 100-ml polypropylene bottles, and acidified to pH<2 with purified nitric acid to avoid trace metal precipitation and adsorption during storage.

The electrical conductivity (EC) and pH were measured *in situ* by using a handheld multiparameter instrument (pH/Cond 340i, WTW, Weilheim, Germany) with a precision of 0.1 µS cm^{-1}. The EC was corrected by nonlinear temperature compensation at 25°C, and the pH was measured by using two pH electrodes, specifically, a SenTix 980 digital IDS and a SenTix HW pH electrode, for low-conducting samples.

Water samples for stable isotope analysis were collected weekly and element-concentration samples were collected biweekly, including event sampling in the main stream (Fig. 3.1) and potential runoff sources. The EC and pH were measured at the time of sample collection.

3.3.3 LABORATORY ANALYSIS

The water isotopic composition was determined at the University of Cuenca with a wavelength-scanned cavity ring-down spectrometer (Picarro L1102-I, Sunnyvale CA, USA). Conforming to the manufacturer's specifications, the precision for $\delta^{18}O$ and $\delta^{2}H$ was ±0.1‰ and ±0.5‰, respectively. Starting from October 2013, all the results were processed by using the ChemCorrect 1.2.0 software (Picarro, Sunnyvale CA, USA) (Picarro, 2010). Two samples with high organic contamination were excluded from further analysis. The results were reported in per mil (‰) units relative to the Vienna Standard Mean Ocean Water indicator (VSMOW).

The concentration of twenty-two elements, including rare earth trace elements (Li, Na, Mg, Al, Si, K, Ca, Fe, Mn, Ni, Cu, Zn, Rb, Sr, Ba, Ce, V, Cr, Y, As, Nd and U), were determined at the Institute for Landscape Ecology and Resource Management of the Justus Liebig University of Giessen by using the ICP-MS analytical technique (Agilent 7500ce, Agilent Technologies). The quality of the measurements was controlled by certified reference material (NIST 1643e – SLRS4 and NIST 1640e – SPSSW2) and internal calibration standards. The inclusion of rare earth trace elements was based on previous studies, where the authors highlighted the importance of those elements in the definition of water sources (Bücker et al., 2010). The results were reported as parts per billion (ppb), representing the mean of two consecutive measurements.

3.3.4 DATA ANALYSIS

A hydroclimatic description, chemical and isotopic characterization of the collected data (first objective) data was performed to conceptualize the uniqueness of each catchment source/sampling site (presented in section 4.1), followed by an EMMA to study the dominant sources of runoff generation (second objective) and a multi-method analysis that was based on EMMA, hydrograph separation and ITTPs to assess the temporal response of the water sources, dynamics in flow paths and water ages (third objective).

3.3.4.1 END MEMBER MIXING ANALYSIS (EMMA)

End-members are defined as functional units of catchments and represent the water sources that physically mix during translocation to the stream channel (James and Roulet, 2006). The recommendations of Christophersen and Hooper (1992) and Hooper (2003) were followed during the application of the EMMA method, including: (1) the identification of conservative tracers (not involved in adsorption or biological processes); (2) a principal component analysis (PCA) and residual error analyses to determine the dimensionality of the hydrologic system; (3) the identification of the best-fit end-members (dimensionality+1); and (4) the computation of the contribution from each end-member to the streamflow.

(1) A set of 22 elements, EC and pH from stream data were tested to identify conservative tracers. First, the outliers of each tracer (in our case, values 1.5 times from the interquartile range) were removed. Bivariate scatter plots (tracers vs. tracer) were developed for all

possible combinations, and the related R^2 and p-values were calculated. A collinear structure in the plots and a R^2 value >0.5 (p-value <0.01) were used to consider a tracer as conservative (Hooper, 2003; James and Roulet, 2006). After assessing the bivariate plots, R^2 values and p-values, 14 tracers (Na, K, Rb, Ba, Ca, Sr, Mg, Si, Al, V, Y, Ce, Nd and EC) were identified as conservative (the data that were used are presented as supporting information).

(2) A PCA with stream data (total stream data set) was applied to identify a sub-dimensional U-mixing space that explains most of the variation in the identified conservative tracers. A procedure by Hooper (2003) was used, including a residual error analysis and the calculation of the Relative root mean square error (RRMSE) between the stream water tracer concentrations and their orthogonal projections in the different subspaces to evaluate the fit of these data in a mixing subspace as defined by their own eigenvectors. The dimension of the mixing subspace is defined by small RRMSE values and the smallest possible space where all plots (residuals against the original concentration) appear to be random (Hooper, 2003; James and Roulet, 2006). Additionally, the residuals were evaluated in light of the analytical precision. Patterns in the plots disappeared and the RRMSE values (Table 3.3) decreased for all the tracers in the third and higher dimensional subspaces. Thus, we used a third mixing space dimension for further analysis.

(3) The medians and standard deviations of all potential end-members were orthogonally projected into the mixing subspaces as defined by the PCA of the stream samples. End-members were selected based on their ability to enclose the stream concentrations in the U3-space. Ideally, end-member solutions should exhibit extreme chemical concentrations compared to stream water, low variability compared to the stream chemistry and exhibit distinctive concentrations between end-members (Hooper, 2001).

(4) The percentage of the contribution from each end-member to the streamflow was computed by solving the set of linear equations that was proposed by Christophersen et al. (1990) (Equations 1 to 4). The mixing-model theory was applied by Christophersen and Hooper (1992) to state that stream samples are a linear mixture of the fraction of end-members that form a convex polygon, where the fractions are non-negative and sum to 1:

$$1 = a_1 + a_2 + a_3 + a_4 \quad (1)$$

$$SW_{U1} = a_1 EM1_{U1} + a_2 EM2_{U1} + a_3 EM3_{U1} + a_4 EM4_{U1} \quad (2)$$

$$SW_{U2} = a_1 EM1_{U2} + a_2 EM2_{U2} + a_3 EM3_{U2} + a_4 EM4_{U2} \quad (3)$$

$$SW_{U3} = a_1 EM1_{U3} + a_2 EM2_{U3} + a_3 EM3_{U3} + a_4 EM4_{U3} \quad (4)$$

where a_1, a_2, a_3 and a_4 are the fractions of the four end-members; SW_{U1}, SW_{U2} and SW_{U3} are the projected stream water observations in the U-space (mixing subspace) coordinates; and EMn_{U1}, EMn_{U2} and EMn_{U3} (n1-4) are the coefficients of the nth end-member as projected in the U-space.

Stream observations that lie outside the domain that is defined by the selected end-members (negative fraction) because of input-data uncertainty or time-dependent end-member variability (Chaves et al., 2008; Christophersen and Hooper, 1992) were projected onto the plane that excluded the end-member with a negative contribution, forcing the negative fraction to be zero, and the other contributions were assumed to be a mixture of the remaining end-members (Liu et al., 2004) (see Appendix A). Additionally, the quality of the selected end-members was determined in terms of the good fit between the observed and predicted stream concentrations for each solute. The predicted stream concentrations were calculated as the matrix product of the contributions from every end-member for each stream observation and the projected end-member medians in terms of the original solutes following Christophersen and Hooper (1992) and Hooper (2003).

Table 3-3. Relative root-mean-square error for projection of stream water observations in a mixing subspace created by its own eigenvectors.

Dimensionality[a]	Na	K	Rb	Ba	Ca	Sr	Mg	Si	EC	Al	V	Y	Ce	Nd
1	0.006	0.015	0.014	0.008	0.012	0.009	0.008	0.011	0.01	0.032	0.016	0.022	0.033	0.026
2	0.006	0.013	0.009	0.008	0.011	0.007	0.007	0.011	0.009	0.017	0.011	0.013	0.024	0.011
3	0.006	0.008	0.006	0.004	0.011	0.007	0.005	0.011	0.007	0.014	0.011	0.010	0.019	0.010
4	0.005	0.008	0.005	0.004	0.010	0.006	0.005	0.011	0.007	0.014	0.011	0.008	0.018	0.009

[a]RRMSE values from the first four dimensions.

3.3.4.2 TWO-COMPONENT HYDROGRAPH SEPARATION

Although two stable water isotopes, namely, $\delta^{18}O$ and $\delta^{2}H$, were monitored, we only used $\delta^{18}O$ for further analysis, which is in accordance with Mosquera et al. (2016a), who stated that both isotopes yield comparable results. Variations in the isotopic content of weighted precipitation and stream water permitted the use of a simple mass-balance approach to separate hydrographs into its event and pre-event components. Weekly isotopic $\delta^{18}O$ time series were used as input data (the data that were used are presented as supporting information). The pre-event signature in the streamflow was defined as the previous day streamflow signature (Tetzlaff et al., 2014). We adapted this concept to our time-scale resolution (previous week):

$$\frac{Q_{pre}}{Q_t} = \frac{\delta_e - \delta_t}{\delta_e - \delta_{pre}} \quad (5)$$

where Q_{pre} is the pre-event contribution to the total discharge Q_t; δ_e (‰) and δ_t (‰) are the observed event signature in the precipitation and streamflow, respectively; and δ_{pre} is the pre-event signature in the streamflow. Altitudinal effects on the isotopic composition of precipitation were reported in the region (Mosquera et al., 2016a; Windhorst et al., 2013). Consequently, the isotopic signature of precipitation (δ_e) was corrected by -0.31‰ per 100-m elevation increase according to Mosquera et al. (2016a). The Gaussian error propagation technique by Genereux (1998) was applied to compute the total uncertainty in the hydrograph separation. The uncertainty terms (stream water, new water and old water) for the weekly hydrograph separation are all based on a single sample, using an instrumental precision of ±0.1‰ $\delta^{18}O$ instead of the standard deviation (Liu et al., 2004), and weighted by multiplying this value with the asymptotic Student's t value (Genereux, 1998) at a confidence level of 95%.

3.3.4.3 INVERSE TRANSIT TIME PROXIES (ITTPS) FOR THE DIFFERENT SOURCES

ITTPs are based on a simple measure of tracer damping, which is calculated as the ratio of the standard deviation of $\delta^{18}O$ in stream water to the standard deviation of $\delta^{18}O$ in precipitation (Tetzlaff et al., 2009). In previous studies, ITTPs were shown to be proportional to the MTT

estimates (Capell et al., 2012; Seeger and Weiler, 2014; Tetzlaff et al., 2009); stronger damping indicates longer MTTs. Birkel et al. (2016) presented ITTPs as a strong predictor of MTT with an exponential relationship of R^2=0.59. In our study, we correlated published MTT values of seven tributaries and the main stream (Mosquera et al., 2016b) with ITTPs that were derived from the corresponding isotope time series to verify the feasibility of using the ITTPs approach as an indicator of MTT. We found good agreement between both indicators with a determination coefficient of 0.85 ($p<0.01$). After verification, the same concept (measure of tracer damping) was applied for $\delta^{18}O$ isotope time series from different water sources.

An 8-week moving window was applied to the $\delta^{18}O$ isotope time series to calculate the ITTPs of different water sources (one-week time step). The time of the window was estimated by the shifts in the isotope peaks of the precipitation inputs and source-water outputs during extreme events. During this period, consecutive peaks in the rainfall-isotope time series, one depleted and one enriched, were observed in all cases. Here, ±50% of the estimated time window was used as an error band to explain the uncertainty.

3.4 RESULTS

3.4.1 HYDRO-CLIMATIC, HYDRO-CHEMICAL AND ISOTOPIC CHARACTERIZATION

Our analysis of the hydrograph indicated that close to 10% of the recorded flow rates were high, 55% of the flow rates were moderate and 35% were low during the study period (Q90 = 45 l s^{-1} km^{-2} and Q35 = 10 l s^{-1} km^{-2} were used as thresholds). The low flows were mainly observed during two periods: July-October 2012 and October-December 2013. The annual amount of streamflow varied between 915 (2012) and 740 mm (2013), consistent with the annual precipitation, which varied from 1,420 to 1,180 mm yr^{-1} during the same period. High precipitation intensities (>0.5 mm h^{-1}) were registered between October and June, representing 0.3% of the events, and a maximum value of 13 mm h^{-1} was observed in December 2013. The most common recorded intensity was 0.061 mm h^{-1}.

The median and standard deviation values of geochemical tracers from the stream and potential end-members are depicted in Figure 3.2. The tracers were grouped according to

similar tendencies in the median source values among the elements, including alkali and alkaline earth metals (Na, K, Rb, Ba, Ca, Sr, and Mg) and semi-metals (Si) as Group 1 (G1) and transition elements, including Al, as Group 2 (G2). The median EC values showed comparable behavior to the elements in G1, so this variable was included in this group. The EC of stream water, which had a median value of 28 µS cm^{-1}, showed the greatest similarities to the HS1.1 (29.9 µS cm^{-1}) and OF values (27.6 µS cm^{-1}).

RF depicted the lowest values for G1 compared to stream water and other potential end-members (Fig. 3.2). In G1, the median values for RF and water from AN1.1 were similar, while RF was in the range of SW and OF in G2. Rare earth elements in RF were one order of magnitude lower than in stream water. The Andosols presented generally lower median concentrations of all soil sources, except for the different patterns that were observed for K and Rb. For G1, HS1 had higher average values than HS2; the latter displayed the highest median concentration for the elements in G2, while SW displayed the highest value in G1. The SW (G1) values were around 4 times higher than the concentrations of those elements in stream water.

Horizon analyses revealed that the solute concentrations of G1 in the Andosols increased with depth, in contrast to the behavior of the G2 elements. For HS1, the most diluted water was originated from a depth of 0.35 m below the surface. HS1 and HS2 did not exhibit a clear trend of either high or low concentrations. Nevertheless, an overall higher concentration of elements could be observed in the deeper horizons of all the soils.

The isotope signal of rainfall varied from -23.4‰ to -0.9‰, with lower $\delta^{18}O$ values observed during May and June (lower than -14.0‰) and higher $\delta^{18}O$ values (higher than -5.0‰) in August and September (Fig. 3.3a), when the lowest temperature values were recorded. The streamflow variations were attenuated but still showed a high responsiveness to the input of rainfall. The isotopic composition ranged from -7.6‰ to -15.7‰, following a comparable pattern of the rainfall. The median values of the rainfall and stream isotope data were similar (-9.04‰ and -9.93‰, respectively), but a four-fold-higher standard deviation was observed for the precipitation.

The isotopic composition of soil water considerably varied, with Andosols exhibiting a higher variability than Histosols and higher $\delta^{18}O$ values in the more porous top soil (Fig 3.3b). The

horizons of the HS1 profile showed the most stable behavior in the signature and were the least responsive to rainfall, with median values between -10.5‰ and -10.8‰ (Fig. 3.3b). This source exhibited the most similar signature to stream water.

Figure 3-2. Tracers characterization, median and standard deviation of stream and potential end-members for the study period 2012-2014.RF = rainfall, AN = Andosols, HS = Histosols; x.1-x.3 = three soil depths; SW = spring water; OF = overland flow. Element concentrations in [ppb] and EC in [µS cm^{-1}]. 3-color scale represents: Red for maximum, yellow for midpoint and green for minimum. [a]SW from 2013 to 2014; [b]OF in April 2014. [a] SW from 2013 to 2014, [b]OF in April 2014

		Na	K	Rb	Ba	Ca	Sr	Mg	Si	EC	Al	V	Y	Ce	Nd
Stream	Median	2235.3	853.4	2.0	24.4	2573.7	47.4	366.2	6275.9	28.0	98.4	0.47	0.10	0.12	0.11
n=146	Std	780.7	253.6	0.4	3.9	748.3	15.5	115.7	1949.9	9.0	46.3	0.17	0.02	0.06	0.04
RF	Median	91.7	319.8	0.2	2.6	240.8	1.1	33.1	33.0	7.3	77.8	0.26	0.01	0.03	0.02
n=54	Std	39.7	149.7	0.2	1.6	120.8	0.6	19.1	27.3	2.0	62.2	0.15	0.01	0.02	0.01
AN1.1	Median	156.2	491.9	1.4	4.6	479.2	5.6	96.4	2081.2	7.5	288.3	0.62	0.08	0.26	0.14
n=54	Std	62.5	386.8	0.9	1.2	168.0	0.8	17.6	318.7	1.8	85.3	0.13	0.01	0.07	0.02
AN1.2	Median	288.5	1087.6	2.7	9.9	581.7	8.1	137.9	2258.6	15.1	250.9	0.46	0.06	0.19	0.10
n=57	Std	69.8	181.1	0.4	3.2	217.4	2.4	33.5	433.8	2.7	94.2	0.11	0.02	0.09	0.03
AN1.3	Median	537.0	934.6	1.2	36.4	926.9	24.3	207.6	2813.3	17.3	148.4	0.24	0.02	0.05	0.03
n=58	Std	148.1	470.0	0.5	10.3	383.7	12.3	80.5	516.0	3.4	65.2	0.07	0.03	0.01	0.02
HS1.1	Median	2041.1	1094.7	2.6	26.8	3034.9	49.1	361.4	7809.0	29.9	162.5	0.32	0.09	0.15	0.14
n=20	Std	336.7	485.1	1.3	6.9	531.4	7.5	39.6	706.2	4.0	72.8	0.13	0.03	0.04	0.04
HS1.2	Median	1861.5	400.1	1.8	30.5	2560.7	45.9	337.0	6814.4	31.4	148.6	0.29	0.08	0.18	0.13
n=56	Std	198.3	235.1	0.4	7.8	607.7	10.1	43.5	1020.8	4.3	61.1	0.16	0.03	0.07	0.04
HS1.3	Median	2262.1	1404.7	4.8	22.5	3174.8	56.1	529.0	7019.2	38.4	185.2	0.29	0.17	0.24	0.18
n=46	Std	296.1	256.3	1.2	6.2	1143.6	18.5	204.6	784.7	5.0	125.8	0.17	0.04	0.07	0.04
HS2.1	Median	1164.8	275.8	0.5	25.6	2248.2	32.9	368.1	3244.3	19.4	617.1	0.60	0.20	0.44	0.40
n=17	Std	360.7	94.8	0.2	3.6	556.9	5.2	43.6	562.0	3.6	163.5	0.19	0.05	0.11	0.19
HS2.2	Median	1059.5	406.5	0.9	12.0	1455.6	17.8	484.7	4697.3	23.5	379.1	0.76	0.38	0.66	0.41
n=17	Std	193.5	316.2	0.8	5.3	363.1	1.5	128.2	1175.6	6.9	738.8	0.60	0.13	0.32	0.12
HS2.3	Median	2146.8	905.7	1.4	35.7	1530.6	18.5	475.0	7145.3	23.4	3025.5	4.35	0.39	0.72	0.60
n=10	Std	327.3	198.2	0.1	9.9	635.0	4.2	99.7	1222.7	1.5	828.6	1.58	0.13	0.30	0.19
[a]SW	Median	7252.1	2855.4	6.0	69.5	11513.2	196.3	2525.4	22405.4	115.5	36.6	1.62	0.01	0.03	0.01
n=28	Std	545.8	243.3	0.5	4.3	901.4	8.0	128.1	3323.2	4.7	20.6	0.09	0.02	0.01	0.01
[b]OF	Median	1704.4	710.5	0.9	27.7	2298.3	42.0	244.0	5129.1	27.6	40.5	0.10	0.01	0.01	0.02
n=15	Std	580.1	283.8	0.5	7.6	577.4	11.8	44.6	1447.8	6.8	20.4	0.08	0.01	0.02	0.02

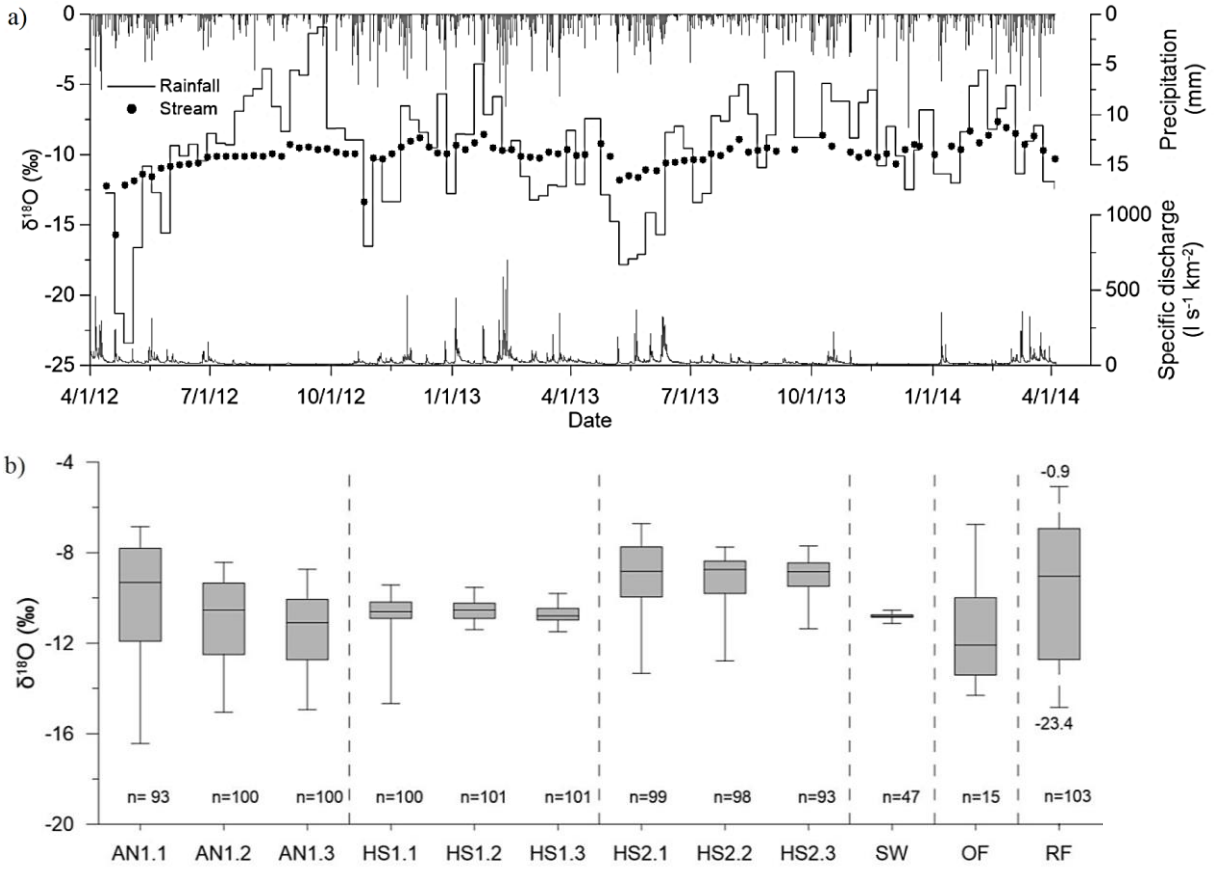

Figure 3-3. (a) Dynamics of the weekly isotope signatures of rainfall and stream water, specific discharge and precipitation time series; and (b) box-plots of isotopic δ18O composition of potential water sources (the central bar in the box represents the median; notches represent the maximum and minimum value and the length of the box indicates the interquartile range). AN = Andosols, HS = Histosols; x.1-x.3 = three soil depths; SW = spring water; OF = overland flow, RF = rainfall. Dotted lines separate water source types.

HS2 showed a higher variability than HS1 and the highest $\delta^{18}O$ median values of all the soil sources. The SW signature revealed the greatest damping behavior, with an isotopic composition from -10.5‰ to -11.1‰. OF presented maximum and minimum values within the range of those in the upper Andosol and Histosol soil horizons and showed the lowest $\delta^{18}O$ median values of all the sources.

3.4.2 SOURCES OF RUNOFF

The PCA of the stream water data explained 60.2% of the variance for the first principal component (U1), 18.4% for the second (U2) and 6.9% for the third (U3). The median values and standard deviations of the end-members projected into the U3-space of the stream water are shown in Fig. 3.4a-3.4c.

U1 mostly explained the variability in the fresh and old water in the system. RF was located on the left side of the stream cloud and SW on the right side (Fig. 3.4); the patterns of the sources' contributions to the streamflow were depicted in this component (Figs. 3.4a and b). The composition of high flow tended to range between RF and Andosols and low flow between Histosols and SW. All the soil horizons from AN1 and HS1 were located between RF and SW.

A large variation in the chemical composition between HS2 and the stream data was observed in U2 and U3 (Fig. 3.4). HS2 plotted far away without enclosing stream observations. In U2 differences in chemical composition between AN1.3 and HS1.3 were identified, while the upper horizons from AN1 and HS1 plotted very close to each other. Infiltration processes throughout the Andosols horizons could be inferred in U3 because the upper horizon plotted near the RF source and progressively deeper horizons became chemically enriched. The median value of OF was located close to HS1.1 and fell within the stream data cloud in the subspace U1-U3.

According to the above-mentioned methodology, the most suitable set of four end-members consisted of RF, SW and water from the bottom horizons of two different soil types (Histosols and Andosols). Most of the stream water observations fell into the domain that was defined by the selected end-members, a tetrahedron in our case. SW represented water with a long contact time with the bedrock material, showing higher solute concentrations from other sources. Although the SW median plotted relative far from the stream water cloud (Fig, 3.4), this value was an essential extreme to define the space that enclosed the stream observations. Satisfactory quality was found for the end-members, with Pearson coefficients between the observed and predicted stream concentrations, specifically, between 0.98 and 0.78 ($p<0.01$). The slope of the regression lines varied from 0.9 to 1.2.

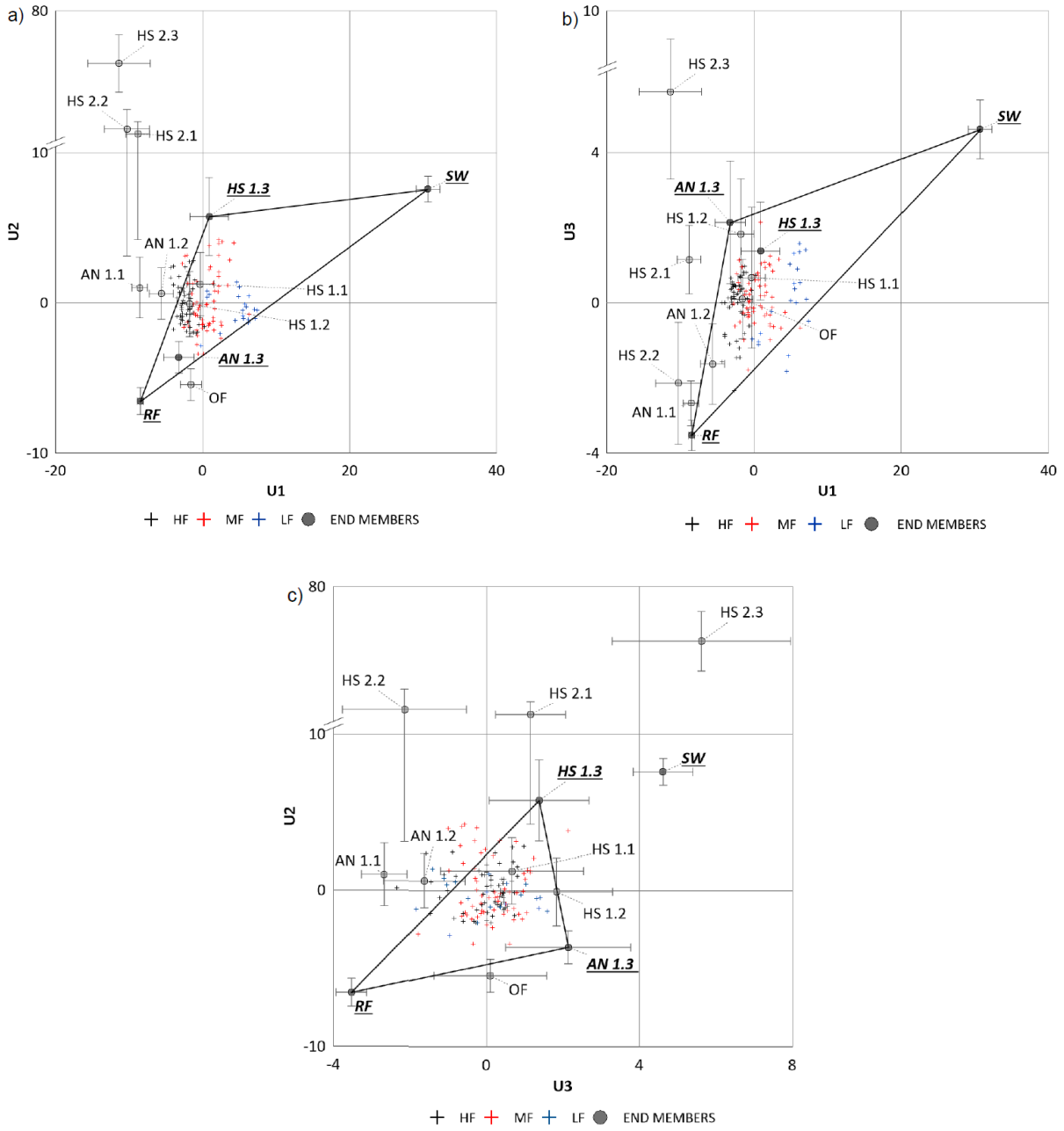

Figure 3-4. Mixing subspaces generated from the main stream water samples: (a) mixing subspace U1-U2; (b) mixing subspace U1-U3; and (c) mixing subspace U2-U3. U1 represents 60.2% of the variance; U2 18.4% and U3 6.9%. HF = high flows (HF>Q90); MF = moderate flows (Q35>MF<Q90); LW = low flows (Q35>LF); RF = rainfall; AN = Andosols; HS = Histosols; x.1-x.3 = three soil depths; SW = spring water; OF = overland flow.

3.4.3 TEMPORAL DYNAMICS IN RUNOFF SOURCES, FLOW PATHS AND TRANSIT TIME PROXIES

In terms of investigating variations in source contributions depending on the hydro-climate conditions, a comparison between the relative contributions to the stream and the specific discharge showed a clear trend for SW (Fig. 3.5), whose contribution potentially decreased with higher specific discharge ($Y=1.48X^{-0.8}$). On the contrary, no clear relationships were found for RF, AN1.3 or HS1.3 and the specific discharge. Only slight trends in stabilizing their contributions with higher specific discharge were observed (Fig. 3.5). To clarify these tendencies, an analysis of the median percentage of the contributions of every end-member was conducted under different flow conditions and during wetter and drier periods.

Under low-flow conditions, HS1.3 and SW contributed the highest proportions to the specific discharge (34% and 31%, respectively; Fig. 3.5), followed by RF (22%) and AN1.3 (13%). Under moderate-flow conditions, the contribution from RF increased to 29%, while the contribution from the soils rose to 40% for HS1.3 and 18% for AN1.3. The contribution from SW decreased to 13%. Under high-flow conditions, HS1.3's contribution increased (42%) and SW's contribution continuously decreased (3%), while the remaining sources displayed contributions of 31% for RF and 24% for AN1.3.

A seasonal analysis revealed that the contribution from RF to the specific discharge slightly decreased from 30% in the wetter season to 22% in the drier season (Fig. 3.5). HS1.3 and SW contributed more to the discharge during the drier season (45% and 23%, respectively), decreasing to 39% and 8% in the wetter season. The median contribution from AN1.3 was nearly two times higher during the wetter season (23%).

The isotope-based two-component hydrograph separation showed that pre-event water was the major component of the streamflow. Most of the time, the fraction of pre-event water was higher than 75% (Fig. 3.6a). Pre-event water was 10% higher during the drier season than the wetter season, averaging 94% and 84%, respectively. The percentage of pre-event water exhibited lower values during the wetter season, occasionally dropping to less than 50%. However, no specific type of runoff event for flow condition could be related to the lower pre-event water component. The uncertainty in the hydrograph separation results ranged from ±2% to ±63% and averaged ±13.5% (Q10 = 4% and Q90 = 27%).

The median values of the ITTPs from the stream data (Fig. 3.6b and 3.6c) showed slight seasonal variation. As Table 3.4 shows, higher median values were obtained from the wetter season compared to the drier season (0.24 and 0.13, respectively). During wet periods, the ITTPs time series of stream water and Andosols (Fig. 3.6b) were particularly close. Relatively older Andosol soil water (at a depth of 0.25 and 0.35 m) appeared during the wetter season. The closest plot of Andosols to the streamflow was that with deeper horizon soil water (Fig. 6b). SW did not exhibit obvious seasonal changes. During the drier season, the stream water was more similar to HS1 (Fig. 3.6c). The high variability in the ITTPs series of water from HS2 (figure not shown) made the delineation of any clear tendency in relation to stream water difficult.

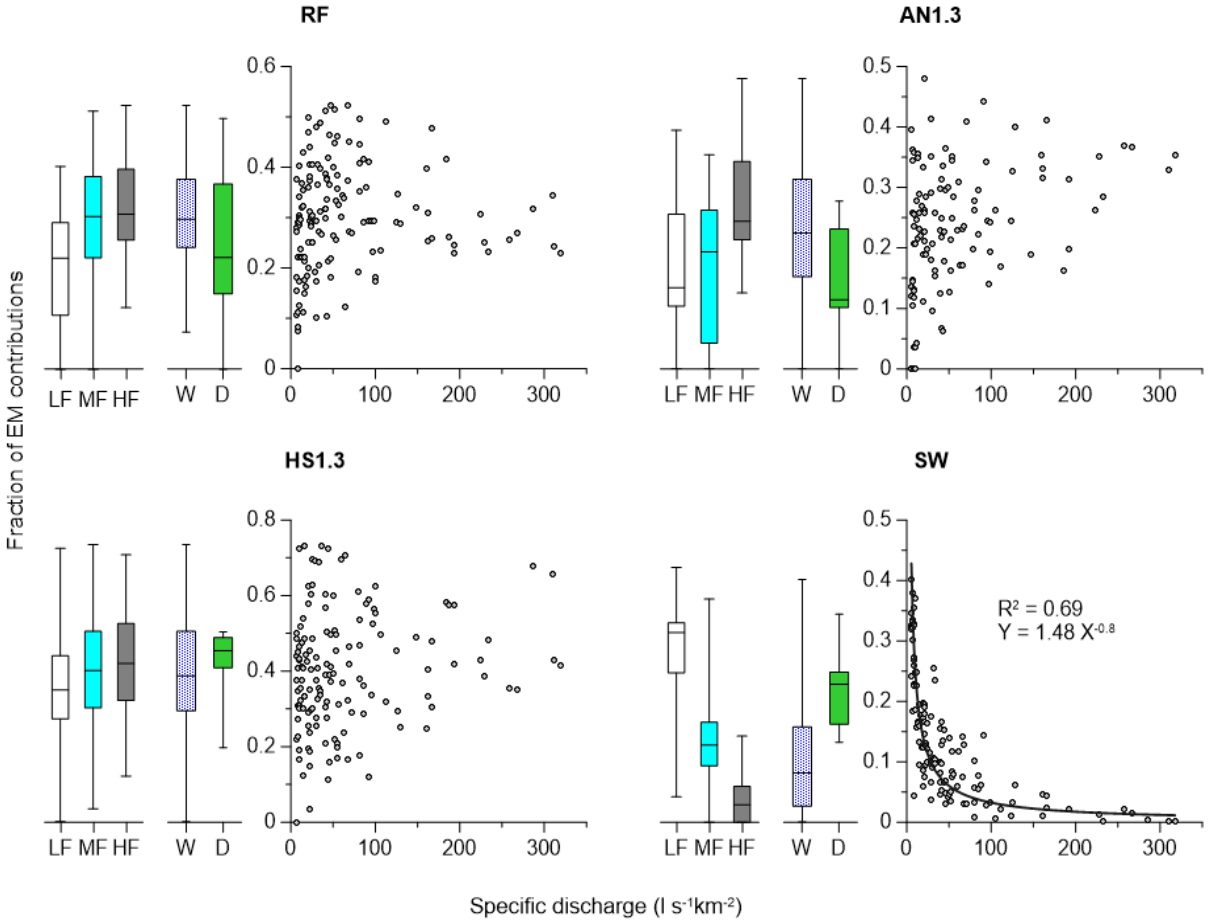

Figure 3-5. Fraction of the end-member contributions versus the specific discharge and box plots of end-member contributions during different flow conditions and in wetter (W) and drier (D) seasons (the central bar in the box represents the sample median; notches represent the maximum and minimum value and the length of the box indicates the interquartile range). RF = rainfall; AN1.3 = Andosol, 3rd soil layer; HS1.3 = Histosol, 3rd soil layer; SW = spring water; HF = high flows (HF>Q90); MF = moderate flows (Q35>MF<Q90); LW = low flows (Q35>LF). Y represents the fraction of end-member contribution and X the specific discharge.

Relatively small increases in the water age proxy could be noted with increasing soil depth (Table 3.4), except for HS2, when the second horizon exhibited relatively older ages than the deepest horizon. The OF source was not included in this analysis because the inadequate time of the sampling resolution did not permit ITTPs analysis.

The results from the error band's 4- and 12-week time window (results not shown) revealed that a shorter window yielded similar median ITTPs (±0.02 on average) but doubled the mean standard deviation (from 0.06 to 0.12 on average) regardless of the season, while a longer window yielded similar results for the median (±0.01 on average) and did not affect the mean standard deviation (0.06 for both cases).

Table 3-4. Median and standard deviation derived from Inverse Transit Time Proxies (ITTPs) using eight weeks as time frame. Values reported for stream water and different water sources correspond to wetter and drier seasons. AN = Andosols, HS = Histosols; x.1-x.3 = three soil depths; SW = spring water.

Sources	Wetter season		Drier season	
	Median	Std	Median	Std
Stream	0.24	0.06	0.13	0.03
AN1.1	0.28	0.09	0.4	0.15
AN1.2	0.25	0.06	0.26	0.1
AN1.3	0.23	0.06	0.16	0.05
HS1.1	0.11	0.07	0.1	0.05
HS1.2	0.09	0.03	0.1	0.03
HS1.3	0.06	0.02	0.09	0.02
HS2.1	0.26	0.1	0.31	0.18
HS2.2	0.08	0.11	0.18	0.08
HS2.3	0.11	0.06	0.26	0.08
SW	0.03	0.01	0.03	0.01

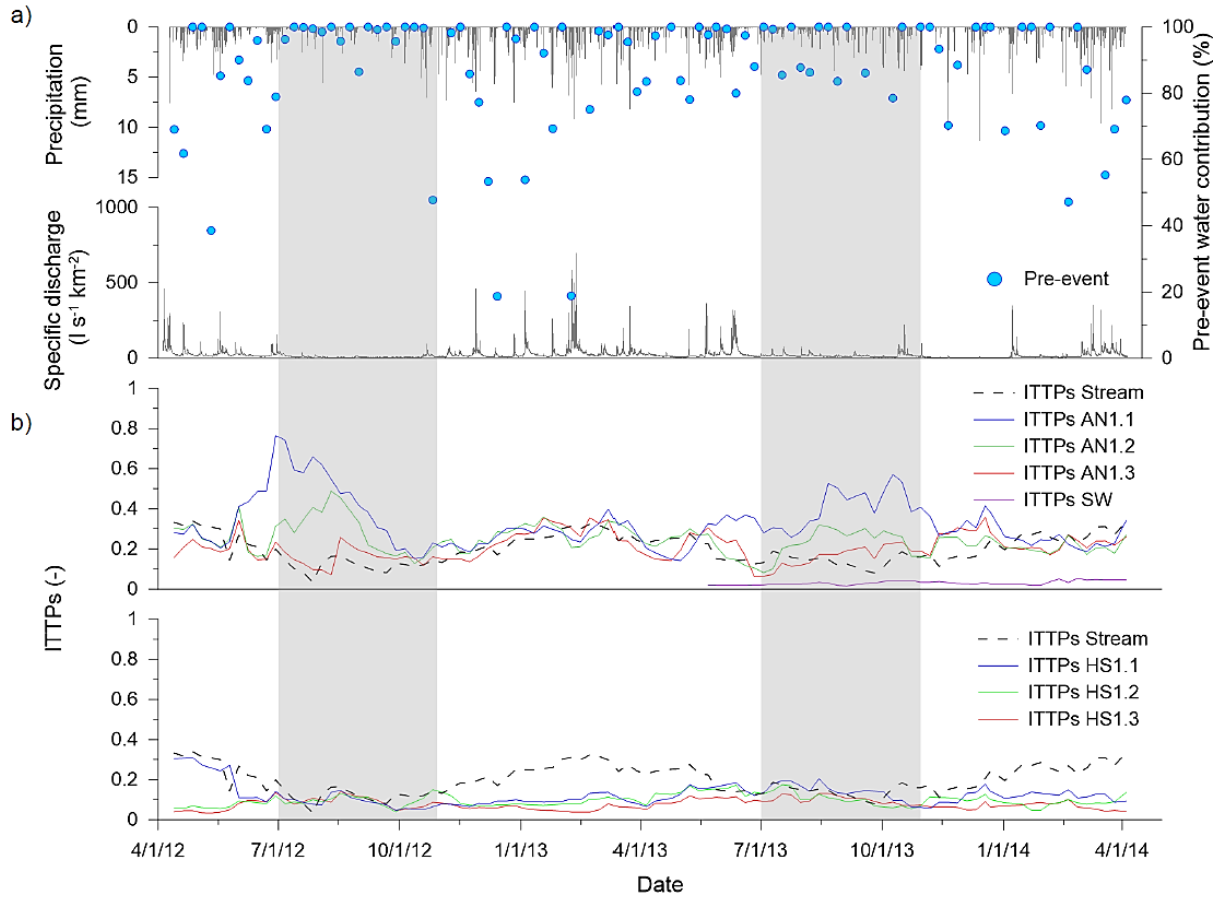

Figure 3-6. (a) pre-event water contributions based on a two-component isotopic hydrograph separation. Blue dots depict the fraction of pre-event water contribution; (b) time series of Inverse Transit Time Proxies (ITTPs) for AN1.1, AN1.2 and AN1.3 representing the three sampled soil depths (0.25, 0.35 and 0.65 m) at the Andosol site and SW spring water; and (c) time series of ITTPs for HS1.1, HS1.2 and HS1.3 representing the three soil depths (0.25, 0.45 and 0.75 m) at the Histosol site. The light grey shaded blocks highlight drier seasons.

3.5 DISCUSSION

3.5.1 SOURCES OF RUNOFF

Combination of several established methods, used to analyze the hydrological processes at the catchment scale, yielded for the Páramo unique system characteristics. Our findings are particularly interesting because they show the feasibility of the EMMA approach beyond the classical three end-member applications. Four end-members are necessary to encompass the mixing space that is generated by two years of stream information and to satisfactorily represent the hydrological system of our study area. The selected end-members were RF, SW and water from two different soil types, namely, AN1.3 on the hillslopes and HS1.3 near and in the valley bottom.

The possibility to identify a higher number of end-members increases when more tracers are available. A large set of tracers reduces the risk of incorrect conclusions regarding catchment functions (Barthold et al., 2011). Usually, authors limit their analysis to two or three end-members (Engel et al., 2016; Hugenschmidt et al., 2014; Katsuyama et al., 2001; Ladouche et al., 2001), even when a fourth end-member is required to explain the variance in stream water chemistry (Ali et al., 2010). Analyzing four or more end-member systems is more mathematically challenging, but this approach presents a more complete conceptualization of the mixing processes when applicable (Barthold et al., 2017; Delsman et al., 2013; Iwasaki et al., 2015; Lee and Krothe, 2001). The research findings by Iwasaki et al. (2015) highlighted the need for five end-members to consistently interpret the influence when studying the upscaling of storm-runoff generation processes in headwater catchments.

The fresh water that enters a system (RF) is an important source to runoff generation (22% - 30%), suggesting direct channel precipitation (Penna et al., 2015, 2016) and some shallow flow from the riparian area. The nearly saturated conditions of the riparian zone cause the storage capacity in these soils to be limited to the top centimeters of the upper soil horizon (von Freyberg et al., 2014; Mosquera et al., 2015); consequently only a small fraction of rainfall can infiltrate (Crespo et al., 2011). This new water flows horizontally above the saturated zone in the Histosols and feeds the stream. A similar picture was presented by Delsman et al. (2013), who described how the water that entered their system only shortly interacted with the soil. Barthold et al. (2017) noted the importance of saturation-excess overland flow in their catchment, but their data suggested that this water was more likely new water. Buytaert et al. (2005, 2007) noted that a virtually impermeable bedrock in high Andean catchments minimized deep infiltration and that groundwater contributions were nearly absent. However, the implementation of tracer techniques enabled Favier et al. (2008) to pinpoint the influence of groundwater on stream generation. The novelty of using multi-tracer data sets from SW revealed the importance of shallow groundwater sources and the weathering of the mineral layers (rocks and soils) in our study area.

In accordance with our results, the essential role of shallow groundwater in headwater catchments was reported by Shaw et al. (2014) in California and high mountain catchments in Scotland with similar hydropedological conditions (Blumstock et al., 2016). In addition to our primary results regarding the relevance of shallow groundwater, detailed studies of its spatio-

temporal variability are still required to better understand its contribution to runoff generation (Lana-Renault et al., 2014; Rinderer et al., 2014, 2016).

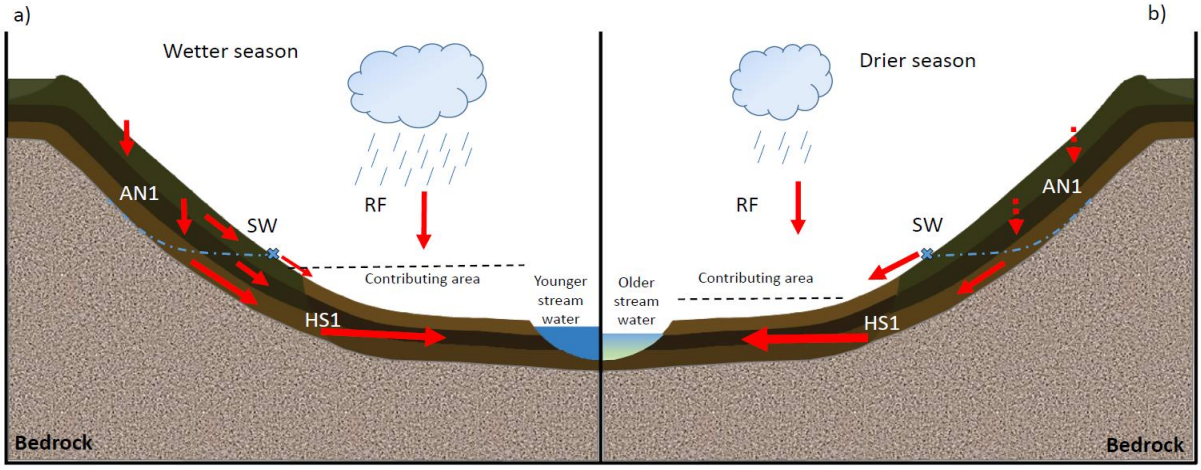

Figure 3-7. Conceptual model showing the relative contributions of the main water sources of runoff generation during the (a) wetter season (November-June) and (b) drier season (July-October). Red arrows = proportional contribution of each source to stream; dotted black line = varying extend of the contributing area; dotted blue line = bedrock-soil interaction; blue cross = location of spring water. AN1 = Andosol; HS1 = Histosol near valley bottom; RF = rainfall, SW = spring water. ITTPs values of 0.24 and 0.13 for younger and older stream water respectively.

The water from Andosols underlined the importance of hillslopes in runoff generation, which should not be underestimated in catchment studies (Iwasaki et al., 2015) because of its important interaction with riparian zones (Ali et al., 2010) and relationship with the hydrological connectivity between uplands and streams (Bergstrom et al., 2016). Based on our analysis, water from Andosols contributed to runoff primarily via the deeper soil horizons (AN1.3). Rainwater infiltrated through the upper porous horizon of the Andosols, percolated through the soil profile and obtained its chemical fingerprint (Fig. 3.2), explaining the importance and usefulness of AN1.3 as a chemical end-member.

HS1.3 stands for water from the foot of the hillslopes, and the riparian zone seemed to exert an important influence on stream generation (von Freyberg et al., 2014), as suggested by plotting close to the stream water in the mixing subspace. Several studies in a range of catchments underlined the essential role of riparian soil water in runoff generation (Blumstock et al., 2015; Jencso et al., 2009; McGlynn and McDonnell, 2003; Tetzlaff et al., 2014).

Mosquera et al. (2016a) identified the shallow subsurface flow that occurs in the top layers of Histosols (HS1.1 and HS1.2) as one of the main discharge contributors based on the similarities in stable isotope signals between soil and stream water. In our study, all the HS1

horizons were active sources, but the top horizons plotted within the stream data lacking the condition of bound the stream water mixing cloud (Fig. 3.4). These observations were a mixture of the distinct chemical signal of the Histosols (HS1.3) and water with a chemical signature closer rainfall (RF) or Andosols (AN1.3). Additionally, we checked the set of end-members, selecting the upper Histosol horizons as end-members in our EMMA. The stream water's chemistry could also be explained, but in a lower proportion than the selected HS1.3 (Fig. 3.4a). HS1.3 bounded the majority of stream water in the mixing cloud, satisfying the end-member condition to explain the highest mixture of stream water (Christophersen and Hooper, 1992). Hence, our findings and those from Mosquera et al. (2016a) do not contradict each other, but rather, lead to the same conclusion, supporting that areas with similar chemical signatures to Histosols are important discharge sources in our study catchment.

Based on the location of the end-members in the mixing space of the EMMA approach, an additional end-member with a chemical signature between SW and HS1.3 could be missing. A mineral soil source below the lowest currently sampled Histosol horizon (HS1.3 at 0.75 m depth) could match this description. Such a source could also explain the long tail of the exponential model that was selected by Mosquera et al. (2016b) to describe the transition of the isotope signal and the currently important contribution from the monitored SW source. These discrepancies highlight the necessity to precisely consider the differences in methods when interpreting the contributions from different sources to flow generation.

3.5.2 TEMPORAL DYNAMICS IN RUNOFF SOURCES, FLOW PATHS AND TRANSIT TIME PROXIES

The dynamics in the RF's contribution revealed this factor's importance under different flow conditions, increasing slightly from low to moderate flows. The contribution from AN1.3 and HS1.3 amplified from low to moderate and high flow conditions, whereas the spring water's contribution considerably decreased when the discharge increased. In our seasonal analysis, water from Histosols was the main contributor to stream water year-round; matching a hydrological system that is dominated by pre-event water. During the drier season, stream water became enriched in solutes with higher contributions from springs. The ITTPs supported these findings, reflecting an increase in stream water age during drier periods and process connectivity within hillslopes under wet conditions.

Figure 3.7 depicts the conceptualization of our findings. The contributing area expanded when

the flow level increased during rainfall-runoff events (Beven and Kirkby, 1979; Correa et al., 2016). This expanded area increased the connectivity with lateral flow from hillslopes to the channel network. The contributing water from hillslopes pushed water from the flat zones into the drainage canals (Tetzlaff et al., 2014), explaining the rise in contribution from both Histosols and Andosols when the flow level increased. Similar connectivity processes were reported by Ali et al. (2010), where scenarios that involved high flow and wet antecedent catchment conditions were associated with increased proportions of soil-water contribution from slopes in a forested headwater catchment in Canada. From this it can be concluded, as stated by Jencso et al. (2009), that the hydrologic connectivity between landscape elements is heterogeneous in time and space.

The increased water contribution from soils near and in the riparian zone when the discharge increased is supported by previous studies in both this region (Correa et al., 2016; Mosquera et al., 2015; Roa-García et al., 2011) and other ecosystems, such as mountainous landscapes in Scotland (Tunaley et al., 2016). The decreasing contribution of SW as a chemical-rich end-member could be explained by dilution processes when the flow level increases (Neill et al., 2011). With higher water levels, stream water is less imprinted by weathering-derived solutes (Blumstock et al., 2015) because of dilution with rainfall and mobile soil water (Bücker et al., 2010).

During the different seasons, RF showed low variations in its contribution to runoff. The nearly saturated riparian soils were hydrologically the most important (Burt, 2005; Mosquera et al., 2016a), even more during the drier season, when 45% of the stream water was estimated to originate from this source. As expected, SW's contributions also played a considerable role during the drier season, while water from the hillslopes barely contributed to the streamflow. The research by Penna et al. (2016) also drew this conclusion.

Based on the isotope two-component hydrograph separation, the studied headwater catchment is dominated by pre-event water (Barthold and Woods, 2015) during wetter and drier seasons. These results are consistent with a previous study in the study area (Mosquera et al., 2016a) and the broadly accepted concept that stored water is primarily controlling runoff generation (Klaus and McDonnell, 2013; McGuire and McDonnell, 2010). According to the seasonal analysis, the pre-event component is slightly reduced during wetter periods, given the higher contribution of water from hillslopes and RF.

Typically for two-component hydrograph separations, small differences between isotopic signatures from the stream and precipitation increased the associated uncertainties to 63%. However, the uncertainty was small throughout the analyzed period (average = 13.5% and Q90 = 27%). Occasionally, the contribution from event water reached high values (>40%). Similarly to previous studies in comparable peat environments, high contributions from event water sporadically occurred during wet periods (Muñoz-Villers and McDonnell, 2012; Tunaley et al., 2016) or under soil saturation conditions (McCartney et al., 1998).

Our analysis of the inter-annual variations in the water ages of the different contributing water sources with ITTPs provides additional insight into the dynamics, connectivity and mixing processes (Soulsby et al., 2015; Tetzlaff et al., 2009). According to the signatures of the soil-water ITTPs, the dampening behavior in HS1 was associated with the likely long transit times from the large storage capacity (porosities >80%) in the soils. AN1 with lower storage capacities and rarely saturation conditions did not store the same amount of water, and therefore, the transport velocity (amplitude of the signature) was higher. The effect of young water sources in HS1 on the overall water storage became less pronounced with depth.

Despite being a simplistic approach, our findings from ITTPs are consistent with those from tracer-aid models that were applied to a sub-annual interpretation of water-age distributions (Birkel and Soulsby, 2016; Tunaley et al., 2016). This study revealed older stream water during drier periods and younger stream water during wetter periods, providing a reference for the movement of water through the landscape in different seasons. In North America, and European rivers, young stream water comprises a third of the global river discharge (Jasechko et al., 2016), and a higher FYW is expected under wetter conditions, similar to our environment (Kirchner, 2016a). The temporal dynamics of stream ITTPs showed additional event-specific dependencies and non-uniform behavior even during low-flow periods.

During the wettest periods, stream water was influenced by all the Andosol horizons, confirming a high connection with the hillslopes (Ali et al., 2010; van Meerveld et al., 2015). Similar results were reported by Penna et al. (2015) in a mountain catchment in the Italian pre-Alps. These authors found important contributions from the hillslope's soil water to stream generation under wet conditions. During the drier season, only the deepest Andosol horizon seemed to contribute to Histosols and thus push stored water into streams, which matches previous findings for the Páramo (Crespo et al., 2011; Mosquera et al., 2016b). The ITTPs and inferred hydrological connectivity exhibited seasonal variations that were

consistent with the research by Detty and McGuire (2010). The younger ITTPs signatures of the superficial horizons during those periods were caused by the low antecedent soil moisture and high porosity of Andosols (Quichimbo et al., 2012). The new water that entered the upper soil horizons rapidly drained towards the bottom without extensive mixing with stored water. In contrast, this mixing occurred during the wetter season and was reflected in an increase in water age (lower ITTP values). During drier periods plotted the older stream water close to the Histosols (Fig. 3.6c), indicating a longer retention time and the overall regulation capacity of the catchment (Mosquera et al., 2016a). Applying ITTPs provided satisfactory results with respect to the interpretation of the hydrologic functioning of the Zhurucay catchment and presented strong potential for isotope data applications. However, this approach represents a rough approximation of the relative water age, and absolute values should be carefully handled (Tetzlaff et al., 2009). Therefore, we used ITTPs to confirm the results from EMMA and hydrograph separation, increasing the credibility of our conceptual model in Fig. 3.7.

3.6 CONCLUSIONS

Combining end-member mixing analysis, hydrograph separation, and water age proxies enabled us to identify and analyze the water flow paths and hydrological processes in a study catchment in the Páramo in southern Ecuador. The relative contribution and timing of different sources from all the methods were in good agreement and strengthened our interpretation of the individual results.

The spatiotemporal dynamics of the dominant water sources and flow paths explained how flow processes change from drier to wetter seasons in the Andean Páramo. A cascade of flow processes is representative for these ecosystems, resulting from the presence of high organic porous soils, a high frequency of precipitation, and the dynamic of the contributing area in the valley bottom, which connects the adjacent hillslopes to the channel network mainly under wet conditions. Rainfall, which is an end-member that represents young water, is a fundamental source to stream water year-round. The contribution of spring water, the oldest water, is higher during the drier season. Under wet conditions, water from the Andosols on the hillslopes contributes via the deeper soil horizons towards the Histosols near and in the lower riparian zone. The latter soils represented the dominant contributing water source to streamflow year-round, highlighting the importance of the riparian zone. Similarly, the large contributions of pre-event water during drier and wetter seasons lead to the same conclusion,

which infers that water from such a hydrologically active zone close to the stream plays a relevant role in runoff generation processes. Additionally, evidence of young streamflow during wetter seasons corroborates connectivity between landscape elements, explaining the influence of water from hillslopes.

The uncertainty that underlies some of the applied methods is often discussed (e.g., selection and number of end-members (Barthold et al., 2011), estimation of mean transit times, (Timbe et al., 2014)). Some studies might suggest focusing more on the uncertainty quantification of individual methods to increase the confidentiality in the obtained results. We used a different approach and applied an ensemble of methods, which enabled us to investigate the structural differences and resulting uncertainty of the various methods and reduce the epistemic uncertainty from our imperfect knowledge of the system. To our knowledge, this study is the first that used the EMMA, hydrograph separation and ITTPs methods to improve the understanding of the hydrological behavior of high mountain tropical catchments. This multi-method approach demonstrated that catchments with perennially humid climates (with drier and wetter periods) and almost stable hydrological conditions can still be characterized by varying inter-annual source contributions. Understanding of the hydrological functioning can be further improved by analyzing the spatial variability of source contributions within the catchment and by conducting studies to elucidate the contributions over short-time scales, e.g., during events.

Appendix A

Spatial geometry was applied to solve the problem of outliers in the four-end-member mixing model, and a scheme is presented in Fig. 3.8a. The stream sample SW plotted outside the tetrahedron that was confined by the 4 end-members EM1, EM2, EM3 and EM4. Assume that the contribution from EM4 is negative and therefore forced to be zero. SW' represents the orthogonal projection of SW onto the plane EM1 EM2 EM3.

A plane is a flat, two-dimensional surface in a three-dimensional space that has the equation

$$Ax + By + Cz + D = 0$$

$\overrightarrow{EM1\ EM2}$ and $\overrightarrow{EM1\ EM3}$ are vectors from the plane. The cross-product of two vectors results in a vector that is perpendicular to both and therefore normal $\vec{n}$ to the plane that contains them:

$$\overrightarrow{EM1\ EM2} = (EM2_{U1} - EM1_{U1},\ EM2_{U2} - EM1_{U2}, EM2_{U3} - EM1_{U3})$$

$$\overrightarrow{EM1\ EM3} = (EM3_{U1} - EM1_{U1},\ EM3_{U2} - EM1_{U2}, EM3_{U3} - EM1_{U3})$$

$$\overrightarrow{EM1\ EM2}\ X\ \overrightarrow{EM1\ EM3} = (A, B, C) = \vec{n}$$

Consequentially,

$$A = (EM2_{U2} - EM1_{U2})(EM3_{U3} - EM1_{U3}) - (EM3_{U2} - EM1_{U2})(EM2_{U3} - EM1_{U3})$$

$$B = (EM2_{U3} - EM1_{U3})(EM3_{U1} - EM1_{U1}) - (EM3_{U3} - EM1_{U3})(EM2_{U1} - EM1_{U1})$$

$$C = (EM2_{U1} - EM1_{U1})(EM3_{U2} - EM1_{U2}) - (EM3_{U1} - EM1_{U1})(EM2_{U2} - EM1_{U2})$$

$$D = -(A * EM1_{U1} + B * EM1_{U2} + C * EM1_{U3})$$

Consider the line in three-dimensional space through the point SW $(SW_{U1}, SW_{U2}, SW_{U3})$ and normal to $Ax + By + Cz + D = 0$. The parametric equations are

$$x = SW_{U1} + A * \lambda$$

$$y = SW_{U2} + B * \lambda$$

$$z = SW_{U3} + C * \lambda$$

The intersection of the plane and normal line that pass through the point SW produces SW':

$$\lambda = \frac{-(D + A * P_{U1} + B * P_{U2} + C * P_{U3})}{A^2 + B^2 + C^2}$$

The coordinates of the projected point SW' are

$$SW'_{U1} = SW_{U1} + A * \lambda$$

$$SW'_{U2} = SW_{U2} + B * \lambda$$

$$SW'_{U3} = SW_{U3} + C * \lambda$$

The fractions of the contributions for 3 end-members (reduction of Eq. 1 - Eq. 4 in the main text) are calculated for SW' following the equations by Christophersen et al. (1990).

If two end-members, such as EM4 and EM1, exhibit negative contributions, both are forced to be zero and the stream sample is projected on the line from EM2 and EM3 (Fig. 3.8b). The fractions of each end-member's contributions are inversely proportional to their distance to SW'. If three end-members exhibit negative contributions, the remaining end-member has a 100% contribution to the stream.

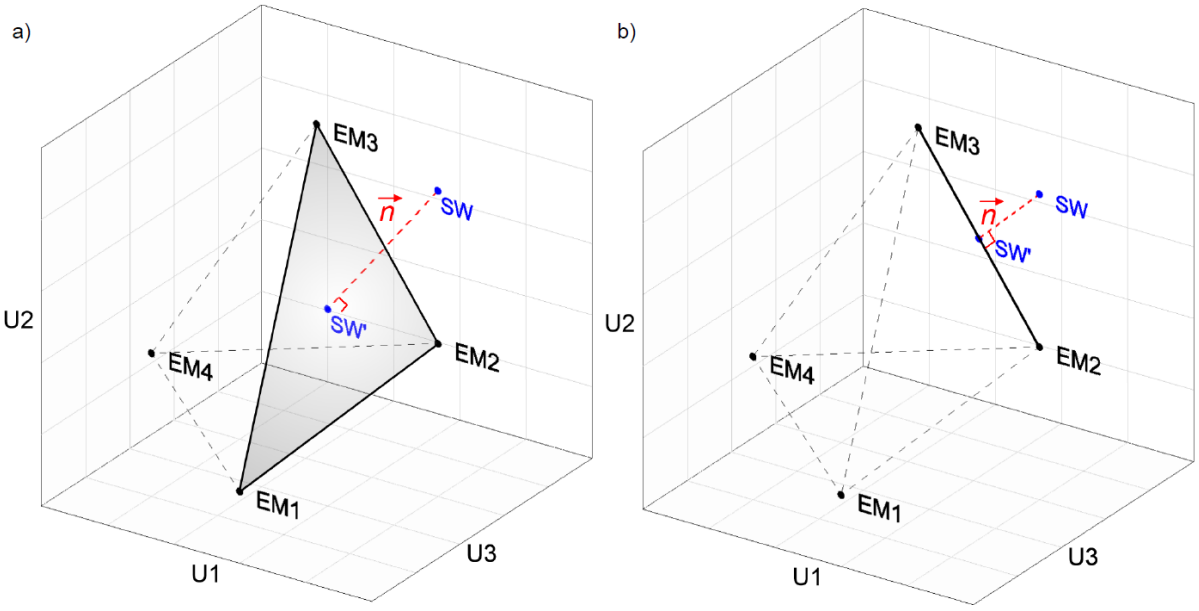

Figure 3-8. 3D diagram illustrating how a stream outlier SW is projected in a: (a) plane or (b) line formed by end-members using a spatial geometrical approach.

Acknowledgments

This research was funded by the Central Research Office (DIUC) of the Universidad de Cuenca through the projects “Identificación de las relaciones entre las propiedades biofísicas y la respuesta hidrológica en cuencas de páramo húmedo” and “Desarrollo de indicadores eco-hidrológicos funcionales para evaluar la influencia de las laderas y humedales en una cuenca de páramo húmedo”, Secretaría de Educación Superior, Ciencia, Tecnología e Innovación (SENESCYT 112-2012), and the German Research Foundation (DFG, BR2238/14-1). The authors would like to thank Matthias Sprenger for his comments on an earlier draft of the manuscript and the staff of Loma Larga Project, Camila Silva, Heike Weller, Irene Cárdenas, Ryan Padrón, Patricio Lazo and students from the Faculties of Civil Engineering and Environmental Engineering of the Universidad de Cuenca for the laboratory work and logistic support during the field campaigns. We are especially grateful for the constructive comments that were provided by the reviewers, which greatly improved the quality of the manuscript.

Supporting data are included as six tables in an .xlsx file.

4 SPATIO-TEMPORAL DYNAMICS OF RUNOFF SOURCES AND EVOLUTION OF STORM EVENTS IN PÁRAMO CATCHMENTS

Abstract

To conceptualize the hydrological functioning of headwater catchments, knowledge about the spatial and temporal dynamics of water quality is needed. This study assessed the consistency of four catchment outlet end-members across five tributaries using diagnostic statistics of stream chemistry. Calculated the contributions of the end-members to streams on the basis of End Member Mixing Analysis (EMMA), and analyzed the evolution of the stream chemistry during storm events. Hydro-chemical data of streams and end-members were sampled biweekly and in event-resolution for three storm events in 2013 and 2014 within a tropical mountain catchment in the Ecuadorian Andes.

The results indicate that the set of end-members (rainfall, spring water, and soil water from Histosols and Andosols) largely explains the catchment's behavior. Source dynamics across the nested system reveal that water from Andosols and Histosols govern the runoff generation during storm events, with average contributions of 35% each. Rainfall contributes around 20% and spring water10%. Water from Andosols presents a higher impact in the tributaries than in the catchment outlet. Clockwise hysteresis patterns in the upper catchments and counterclockwise in the lower catchment suggest opposite evolution during storms indicating different interaction of end-members. Differences in hydro-metrical characteristics of storm events have a relatively negligible impact on the end-members' contribution. Large hydro-chemical data sets including event-resolution provide detailed insight to spatially-distributed hydrological processes on these water towers of the Andes.

Submitted to Water Resources Research as:

Correa, A., L. Breuer, P. Crespo, R. Célleri, J. Feyen, C. Silva, and D. Windhorst, (2017), Spatio-temporal dynamics of runoff sources and evolution of storm events in Páramo catchments, Water Resour. Res.

4.1 INTRODUCTION

Understanding the runoff generation and water source dynamics of headwater mountainous catchments is scientifically and from management point of view a central issue. This is even more the case for remote, mountainous catchments in the Andean Páramo, where these ecosystems can be considered sentinels for climate change (Dangles et al., 2017) and act as water towers, in countries such as Venezuela, Colombia, Ecuador, and Peru. Mountainous headwater catchments in the Páramo typically present two dominant landscape types: hillslopes and riparian zones, each with different hydrological behavior (Camporese et al., 2014; Penna et al., 2016). The riparian zone presents nearly saturated conditions (Mosquera et al., 2015) and acts as a buffer, through which water from the most freely-draining hillslopes passes and contributes to streamflow (McGlynn and McDonnell, 2003; Penna et al., 2016; Uchida et al., 2008). Analysis of g the influence and interaction of the riparian zone on the catchment functioning provides essential insights of streamflow generation processes at different spatial and temporal scales (Brown et al., 1999; Capell et al., 2012; Soulsby et al., 2006). In Andean Páramo, authors found a crucial influence of the riparian zone on the runoff generation and the dominance of pre-event water on catchment runoff behavior (Correa et al., 2017; Mosquera et al., 2016a). In line herewith, Correa et al. (2016) reported the flash response of runoff during storm events and attributed the quick-flow event-component (avg. = 33%) to shallow subsurface lateral flow in the valley bottom.

Conceptualization of the spatial and temporal contribution of water from different landscapes units in runoff generation exploring the hydrochemical composition of the runoff water attracted recently much attention. Based on hydro-chemical mixing models, e.g., end-member mixing analysis (EMMA) (Christophersen and Hooper, 1992), researchers improved tools that help elucidate the hydrological functioning of catchments and quantified the average contributions of dominant runoff sources (end-members) to streams water in a range of scales (Barthold et al., 2010; Correa et al., 2017; Hooper, 2003; Liu et al., 2004). More recent studies focused on comparing the stream chemistry of multiple sub-catchments to identify any similarities or differences in water chemistry, assessing whether the same processes and end-members control different streams (Hooper, 2003; James and Roulet, 2006). Furthermore, special attention was given to analyze the stream chemistry evolution of storms and the relative position of end-members in the storm-mixing subspace (Barthold et al., 2017; Inamdar et al., 2013).

In all EMMA approaches, the hydro-chemical mixing of end-members tries to mimic the hydro-chemical composition of the stream (Christophersen et al., 1990). It therefore relies on the assumption of the conservative behavior of tracers and linear mixing processes (Hooper, 2001). These end-members, defined as functional units of catchments, are typically identified by plotting all potential water sources in the stream mixing space (U-space) and are selected based on their ability to completely circumscribe the stream data (Levia et al., 2011). The notable point of this methodology is that it takes into account the variability of multiple tracers data sets, thus reducing the probability of missing sources and, therefore, the risk of false conclusions about catchment functioning (Barthold et al., 2011, 2017).

To compare hydro-chemical signatures of sub-catchments with the catchment outlet, chemical data from tributaries is projected into the U-space generated by the main stream (Hooper, 2003). Scalar measures of fit define the ability of a main stream mixing model to predict the stream chemical signatures of tributaries (Hooper, 2003; James and Roulet, 2006). The model's capability further suggests the existence of a Representative Elementary Area (REA) (James and Roulet, 2006), which is defined as a threshold scale (e.g. the smallest sub-catchment) beyond which the variability of stream chemistry is reduced (Wolock et al., 1997; Wood et al., 1988).

Insights to conceptualize the storm chemistry evolution can be obtained by analyzing hysteresis patterns, shapes, and directional shifts of storms within the U-space (Levia et al., 2011). Additionally the relative position of stream data with respect to the end-members in the U-space qualitatively define their influence throughout the different storm hydrograph stages (rising limb, falling limb, and recession) (Inamdar et al., 2013).

Analysis of storm hysteresis patterns based on stream chemistry versus discharge have been applied by Evans and Davies (1998) and have drawn attention in recent years (Engel et al., 2016; Fröhlich et al., 2008; Lloyd et al., 2016; Tunaley et al., 2017). Authors focused on predicting the influence and sequence of runoff sources based not only on the stream chemistry versus the discharge approach, but mainly on the stream chemistry in the U-space (Barthold et al., 2017; Inamdar et al., 2013). Inamdar et al. (2013) showed a counterclockwise rotation in all analyzed storm events and hysteresis loops that varied with hydrological conditions, from tighter in wet, well-connected conditions to wider in dry, disconnected conditions. In another study, Barthold et al. (2017) presented relatively open hysteresis loops

in the analyzed storms by only monitoring in wet conditions, pointing out that all sources are fairly distinct and that only limited mixing occurred.

In this context, hydro-chemical data is particularly valuable when used in conjunction with independently-measured hydro-metric data (Buttle, 1994; Inamdar et al., 2013). Several authors used the latter to separate, for example, seasons or independent rainfall-runoff events, where end-members and their relative contributions can be analyzed (Ali et al., 2010; Correa et al., 2017; Morel et al., 2009). Other authors, such as Inamdar and Mitchell (2007), Ali et al. (2010) and Inamdar et al. (2013) showed important variations of end-members' contributions to streams depending on the size of the storm event and the antecedent moisture conditions.

The research presented herein builds on recent work carried out in the same study area in the Ecuadorian Andes (Correa et al., 2017). These authors used multi-tracer sets of stream solutes to assess the temporal dynamics of water sources via EMMA and defined four end-members to represent the hydrological system. The dominant end-members were rainfall, spring water, and water from the bottom soil layers of Histosols and Andosols. Water from Histosols in the riparian zone was the most important source year-round. They also highlighted the influence of water from hillslopes during wetter conditions, an increase of spring water contribution during drier conditions, and homogeneous rainfall contribution throughout the year. However, Correa et al. (2017) limited their analysis to temporal dynamics of the rainfall-runoff process at the outlet, only comparing dry and wet seasons. Here, we take a more spatially-distributed EMMA into account and particularly analyzed the water provenance during storm events.

Data collected in the period 2013- 2014 in the Zhurucay River Ecohydrological Observatory, a high tropical mountainous catchment in Southern Ecuador, were used to reach the following specific objectives: 1) assess the consistency of stream chemistry from tributaries with the stream outlet (site comparison); and 2)calculate the end-member contributions and stream evolution during storm events.

4.2 DATA AND METHODS

4.2.1 STUDY AREA

The Zhurucay River Ecohydrological Observatory (Fig. 4.1) is located in southern Ecuador (3°4′38″S, 79°15′30″O). The observatory encompasses a tropical fourth-order headwater

catchment (7.53 km^2), which ultimately drains into the Pacific Ocean. The mean annual precipitation is 1,345 mm (2011-2014), of which 15% is fog water (Padrón et al., 2015), and the estimated annual reference evapotranspiration is 723 mm (Córdova et al., 2015). Mean annual discharge is 864 mm yr^{-1} with an average runoff coefficient (RC) of 0.68 (Mosquera et al., 2015). This coefficient can increase to 0.80 during isolated storms (Correa et al., 2016). The storm events are characterized by peaks that range from 50 to 700 l s^{-1} km^{-2}, most of which fall between 150 to 400 l s^{-1} km^{-2}. The mean air temperature in Zhurucay River Ecohydrological Observatory is 6°C. Temperatures below 0°C are rarely and occur only for limited time, a couple of hours, preventing freezing. The elevation range varies between 3,505 and 3,900 m a.s.l. The glacial-formed valley has an average slope of 17%, in some places reaching 40%.

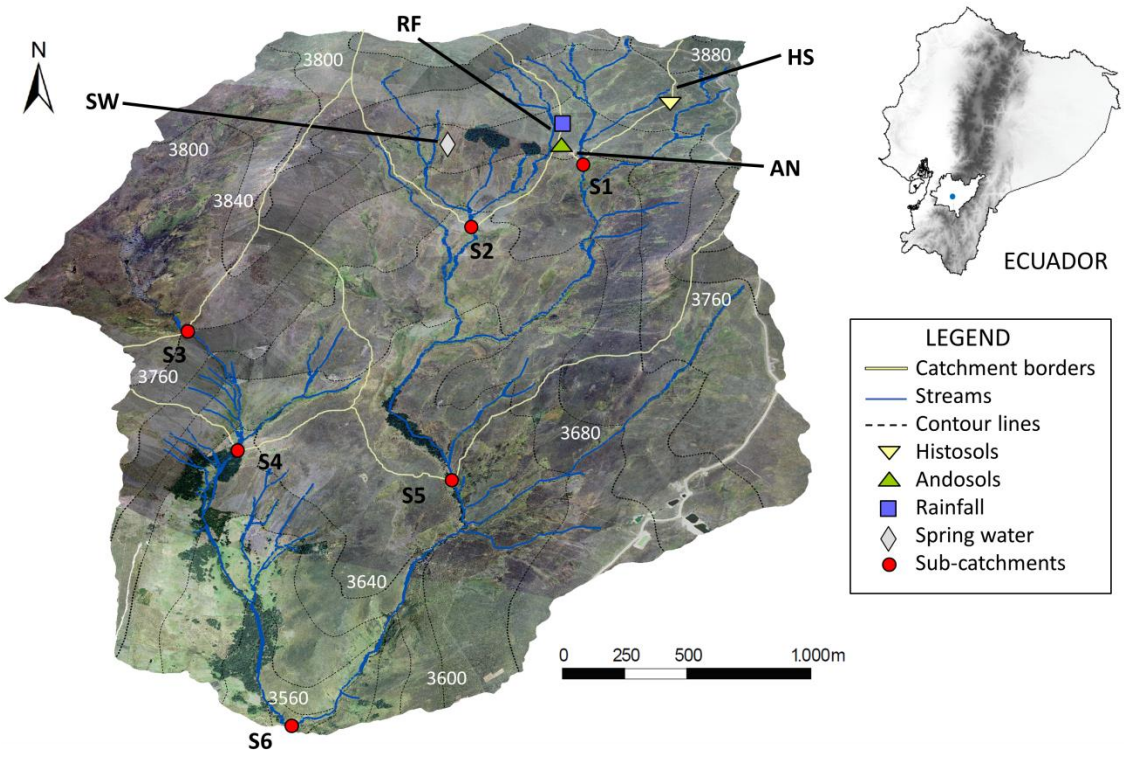

Figure 4-1. The Zhurucay River Ecohydrological Observatory located in southern Ecuador, showing sites of water sampling: HS (Histosol) and AN (Andosol) represent soil sampling sites; RF, rainfall; SW, spring water, S1-S6 stream monitoring sites.

The geology of the catchment is mainly dominated by the Quimsacocha Formation (56%) (basalt flows with plagioclase, feldspar, and andesitic pyroclastic deposits) (Pratt et al., 1997), followed by the volcano-sediment Turi Formation (31%) (accumulation of a thick sequence of conglomerates, fluvial sands, clays, tuffs, and volcanic breccia) (Coltorti and Ollier, 2000) on the valley bottom. Both formations belong to the late Miocene geological period. The

remaining 13% belongs to Quaternary deposits (glacial moraines), generally located in escarpments and steep slope areas (Table 4.1).

The two dominating soil types in the study area, formed from the volcanic ash of the Sangay and Tungurahua volcanoes (Quichimbo et al., 2012), are Histosol (24%) and Andosol (72%) soils (IUSS Working Group WRB, 2015). Both soil types are rich in organic matter (on average 380 g kg^{-1}), strongly acidic (pH values of 4.8), and extremely porous with high infiltration and water retention capacity. The Histosols are located at the foot of the hillslopes and at the bottoms of valleys present nearly saturated conditions year-round (Buytaert and Beven, 2011; Mosquera et al., 2015) and are mainly covered by cushion plants. These soils contain a high fraction of non-decomposed plant fibers in the top organic horizon (Beck et al., 2008). Andosols are general characterized by less-developed horizons and mainly cover hillslopes, where vegetation is dominated by tussock grass. The organic layer consists of short-range-order minerals and organo-metallic complexes. Both soils overlay an organic mineral interface horizon. The saturated hydraulic conductivity is higher in the Histosols than in the Andosols, declines in both soils from the shallow to deeper horizons (Histosols 1.55 cm h^{-1} to 0.72 cm h^{-1} and Andosols 0.89 cm h^{-1} to 0.28 cm h^{-1}), and is inversely related to the bulk density (Mosquera et al., 2016a). Shallow organic Leptosols (4%) on steep slopes cover the remaining catchment area. Land use is limited to extensive grazing with low animal density. Physiographic characteristics are presented in Table 4.1.

Table 4-1. Catchment characteristics of the nested sub-catchments (TWI = topographic wetness index)

Catchment	Area	Perimeter	Altitude (m asl)		Slope (%)		Mainstream length	Drainage density	Drainage slope	TWI
	(km²)	(km)	Range	Avg	Range	Avg	(km)	(km/km^2)	(%)	(-)
S1	0.38	3.06	3,770 – 3,900	3,835	0 - 30.73	24	0.79	6.92	1.9	12.75
S2	0.65	3.23	3,715 – 3,850	3,782	0 - 25.35	18	1.28	6.76	2.0	12.46
S3	1.22	5.54	3,771 – 3,830	3,820	0 - 25.52	12	0.40	0.33	1.7	10.00
S4	1.72	7.20	3,640 – 3,880	3,760	0 - 34.42	16	0.85	1.70	2.2	13.12
S5	3.28	8.09	3,676 – 3,900	3,788	0 - 45.80	18	3.29	4.21	1.8	8.23
S6	7.53	12.09	3,505 – 3,900	3,702	0 - 45.80	17	4.63	3.26	1.9	16.72

Catchment	Distribution of soil types (%)			Geology (%)			Land cover (%)			
	Andosols	Histosols	Leptosols	Quarternay deposits	Turi	Quimsacocha	Tussock grass	Cushion plants	Polylepis forest	Pine forest
S1	83	15	2	33	1	66	87	13	0	0
S2	76	20	4	1	48	51	79	18	3	0
S3	37	59	4	13	0	87	35	65	0	0
S4	50	45	5	14	14	72	54	46	0	0
S5	74	22	4	20	30	50	73	24	1	2
S6	72	24	4	13	31	56	72	24	2	2

4.2.2 HYDRO-METRIC DATA

A sampling network of six, nested sub-catchments (0.38–7.53 km^2) was established, and their hydro-metric characteristics are presented in Table 4.2. The sub-catchments were instrumented either with a custom build V-notch weir (S1 to S5) or a rectangular weir (S6) and equipped with a water-level sensor (Diver, Schlumberger, NC, USA). The water level was recorded at 5-min intervals. The theoretical Kindsvater-Shen equation was used to convert the water level into discharge, and the discharge equation was calibrated following the Moore's technique (2004).

Precipitation was measured 1 m above ground surface using four tipping-buckets with a resolution of 0.2 mm (RG3-M Onset, MA, USA). Precipitation time series were corrected to account for fog (+15 %) (Padrón et al., 2015). The area-weighted precipitation was calculated for each sub-catchment by applying the Thiessen polygon method.

Hydro-metric characteristics of storm events were calculated and are presented in Table 4.2. From specific discharge measurements, we derived respectively the amount of specific discharge (amount; mm), the specific peak flow rate (peak; l s^{-1} km^{-2}), and the average specific discharge for a 24 h period prior to the event (AQ24hr; mm hr^{-1}). From the precipitation data we derived the total amount (amount; mm), the 5 min maximum intensity (5 min Intensity; mm), and the antecedent precipitation index (API) as total amount of precipitation fallen during the 7 and 14 days preceding the event (API7, API14; mm). APIs and AQ24 were used to characterize the antecedent moisture conditions in the catchment prior to the storm events (Inamdar et al., 2013). Additionally, the runoff coefficient (RC) was determined as the ratio of discharge and total precipitation amount and the time lag, as the time between the maximum precipitation and specific peak discharge (LAG; h).

Table 4-2. Hydro-metric variables of the six nested sub-catchments (2013) and the 3 selected storm events in 2013-2014

		Specific discharge					
		S1	S2	S3	S4	S5	S6
Amount[a] (mm yr^{-1})		588	688	710	699	689	756
Amount (mm)	E1	9.3	10.1	10.2	9.6	10.5	10.4
	E2	2.5	2.6	3.1	2.5	3.3	4.0
	E3	8.9	10.4	13.3	12.3	11.3	13.3
Peak ($l\ s^{-1}\ km^{-2}$)	E1	309	500	190	342	301	202
	E2	96	116	56	66	106	115
	E3	154	425	270	296	357	320
AQ24 (hr)	E1	27	29	65	10	35	38
	E2	4.2	9.6	11.0	7.0	11.0	12.8
	E3	12.2	12.6	15.1	8.7	13.4	21.4
		Precipitation					
Amount[b] (mm yr^{-1})		1107	1095	1052	1039	1069	1084
Amount (mm)	E1	11.7	11.7	11.4	11.2	11.7	11.1
	E2	6.5	6.6	5.5	5.8	7.0	6.9
	E3	17.9	19.4	22.7	23.3	21.3	22.1
5 min Intensity (mm)	E1	2.2	2.1	1.8	2.1	1.9	2.0
	E2	1.0	0.9	0.6	0.7	0.8	0.7
	E3	1.6	1.6	3.0	2.9	1.9	2.0
API7 (mm)	E1	30.2	30.0	27.4	26.6	29.8	30.9
	E2	16.9	17.4	23.2	22.5	18.8	21.0
	E3	25.9	26.2	30.5	30.1	27.4	29.9
API14 (mm)	E1	51.0	50.1	42.8	38.4	40.8	44.8
	E2	21.0	21.4	27.1	26.3	22.7	25.0
	E3	55.6	56.4	65.5	65.9	61.0	70.3
RC[c] (-)		0.53	0.63	0.67	0.67	0.64	0.70
RC (-)	E1	0.79	0.86	0.89	0.86	0.9	0.94
	E2	0.38	0.39	0.56	0.43	0.47	0.59
	E3	0.50	0.54	0.59	0.53	0.53	0.6
LAG (h)	E1	2.8	2.3	7.4	2.2	1.9	3.5
	E2	1.0	2.0	6.2	2.8	2.0	2.6
	E3	1.6	2.5	6.2	1.5	1.9	3.3

[a] Total annual amount of runoff; [b] Total annual amount of precipitation; [c] Runoff coefficient E1 = storm event 18-21 March 2013; E2 = storm event 1-2 March 2014; E3 = storm event 15-18 March 2014.

4.3 WATER SAMPLING COLLECTION AND LABORATORY ANALYSES

From March 2013 to April 2014, stream and end-members water samples from the six nested headwater catchments (S1-S6) and the end-members were collected, biweekly and during two

field campaigns in (March 2013 and March 2014) on an event-based resolution (Fig. 4.1). End-members included rainfall (RF), soil water from the bottom layer of Andosol (AN) and Histosols (HS) and spring water (SW). The event-based monitoring included three storm events with 5-240 min resolution in the streams, except for catchments S2 and S4, where, only two storms were monitored due to logistic reasons. An automatic water sampler (3700 Full-Size Portable Sampler, ISCO, NE, USA) was used at the catchment outlet (S6), and water samples were collected manually at all other tributaries (S1-S5). Water samples from end-members were collected in variable time steps, depending on the logistic access to sites and the required amount of water per sample (100 ml).

Circular funnels (diameter = 16 cm) connected to polypropylene collectors were used to collect rain water (RF). Soil water from AN and HS was sampled using wick samplers below the surface, at 0.65 m and 0.75 m, respectively (Boll et al., 1992). All water samples were filtered *in situ* (0.45 µm polypropylene membrane filters, Puradisc 25PP Whatman Inc., Clifton, NJ, USA), acidified with purified nitric acid (pH < 2) to avoid trace metal precipitation and adsorption, and stored in acid-washed 100 ml polypropylene bottles.

Electrical conductivity (EC) of each sample was measured using a portable multiparameter instrument (pH/Cond 340i, WTW, Weilheim, Germany) with instrumental precision of 0.1 µS cm^{-1}. EC results were established at 25°C by nonlinear temperature compensation.

Thirteen-solutes concentration, defined as conservatives by Correa et al. (2017) including Na, Mg, Al, Si, K, Ca, Rb, Sr, Ba, Ce, V, Y, and Nd, were determined at the Institute for Landscape Ecology and Resource Management of the Justus Liebig University using an ICP-MS (Agilent 7500ce, Agilent Technologies). Results were reported as parts per billion (ppb) as the mean of two consecutive measurements (see Fig. 4.2 and Table 4.3). Certified reference material (NIST 1643e – SLRS4 and NIST 1640e – SPSSW2) and internal calibration standards were measured to ensure the analytical quality. ring water, S1-S6 stream monitoring sites.

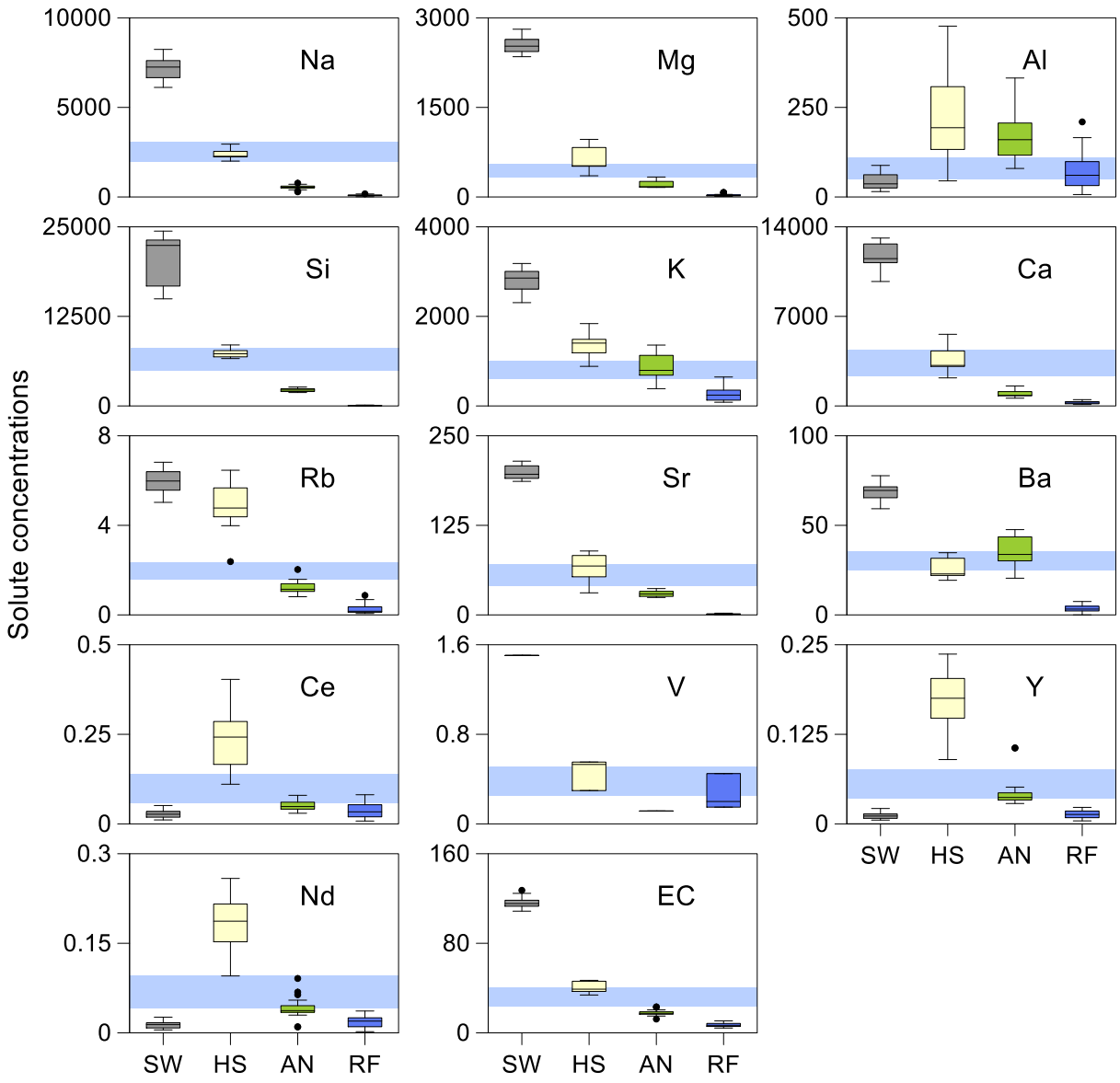

Figure 4-2. Boxplots of solute concentrations of end-members for the study period 2013–2014, concentrations in (ppb) and EC in (µS cm^{-1}) (the central bar in the box represents the median; notches represent the 95% confidence intervals; whiskers 1.5 times the interquartile range and circles represent outliers). SW, spring water; HS, Histosol; AN, Andosol; RF, rainfall. Light blue bars represent the 95% confidence intervals of stream data (including: S1, S2, S3, S4, S5 and S6).

Table 4-3. Median and standard deviation of stream solutes at S6 and tributaries (S1, S2, S3, S4 and S5) for the study period 2013-2014. Element concentrations in (ppb) and EC in (µS cm^{-1}).

		Na	Mg	Al	Si	K	Ca	Rb	Sr	Ba	Ce	V	Y	Nd	EC
S1	Median	2568	385	50.9	7359	682	3767	1.9	60.7	27.1	0.05	0.18	0.03	0.04	32.8
n=65	Std	752	93	27.9	2344	152	1230	0.4	14.6	6.0	0.01	0.04	0.01	0.01	7.0
S2	Median	2982	684	110.1	7768	972	4259	2.2	72.4	39.2	0.15	0.60	0.07	0.11	38.8
n=74	Std	1454	444	48.9	4253	493	2261	0.9	36.4	9.3	0.06	0.26	0.03	0.04	23.9
S3	Median	1168	305	96.9	2580	475	1634	0.5	27.7	33.4	0.13	0.15	0.02	0.03	16.5
n=38	Std	197	834	22.7	482	72	486	0.2	7.8	12.9	0.02	0.04	0.01	0.01	4.1
S4	Median	2389	371	83.3	6190	641	2749	1.6	46.0	26.9	0.08	0.31	0.05	0.07	29.1
n=84	Std	896	133	28.9	2287	197	1127	0.4	16.7	5.4	0.04	0.09	0.01	0.02	9.7
S5	Median	2465	411	83.6	7503	844	3168	2.1	57.6	32.8	0.11	0.35	0.06	0.08	31.3
n=91	Std	780	150	43.5	2545	276	1214	0.6	16.9	4.6	0.05	0.09	0.02	0.03	10.4
S6	Median	2228	391	88.1	6276	819	2574	2.0	47.3	24.4	0.10	0.46	0.08	0.11	27.6
n=125	Std	796	120	44.1	1984	258	762	0.4	15.8	3.8	0.06	0.16	0.03	0.04	9.5

4.3.1 SITE COMPARISON

Conservative solutes and EC were used as set of tracers to perform a site comparison following Hooper's methodology (2003), which only requires stream data. The analyzes was performed in a three-dimensional space (U3-space) (Correa et al., 2017). The main outlet of catchment (S6) was considered as the *reference site*, being a well-characterized site against which the chemistry of the *other sites'* (S1-S5) chemistry can be compared (Hooper, 2003; James and Roulet, 2006). Principal component analysis (PCA) was applied to the data from the main outlet, and three eigenvectors were obtained. The *other sites* were projected into the U3-space generated for the main outlet. Scalar measures of fit as relative bias (RBias) and relative root-mean-square error (RRMSE) were computed from residuals between the projected and original values (Hooper, 2003). Solute measures were scaled by the mean concentration of each solute to make them unit less. The evaluation of scalar measures of fit of one site into the mixing subspace of a different site, permits an assessment of the consistency of controlling end-members across sites (Hooper, 2003). Thresholds of ±50% and 15% for RBias and RRMSE, respectively, were established to consider one site fitting into the mixing subspace of the *reference site*.

The mathematical procedure (Hooper, 2003) for the errors residual analysis is described as follows: X represents an (n x p) matrix of stream chemical data consisting of n samples on which p solutes were measured, X^* is the matrix of standardized values, where $\bar{x}_j$ is the mean of the j^{th} solute and s_j its standard deviation, each element of this matrix is x_{ij}^* (Eq. 1).

$$x_{ij}^* = \frac{(x_{ij} - \bar{x}_j)}{s_j} \quad (1)$$

V represents the matrix formed by the first m eigenvectors from the PCA analyses, V^T its transpose and $\hat{X}^*$ the orthogonal projection of X^*.

$\hat{X}^*$can be calculated with Eq. 2.

$$\hat{X}^* = X^* V^T (V V^T)^{-1} V \quad (2)$$

$\hat{X}$ represents the destandardized $\hat{X}^*$ and each element of this matrix $\hat{X}$ is $\hat{x}_{ij}$ (Eq. 3)

$$\hat{x}_{ij} = \hat{x}^*_{ij} s_j + \bar{x}_j \quad (3)$$

The residuals errors (E) between the projected and original data were calculated with Eq. 4, as:

$$E = \widehat{X} - X \quad (4)$$

4.3.2 END-MEMBERS' CONTRIBUTION AND STREAM CHEMICAL EVOLUTION

The suggested four end-members that explain the stream water chemistry were used to calculate the end-member fractions during storm events. Their weighted medians and standard deviations were orthogonally projected into the mixing U3-space defined by the PCA of the stream outlet samples and the percentage of contribution of each end-member to streamflow was calculated according to Christophersen et al. (1990).

The median concentrations of the end-members should circumscribe the streamflow data, and the percentage of contribution should sum up to 100%. Negative contribution of an end-member suggests that stream observations fall outside of the end-member's domain as result of input data uncertainty (Christophersen and Hooper, 1992). According to Liu et al. (2004), these points were projected onto the domain space, forcing the negative fraction to be zero and the other contributions to be a mixture of the remaining end-members. In this study, an extension of the Liu et al.'s (2004) methodology for the U3-space (Correa et al., 2017) was applied and the samples were projected onto the tetrahedron defined by the four selected end-members.

Stream chemical evolution of storm events was analyzed in the U3-space, based on hysteresis patterns, shapes, and directional shifts of stream data. Likewise, the relative positions of stream data, with respect to end-members, was used to qualitatively identify periods of higher influence of those on storm events (Barthold et al., 2017; Inamdar et al., 2013).

4.4 RESULTS

4.4.1 HYDRO-METRICAL OBSERVATIONS

The annual runoff ranged from 588 mm yr^{-1} at S1 to 765 mm yr^{-1} at catchment outlet S6. Similarity, the RC varied from 0.53 to 0.7 for the sub-catchments. The annual precipitation for the study period (avg. = 1107 mm yr^{-1})was lower than the mean value reported by Padrón et al. (2015). Values of annual precipitation were slightly higher in the upper, and lower in the western sub-catchments in relation to S6.

Event 1 (E1: 18-21 March 2013) presented a similar amount of runoff as event 3 (E3: 15-18 March 2014) and on average a 3.5 times higher amount than event 2 (E2: 1-2 March 2014) for all sub-catchments. Peak values ranged from 500 to 190 l s^{-1} $km^{-2}$for E1, 116 to 56 l s^{-1} km^{-2} for E2, and 425 to 154 l s^{-1} km^{-2} for E3. S2 presented the highest peak values for all storms. In E1, the precipitation amount presented a homogeneous spatial distribution over the entire catchment. S3 and S4 showed slightly lower precipitation values in E2, similar to S1 and S2 in E3. On average, 11 mm of precipitation was recorded during E1, 6 mm during E2, and 21 mm during E3. Average 5 min intensities of 2 mm were reported for E1 and E3, and 0.8 mm 5 min^{-1} for E2. AQ24 and API7 presented the highest values for E1, followed by E3 and E2, except for S4, where E3 depicts the maximum API7. E3 showed the highest API14 of all the storm events. Average RCs of 0.87, 0.45, and 0.54 were reported for E1, E2, and E3, with minimum values in the headwater catchment and maxima in the main outlet. LAG values of 3.3 h for E1, 2.6 h for E2, and 2.8 h for E3 were reported. S3 always presented the longest LAG times, being on average 3 times longer than the LAG times for all other sub-catchments.

4.4.2 HYDRO-CHEMICAL OBSERVATIONS

Boxplots of fourteen geochemical tracers from the streams and end-members are depicted in Fig. 4.2. Similar patterns of end-members were evident for Na, Mg, Si, K, Ca, Rb, Sr, Ba, and EC. SW generally presented the highest concentrations, with on average three times higher medians than for HS. Differences between HS and AN were smaller but still evident, and AN presented the lowest variability in the distribution of data in general. We found higher median value and a larger variability for AN than for HS only in the case of Ba. In all cases, RF showed the smallest concentrations and lowest variability of all end-members. For V, end-

members followed a similar pattern, with the exception that the median of RF was higher than the median of AN and the almost non-existent variability of concentrations for SW and AN. By analyzing the entire distribution of the end-members (boxplots) in relation to the 95% confidence interval of all stream data (blue ribbon in Fig. 4.2), SW always plotted considerably above of the stream data ribbon. RF was commonly below, touched the blue ribbon in case of K, and overlapped with it in the case of V. AN almost always plotted below, except for K and Ba, where the mentioned end-member superposed the confidence interval. HS overlapped the stream sector, with the sole exception of Rb, where the concentration of HS was considerably higher.

In the cases of Ce, Y, and Nd (rare earth elements), the end-members presented a different pattern. HS showed a wider distribution in relation to the remaining sources and the highest median concentration, followed by AN, RF, and SW. In contrast with the pattern described above, SW always plotted below the stream data ribbon and presented similar median values than RF. AN overlapped the stream data confidence interval. The end-members followed the same arrangement for Al, with the difference that AN presented a wide distribution of concentrations and plotted above the stream data. The stream data ribbon was superposed by RF.

4.4.3 SITE COMPARISON

The three-dimensional mixing space defined by the stream data from the *reference sit*e (main outlet S6) explained 59.6%, 19.7%, and 7.4% of the variance for the three principal components U1, U2, and U3. The five upstream sub-catchments (S1-S5) were projected into the previously-mentioned space. Residuals for each sub-catchment were computed, and the corresponding RBias and RRMSE as scalar measures of fit are presented in Fig. 4.3. The RBias (Fig. 4.3a) and RRMSE (Fig. 4.3b) values of the upstream sub-catchments can be compared to S6 based on the height of the bars. As expected, S6 exhibits no bias, and has the lowest RRMSE values (2%) in relation to the projected upstream sub-catchments. Fig. 4.3a shows that S5, located in close vicinity to S6, gives the best fit with regard to RBias, showing a maximum of 20% for V and -20% for Ce, followed by S4 (33% for Ce). In the upstream sub-catchments, fits deteriorate for S2 (38% for Ce) and S1 (48% for V). In general, for the mentioned sub-catchments, the RBias indicates that stream water concentrations are over-

predicted (positive values) in the case of V and under-predicted (negative values) in the case of Ce. Solutes such as Na, K, Sr, Ba, Y, and Nd are generally predicted more precisely, being randomly over- or under-predicted. Stream concentrations of Si and EC presented the smallest values therefore they are the best-predicted solutes. Fig. 4.3b depicts similar patterns. The lower sub-catchments, S5 and S4, fit best into the mixing space of the *reference site*, with maximum RRMSE values of 5% for V, followed by sub-catchment S2 (6% for Ce) and S1 (12% for V). Overall, Ce, V, and Al presented the highest RMMSEs values.

Both bar-chart plots, Fig. 4.3a & b, clearly depict lack of consistency for the northwestern part of the catchment (S3). Here, RBias and RRMSE reached values one order of magnitude higher than all other sub-catchments, with 178% and 50%, respectively. Particularly in the case of Rb, stream concentrations are largely over-predicted. In S3 (Fig. 4.3a), solutes Rb, Y (over-predicted), Ce, and Al (under-predicted) exceeded established thresholds for RBias, and Rb, Ce, and Y for RRMSE (Fig. 4.3b).

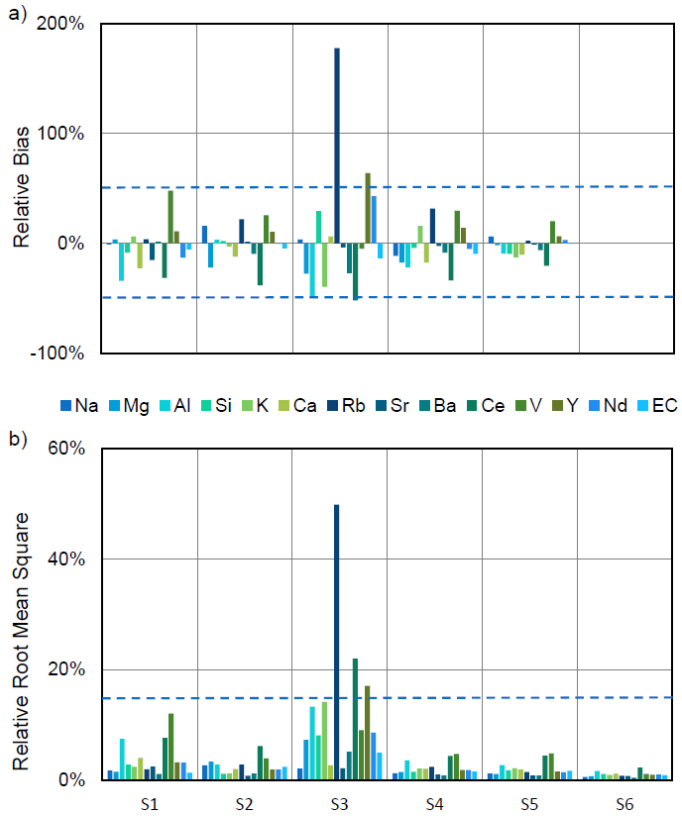

Figure 4-3. Diagnostic statistics for tributaries (S1-S5) projected into three-dimensional mixing space of the main stream outlet (S6). Figures 4.3a and 4.3b show the projected Relative Bias (RBias) and Relative Root Mean Squared Error (RRMSE), respectively. Blue dotted lines represent thresholds, i.e. ±50% for RBias and 15% for RRMSE.

4.4.4 END-MEMBERS INFLUENCE ON STORM EVENTS

As outlined above, three storm events were analyzed to improve our understanding of the rain-fall runoff generation. From the potentially eighteen cases (6 sub-catchments x 3 events), thirteen storm events were considered to characterize the influence of end-members on stream water mixing under extreme conditions (Fig. 4.4). S3 was excluded from the analysis due its lack of consistency with the *reference site*, and consequently, it is unlikely that the selected end-members control this sampling site.

For all the considered storm events, one of the soil end-members (AN or HS) was the highest source contributor (AN in the sub-catchments S1, S4, and S5, and HS in S6). HS in S6 presented on average two times higher values than the succeeding contributor. SW was the lowest contributor in the majority of cases, except for S2 (the geographically closest sub-catchment to SW).

During event E1, RF presented similar contributions (25% to 30%) for all sub-catchments. AN, the highest contributor for the tributaries, reached around 40% and only 25% at the outlet, where HS presented 44%. SW contributions were always lower than 15%. In E2, the increases of HS contributions in relation to E1 (increase on average 15%) were evident in the majority of sub-catchments, except for S1. During this event, AN and RF were the most-influencing end-members in S1 and S4. Contributions of HS during E3 were very similar to those in E1 for the sub-catchments S5 and S6. Overall, patterns in end-member contributions were rather stable, thus following the same arrangement when comparing events for each sub-catchment.

The end-member hydrograph separation showed an influence of RF throughout the events in the majority of cases, with higher impacts in falling limbs, except for S2, where the influence is negligible in the mentioned period. Soil end-members contributed during the entire events in the same manner as SW, but the latter with very small overall contributions.

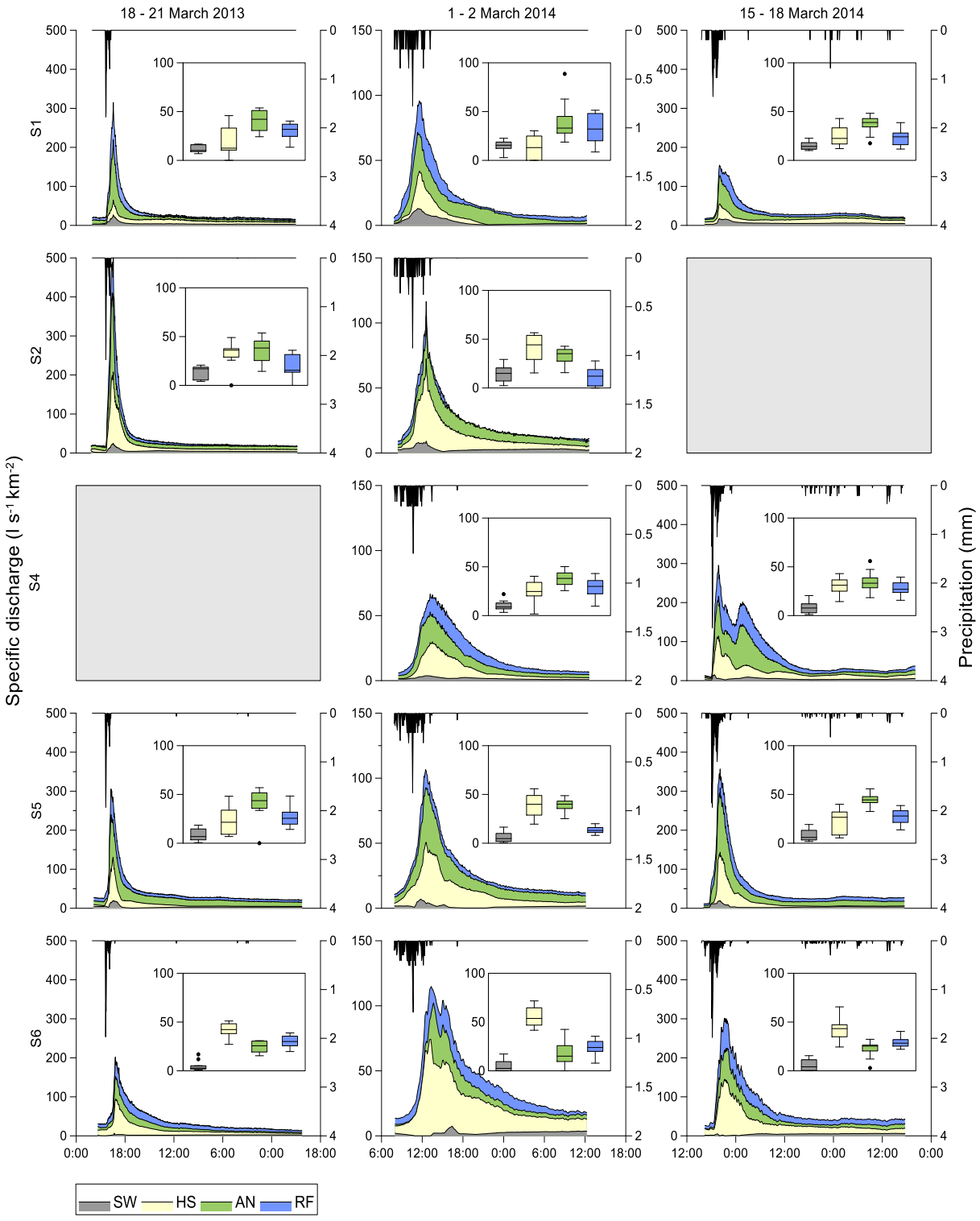

Figure 4-4. Hydrograph separation with end-member contributions during three storm events in the nested catchment system. Inlet boxplots show the percentage of end-member contributions. Estimation of end-member contribution was not possible for S3 due the lack of fit into the mixing subspace of S6. Grey fields reflect not monitored storms.

4.4.5 EVENT-BASED STREAM EVOLUTION

Stream water and end-members in the EMMA subspace are presented in Fig. 4.5. Hysteresis patterns of stream water across the nested system reveals that stream water for all storms develops mainly along the U1 and U3 axes, apart from the major outlet S6 that also indicates a considerable spread along the U2 axis. Soil water end-members show a small difference in median concentrations in the U3 axis, reducing, to a certain degree, the interpretation of their influence in the evolution of storms along this axis. Stream water from storm events generally starts out near end-members with higher solute concentrations. During the rising limb of the specific discharge hydrographs, they move to the left of less-imprinted end-members (an area between soils and rainfall). Afterwards, at times of falling limbs and recessions, they return to the area where they began.

Hysteresis loops of the upper sub-catchments (S1 and S2, Fig. 4.5a) show in general a clockwise direction (except for E1 in S1, U1-U3 mixing space). They depict a quick contribution from rapidly-responding end-members RF and AN during the hydrograph's rising limb and peaks. During the further development of the hydrograph, the contribution of soil water from AN and HS increases. Towards the end of the event, at falling limbs and during the recession, stream water is more and more dominated by HS and SW.

Contrarily, storm events in lower sub-catchments (S4, S5, and S6) exhibit counter-clockwise hysteresis and, therefore, a different arrangement of the end-members. Storm events clearly depict the influence of HS soil water at the beginning of the rising limb. During the rising limb, peaks, and falling limbs, AN and RF dominates the discharge, followed by HS and SW, which primarily impact the recessions.

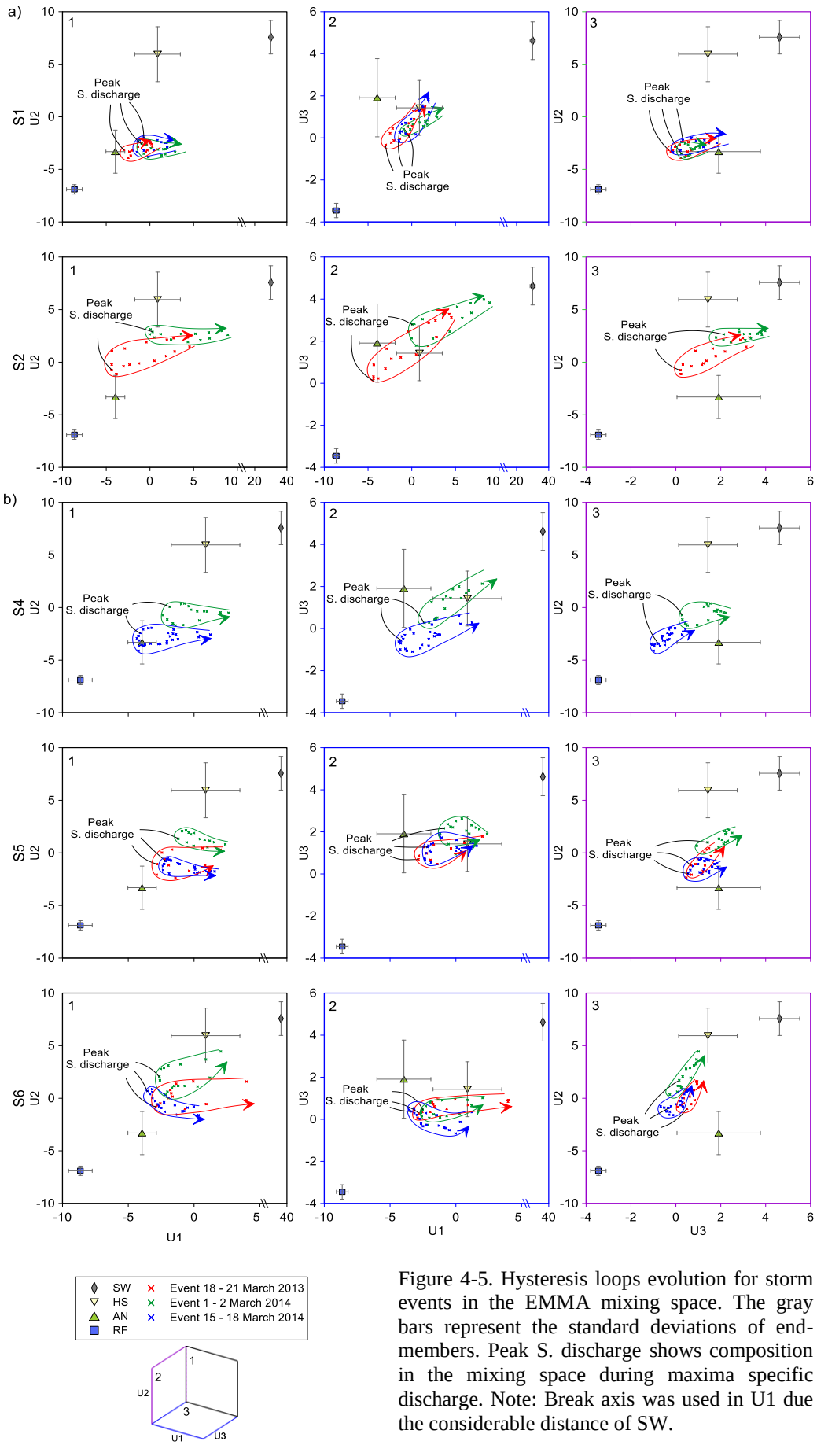

Figure 4-5. Hysteresis loops evolution for storm events in the EMMA mixing space. The gray bars represent the standard deviations of end-members. Peak S. discharge shows composition in the mixing space during maxima specific discharge. Note: Break axis was used in U1 due the considerable distance of SW.

4.5 DISCUSSION

4.5.1 END-MEMBERS AND SITE COMPARISON

Tracer-based analysis is invaluable when trying to gain a general understanding of hydrological catchment functioning and the delineation of the sources contributing to runoff. Our findings are particularly interesting, because they clearly show the spatio-temporal variability of stream water chemistry and end-member contributions during storm events in a remote Páramo headwater catchment in Southern Ecuador with relative homogeneous climate and landscape characteristics.

In this study, the four end-members identified for the catchment outlet of our study area (Correa et al., 2017) enable conceptualization in space and time of the chemical signatures of the different water sources and sub-catchments. SW, the chemical richest end-member, underlined the influence of shallow groundwater, even though its contribution to event-based runoff remains often small. The importance of this type of water source was previously reported for other headwater catchments under comparable geomorphological and hydro-pedological features (Blumstock et al., 2016; Favier et al., 2008). The RF had a small chemical signature, representing direct channel precipitation (Penna et al., 2015), overland flow (which rarely occurred), and water that short interacted with the soils (Delsman et al., 2013). The soil end-members AN and HS showed solute concentrations between the extremes SW and RF and are, in general, plotted closer to the stream water data (Fig. 4.2). In line with our results, the crucial role of soil water from hillslopes (AN) and from the riparian area (HS) in the streamflow generation were earlier reported in several studies (Blumstock et al., 2015; Iwasaki et al., 2015; McGlynn and McDonnell, 2003; Tetzlaff et al., 2014). The hydrological connectivity of these landscape units were analyzed by von Freyberg et al. (2014), highlighting that the riparian zones were the most important storm event water source.

Water samples from tributaries projected into the main outlet mixing space permitted to compare the stream water chemistry of the nested system, identify sources and sub-catchments, and determine those solute concentrations that are controlled by physical mixing (James and Roulet, 2006). The spatio-temporal differences in the geochemical signature of stream water is influenced by land use (Camporese et al., 2014), the spatial distribution of

geological formations and soil composition (James and Roulet, 2006), and the contact time of water with the bedrock and soils (Blumstock et al., 2015; Mosquera et al., 2016b).

The EMMA model, generated with stream chemistry of the main stream (7.53 km^2), represents based on the small RBias and RMMSEs more successfully the nearby lower sub-catchments S5 (3.28 km^2) and S4 (1.72 km^2). The capacity of the mixing model to predict the stream water chemistry of S5 and S4 led to the conclusion that the REA of the Zhurucay River Ecohydrological Observatory is equal to 1.72 km^2. After studying a set of 18 nested catchments in the Neversink River watershed in New York, Wolock et al. (1997) reported an REA of 3 km^2 as the threshold at which the variability in concentrations of stream chemistry solutes was evident and above which such concentrations stabilize at relatively invariant values. James and Roulet (2006) reported a REA of 0.9 km^2 in an EMMA study of eight nested catchments in Quebec. Hence, our value is in between the previously-reported areal values, indicating the size of a spatial entity (in our case a sub-catchment S4) above which the hydrological response of the catchment can be represented without the undefinable complexity of local heterogeneity.

Upstream, we found large RBias and RMMSEs for the northwestern catchment (S3), suggesting a different composition of stream chemistry than in the other sub-catchments. Results suggest that tracers in S3, such as Ce, Al, Rb, and Y, are not mixing with the same ratios in the tributaries as in the main stream. A different hydrological functioning of S3 is further supported by water isotope data (Mosquera et al., 2016a), which revealed that this tributary is influenced by precipitation to a larger degree than the rest of the nested streams in the Zhurucay River Ecohydrological Observatory. This sub-catchment is likely further influenced by water from a pounded wetland in the hilltop and the nearby shallower soils.

The projected RRMSEs and RBias are substantially smaller for the upper sub-catchments S1 and S2 when compared to S3, indicating that the main stream model is able to represent these tributaries. In these two sub-catchments, small temporal tributaries were observed during wet conditions. We assume that the variable drainage density in the rather small headwater catchment areas affects the concentration of solutes. On the one hand, we observed some stream chemical differences compared to the main stream, and found over- and under-predicted solute concentrations across the nested system, specifically for V, Ce, and Al.

Following the diagnostic statistics of RBias and RRMSE, the main stream S6 mixing model largely explained the hydro-chemical behavior of the tributaries (except for S3). In line with Hooper's (2003), findings well-explained tributaries are controlled by the same set of end-members. Therefore, the defined set of end-members, SW, HS, AN, and RF consistently control the main outlet and four tributaries in the studied catchment.

4.5.2 INFLUENCE OF END-MEMBERS DURING STORM EVENTS

The potential information extracted from storm events was previously reported in the catchment area by analyzing hydro-metrical data (Correa et al., 2016). The dynamics of end-member contributions to storm events, presented in Fig. 4.4, were only monitored in the wetter season, similar to the study presented by Barthold et al. (2017). Nevertheless, the analyzed storm events presented differences in antecedent moisture conditions and event characteristics across the nested system.

Results from the headwater catchment S1 underlined the importance of considering soil water from hillslopes (AN) as a relevant stream water source (Iwasaki et al., 2015; van Meerveld et al., 2015). In our case, it is the dominant end-member contributor, independent of storm event conditions, in line with findings of Penna et al.(2015). These authors stated that there are important contributions from the hillslopes' soil water to stream generation under wet conditions in a mountain catchment in the Italian pre-Alps. Sub-catchment S1 presented the largest share of Andosols and the highest average slope of all sub-catchments. The combination of steep slopes and wet catchment conditions also resulted in a rather high contribution of new water (RF) to stream discharge. This water flows laterally near-surface and, occasionally, under storm conditions, even overland (Barthold et al., 2017; Barthold and Woods, 2015). The reduced amount of Histosols in S1 limited the contribution of water from riparian areas (Mosquera et al., 2015). Similarly, contributions of SW are small during high flows, as stream water was less imprinted by weathering-derived solutes (Blumstock et al., 2015; Correa et al., 2017; Neill et al., 2011). Streamflow seemed to be influenced by RF during the entire cycle of the three storm events.

The contribution of HS was more apparent in S2 compared to S1, particularly during E2. The rather small peak discharge (around 100 l s^{-1}) and the lowest antecedent soil moisture suggests that the water entering the system filled the unsaturated soils and pushed water from the

riparian zone into the drainage canals (Tetzlaff et al., 2014). In event 1, rainfall nearly saturated the top soils and resulted in an expansion of the streamflow contributing area, enhancing the connectivity of the overland flow and/or lateral flows in the top nearly saturated soils with the channel network (Beven and Kirkby, 1979). This is corroborated by the RF influence during the rising and falling limb. During the recession of the streamflow, the influence of RF declined and increased the contribution of HS and AN. In particular, the latter end-member gaining importance indicates a growing interaction between the riparian area and hillslopes (Ali et al., 2010). Similar results were presented by Morel et al. (2009) by applying the end-member approach in a headwater catchment in northwest France.

The important contributions of RF and AN in the two events of S4 reflect the high influence of precipitation and the little formation of ponds (Mosquera et al., 2016a) in the nearby upper catchment, S3. Water is quickly released and impacts downstream tributaries. In S5, AN was the highest source contributor followed by RF, HS, and SW for E1 and E3. These storm events show higher peak discharge, antecedent catchment moisture, and amount of precipitation than E2.

For the main stream outlet, water contribution from soils near and in the riparian zone (HS) appeared the most important stream source (Burt, 2005; Roa-García et al., 2011), with values that surpass 43% in all storm events. Results are in line with a recent study in the catchment (Correa et al., 2017), where HS values reached as high as 40% in the wet season. RF and AN contributed in similar proportions, and the influence of SW was insignificant. The latter result is in line with previous studies in headwater catchments of the Scottish highlands, where Blumstock et al. (2016) reported limited controls of groundwater on stream generation during wet catchment conditions.

4.5.3 EVENT-BASED STREAM EVOLUTION

Study results enabled to assess the spatio-temporal evolution of stream water chemistry (hysteresis loops, shapes, and directional shift) and to qualitatively describe how end-members influence stormflow generation (Evans and Davies, 1998). Storm chemical evolution patterns in the U-space depicted differences between the upper (S1 and S2) and lower catchments (S4, S5, and S6), indicated by shifts in the direction of RF and AN end-members. This observation was only possible via high-resolution sampling, which recently

was highlighted in several studies. The approach allows the detection of formerly unknown hydrological processes (Aubert et al., 2016; Aubert and Breuer, 2016; Barthold et al., 2017; Engel et al., 2016).

Shapes of the hysteresis loops show the tendency of the storm events under wetter conditions (E1 and E3), plotting closer to "new water" end-members, in line with a previous study which showed clearly the strong influence of surficial sources in more wet events (Inamdar et al., 2013). Similar shapes for all storms in each sub-catchment suggest a reduced impact of hydrometrical storm characteristics and catchment conditions on the chemical evolution. This results are conform with the findings of Barthold et al. (2017) who found similar event shapes, monitoring a single catchment in wet conditions. By comparing the sub-catchments, longer loops for S2 in the U-space, suggest more variability in the chemical composition of stream water. Overall, in our storm events (wetter conditions) relatively narrowed linear hysteresis shapes and well-defined mixing loops where found for all events, suggesting end-members hydrologically connected and contributions from all major end-members in different storm hydrograph stages (Ali et al., 2010; Inamdar et al., 2013; Rice and Hornberger, 1998).

A number of studies showed consistent counterclockwise hysteresis with early surficial end-member contributions and delayed influence of near-stream soil water and/or groundwater (Inamdar et al., 2013; Inamdar & Mitchell, 2007; Morel et al., 2009; Wenninger et al., 2004). Engel et al. (2016) reported different hysteresis loop patterns during storm events for upper (clockwise) versus lower sub-catchments (counterclockwise). They assumed that this difference is related to the seasonal contribution of a chemically-rich source, present in a small catchment area (and therefore present short propagation times) upstream of the lower sub-catchment.

The general clockwise hysteresis patterns for the upper sub-catchments we found propose a conceptualization of storm event behavior. For this part of the catchment, the rising limb and peak of the hydrograph are dominated by rainfall and soil water from the hillslopes, whereas during the falling limb and recession periods soil water from the riparian zone and shallow groundwater (in very small proportions) take over. This behavior is likely due to the presence of temporal tributaries and lateral flow in near-surface flow paths of saturated soils during wet conditions. Inamdar et al. (2013) proposed a similar conceptual model by studying a small, forested catchment in Maryland, where precipitation, throughfall, and overland flow influence

the rising limb, and soil water and/or shallow groundwater contributions subsequently gain importance. The relative position of HS was closer to stream data for S2 than S1. Additionally the developed hysteresis of the storm events in S2 suggested higher influence of imprinted end-members (SW) before and after the storm events (Inamdar & Mitchell, 2007; Rice & Hornberger, 1998).

The rotational directions of hysteresis loops changed in the lower sub-catchments and were consistent for all storms. The conceptualization for these sub-catchments include an early influence of HS, suggesting that water stored in the riparian area is pushed by soil water from the hillslopes (Correa et al., 2017; Crespo et al., 2011; Tetzlaff et al., 2014). Nevertheless, the wet catchment conditions made the "new water" end-members (AN and RF) act immediately thereafter. The lower catchments have wider valley bottoms and thus a large share of HS compared to the upper catchments, S1 and S2. The propagation times for RF and water from the hillslopes (AN) seem to be longer than the required times to start impacting the rising limb of the hydrograph during storm events, when water from the riparian zone (HS) plays an important role.

4.6 CONCLUSIONS

We compared the stream chemistry among a nested catchment system of the Zhurucay River Ecohydrological Observatory in the Andean Páramo, assessed the consistency of the four, established end-members, calculated their contributions to runoff during storm events, and analyzed the stream chemistry evolution based on event hysteresis loop patterns. Four of the five tributaries presented similar stream water chemistry and fit into the mixing model generated for the main outlet. The end-members rainfall, spring water, and water from the riparian area (HS) and hillslopes (AN) largely explained the hydro-chemical behavior of the catchment. Results suggests that internal stream chemical information is necessary to avoid false conclusions about the hydrological functioning, compared to the findings considering only a fixed set of end-members for the entire catchment. Different hydrological behavior in the upper compared to the lower sub-catchments became evident. This study confirmed the usefulness of multi-tracer sets with event data resolution to provide insights into the complex, spatio-temporal, distributed hydrological processes in mountain ecosystems. The authors believe that information on the spatio-temporal runoff-generation process is very helpful in

evaluating process-based hydrological models. Instead of merely calibrating those models to gauged point information, we advocate simulating mixing processes and comparing them to observations like the ones presented here.

Acknowledgement

This research was funded by the Secretaría de Educación Superior, Ciencia, Tecnología e Innovación (SNESCYT), the Central Research Office (DIUC) of the Universidad de Cuenca through the project ‘‘Desarrollo de indicadores hidrológicos funcionales para la evaluación del impacto del cambio global en ecosistemas Andinos’’, and the German Research Foundation (DFG, BR2238/14–1). AC was funded by SENESCYT sholarship 112–2012. The authors thank the project “Identificación de las relaciones entre las propiedades biofísicas y la respuesta hidrológica en cuencas de páramo húmedo” to provide part of solute concentration data. Please contact the authors for access to the data used in this paper.

5 REFERENCES

Acreman, M. C. and Sinclair, C. D.: Classification of drainage basins according to their physical characteristics; an application for flood frequency analysis in Scotland, J. Hydrol., 84(3), 365–380, doi:10.1016/0022-1694(86)90134-4, 1986.

Ali, G., Tetzlaff, D., Soulsby, C. and McDonnell, J. J.: Topographic, pedologic and climatic interactions influencing streamflow generation at multiple catchment scales, Hydrol. Process., 26(25), 3858–3874, doi:10.1002/hyp.8416, 2012.

Ali, G. A., Roy, A. G., Turmel, M.-C. and Courchesne, F.: Source-to-stream connectivity assessment through end-member mixing analysis, J. Hydrol., 392(3–4), 119–135, doi:10.1016/j.jhydrol.2010.07.049, 2010.

Aubert, A. H. and Breuer, L.: New Seasonal Shift in In-Stream Diurnal Nitrate Cycles Identified by Mining High-Frequency Data, PLOS ONE, 11(4), e0153138, doi:10.1371/journal.pone.0153138, 2016.

Aubert, A. H., Thrun, M. C., Breuer, L. and Ultsch, A.: Knowledge discovery from high-frequency stream nitrate concentrations: hydrology and biology contributions, Sci. Rep., 6, srep31536, doi:10.1038/srep31536, 2016.

Barthold, F. K. and Woods, R. A.: Stormflow generation: A meta-analysis of field evidence from small, forested catchments, Water Resour. Res., 51(5), 3730–3753, doi:10.1002/2014WR016221, 2015.

Barthold, F. K., Wu, J., Vaché, K. B., Schneider, K., Frede, H.-G. and Breuer, L.: Identification of geographic runoff sources in a data sparse region: hydrological processes and the limitations of tracer-based approaches, Hydrol. Process., 24(16), 2313–2327, doi:10.1002/hyp.7678, 2010.

Barthold, F. K., Tyralla, C., Schneider, K., Vaché, K. B., Frede, H.-G. and Breuer, L.: How many tracers do we need for end member mixing analysis (EMMA)? A sensitivity analysis, Water Resour. Res., 47(8), W08519, doi:10.1029/2011WR010604, 2011.

Barthold, F. K., Turner, B. L., Elsenbeer, H. and Zimmermann, A.: A hydrochemical approach to quantify the role of return flow in a surface flow-dominated catchment, Hydrol. Process., 31(5), 1018–1033, doi:10.1002/hyp.11083, 2017.

Bazemore, D. E., Eshleman, K. N. and Hollenbeck, K. J.: The role of soil water in stormflow generation in a forested headwater catchment: synthesis of natural tracer and hydrometric evidence, J. Hydrol., 162(1), 47–75, doi:10.1016/0022-1694(94)90004-3, 1994.

Beck, E., Makeschin, F., Haubrich, F., Richter, M., Bendix, J. and Valarezo, C.: The Ecosystem (Reserva Biológica San Francisco), in Gradients in a Tropical Mountain Ecosystem of Ecuador. Ecological Studies, vol. 198, edited by E. Beck, J. Bendix, I. Kottke, F. Makeschin, and R. Mosandl, pp. 1–14, Springer, Berlin, Germany., 2008.

Bendix: Precipitation dynamics in Ecuador and northern Peru during the 1991/92 El Nino: A remote sensing perspective, Int. J. Remote Sens., 21(3), 533–548, doi:10.1080/014311600210731, 2000.

Berger, K. P. and Entekhabi, D.: Basin hydrologic response relations to distributed physiographic descriptors and climate, J. Hydrol., 247(3–4), 169–182, doi:10.1016/S0022-1694(01)00383-3, 2001.

Bergstrom, A., Jencso, K. and McGlynn, B.: Spatiotemporal processes that contribute to hydrologic exchange between hillslopes, valley bottoms, and streams: UPLAND AND VALLEY BOTTOM INFLUENCES ON STREAM WATER BALANCE, Water Resour. Res., 52(6), 4628–4645, doi:10.1002/2015WR017972, 2016.

Beven, K.: Towards integrated environmental models of everywhere: uncertainty, data and modelling as a learning process, Hydrol Earth Syst Sci, 11(1), 460–467, doi:10.5194/hess-11-460-2007, 2007.

Beven, K. J. and Kirkby, M. J.: A physically based, variable contributing area model of basin hydrology / Un modèle à base physique de zone d'appel variable de l'hydrologie du bassin versant, Hydrol. Sci. Bull., 24(1), 43–69, doi:10.1080/02626667909491834, 1979.

Birkel, C. and Soulsby, C.: Linking tracers, water age and conceptual models to identify dominant runoff processes in a sparsely monitored humid tropical catchment: Linking Tracers, Water age and Conceptual Models in the Humid Tropics, Hydrol. Process., doi:10.1002/hyp.10941, 2016.

Birkel, C., Geris, J., Molina, M. J., Mendez, C., Arce, R., Dick, J., Tetzlaff, D. and Soulsby, C.: Hydroclimatic controls on non-stationary stream water ages in humid tropical catchments, J. Hydrol., doi:10.1016/j.jhydrol.2016.09.006, 2016.

Blume, T., Zehe, E. and Bronstert, A.: Rainfall—runoff response, event-based runoff coefficients and hydrograph separation, Hydrol. Sci. J., 52(5), 843–862, doi:10.1623/hysj.52.5.843, 2007.

Blumstock, M., Tetzlaff, D., Malcolm, I. A., Nuetzmann, G. and Soulsby, C.: Baseflow dynamics: Multi-tracer surveys to assess variable groundwater contributions to montane streams under low flows, J. Hydrol., 527, 1021–1033, doi:10.1016/j.jhydrol.2015.05.019, 2015.

Blumstock, M., Tetzlaff, D., Dick, J. J., Nuetzmann, G. and Soulsby, C.: Spatial organization of groundwater dynamics and streamflow response from different hydropedological units in a montane catchment: Groundwater and Stream Dynamics Across Different Hydropedological Units, Hydrol. Process., 30(21), 3735–3753, doi:10.1002/hyp.10848, 2016.

Boll, J., Steenhuis, T. S. and Selker, J. S.: Fiberglass Wicks for Sampling of Water and Solutes in the Vadose Zone, Soil Sci. Soc. Am. J., 56(3), 701, doi:10.2136/sssaj1992.03615995005600030005x, 1992.

Brown, V. A., McDonnell, J. J., Burns, D. A. and Kendall, C.: The role of event water, a rapid shallow flow component, and catchment size in summer stormflow, J. Hydrol., 217(3–4), 171–190, doi:10.1016/S0022-1694(98)00247-9, 1999.

Bücker, A., Crespo, P., Frede, H.-G., Vaché, K. and Cisneros, F.: Identifying Controls on Water Chemistry of Tropical Cloud Forest Catchments: Combining Descriptive Approaches and Multivariate Analysis, , 16(1), 127–149, 2010.

Burt, T. P.: A third paradox in catchment hydrology and biogeochemistry: decoupling in the riparian zone, Hydrol. Process., 19(10), 2087–2089, doi:10.1002/hyp.5904, 2005.

Buttle, J. M.: Isotope hydrograph separations and rapid delivery of pre-event water from drainage basins, Prog. Phys. Geogr., 18(1), 16–41, doi:10.1177/030913339401800102, 1994.

Buytaert, W. and Beven, K.: Regionalization as a learning process, Water Resour. Res., 45(11), 1–13, doi:10.1029/2008WR007359, 2009.

Buytaert, W. and Beven, K.: Models as multiple working hypotheses: hydrological simulation of tropical alpine wetlands, Hydrol. Process., 25(11), 1784–1799, doi:10.1002/hyp.7936, 2011.

Buytaert, W., Wyseure, G., De Bièvre, B. and Deckers, J.: The effect of land-use changes on the hydrological behaviour of Histic Andosols in south Ecuador, Hydrol. Process., 19(August), 3985–3997, doi:10.1002/hyp.5867, 2005.

Buytaert, W., Célleri, R., De Bièvre, B., Cisneros, F., Wyseure, G., Deckers, J. and Hofstede, R.: Human impact on the hydrology of the Andean páramos, Earth-Sci. Rev., 79(1–2), 53–72, doi:10.1016/j.earscirev.2006.06.002, 2006.

Buytaert, W., Iñiguez, V. and Bièvre, B. D.: The effects of afforestation and cultivation on water yield in the Andean páramo, For. Ecol. Manag., 251(1–2), 22–30, doi:10.1016/j.foreco.2007.06.035, 2007.

Buytaert, W., Célleri, R., De Bièvre, B. and Cisneros, F.: Hidrología del páramo andino: propiedades, importancia y vulnerabilidad, Descargado Ftpftp Ciat Cgiar OrgHIDROLOGIADELPARAMO En Oct. [online] Available from: https://www.researchgate.net/profile/Felipe_Cisneros/publication/228459137_HIDROLOGA_DEL_PRAMO_ANDINO_PROPIEDADES_IMPORTANCIA_Y_VULNERABILIDAD/links/0deec528f8f8e65d5e000000.pdf (Accessed 25 April 2016a), 2010.

Buytaert, W., Vuille, M., Dewulf, A., Urrutia, R., Karmalkar, A. and Célleri, R.: Uncertainties in climate change projections and regional downscaling in the tropical Andes: implications for water resources management, Hydrol Earth Syst Sci, 14(7), 1247–1258, doi:10.5194/hess-14-1247-2010, 2010b.

Camporese, M., Penna, D., Borga, M. and Paniconi, C.: A field and modeling study of nonlinear storage-discharge dynamics for an Alpine headwater catchment, Water Resour. Res., 50(2), 806–822, doi:10.1002/2013WR013604, 2014.

Capell, R., Tetzlaff, D., Hartley, A. J. and Soulsby, C.: Linking metrics of hydrological function and transit times to landscape controls in a heterogeneous mesoscale catchment, Hydrol. Process., 26(3), 405–420, doi:10.1002/hyp.8139, 2012.

Célleri, R.: Rainfall variability and rainfall-runoff dynamics in the Paute river basin - Southern Ecuadorian Andes, PhD thesis, Katholieke Universiteit Leuven, Leuven, Belgium, 26 June. [online] Available from: https://lirias.kuleuven.be/handle/1979/899 (Accessed 25 April 2016), 2007.

Célleri, R. and Feyen, J.: The Hydrology of Tropical Andean Ecosystems: Importance, Knowledge Status, and Perspectives, Mt. Res. Dev., 29(4), 350–355, doi:10.1659/mrd.00007, 2009.

Célleri, R., Buytaert, W., De Bièvre, B. and Tobón, C.: Understanding the hydrology of tropical Andean ecosystems through an Andean Network of Basins, in Status and Perspectives of Hydrology in Small Basins, pp. 209–212., 2009.

Chapman, T. G.: Comment on "Evaluation of automated techniques for base flow and recession analyses" by R. J. Nathan and T. A. McMahon, Water Resour. Res., 27(7), 1783–1784, doi:10.1029/91WR01007, 1991.

Chaves, J., Neill, C., Germer, S., Neto, S. G., Krusche, A. and Elsenbeer, H.: Land management impacts on runoff sources in small Amazon watersheds, Hydrol. Process., 22(12), 1766–1775, doi:10.1002/hyp.6803, 2008.

Christophersen, N. and Hooper, R. P.: Multivariate analysis of stream water chemical data: The use of principal components analysis for the end-member mixing problem, Water Resour. Res., 28(1), 99–107, doi:10.1029/91WR02518, 1992.

Christophersen, N., Neal, C., Hooper, R. P., Vogt, R. D. and Andersen, S.: Modelling streamwater chemistry as a mixture of soilwater end-members - A step towards second-generation acidification models, J. Hydrol., 116(1–4), 307–320, 1990.

Coltorti, M. and Ollier, C. D.: Geomorphic and tectonic evolution of the Ecuadorian Andes, Geomorphology, 32(1–2), 1–19, doi:10.1016/S0169-555X(99)00036-7, 2000.

Córdova, M., Carrillo-Rojas, G., Crespo, P., Wilcox, B. and Célleri, R.: Evaluation of the Penman-Monteith (FAO 56 PM) Method for Calculating Reference Evapotranspiration Using Limited Data: Application to the Wet Páramo of Southern Ecuador, Mt. Res. Dev., 35(3), 230–239, doi:10.1659/MRD-JOURNAL-D-14-0024.1, 2015.

Correa, A., Windhorst, D., Crespo, P., Célleri, R., Feyen, J. and Breuer, L.: Continuous versus event based sampling: How many samples are required for deriving general hydrological understanding on Ecuador's páramo region?: Comparison of continuous versus event based sampling, Hydrol. Process., 30, 4059–4073, doi:10.1002/hyp.10975, 2016.

Correa, A., Windhorst, D., Tetzlaff, D., Crespo, P., Célleri, R., Feyen, J. and Breuer, L.: Temporal dynamics in dominant runoff sources and flow paths in the Andean Páramo, Water Resour. Res., doi:10.1002/2016WR020187, 2017.

Crespo, P. J., Feyen, J., Buytaert, W., Bücker, A., Breuer, L., Frede, H.-G. and Ramírez, M.: Identifying controls of the rainfall–runoff response of small catchments in the tropical Andes (Ecuador), J. Hydrol., 407(1–4), 164–174, doi:10.1016/j.jhydrol.2011.07.021, 2011.

Dangles, O., Rabatel, A., Kraemer, M., Zeballos, G., Soruco, A., Jacobsen, D. and Anthelme, F.: Ecosystem sentinels for climate change? Evidence of wetland cover changes over the last 30 years in the tropical Andes, edited by A. J. Green, PLOS ONE, 12(5), e0175814, doi:10.1371/journal.pone.0175814, 2017.

Delsman, J. R., Essink, G. H. P. O., Beven, K. J. and Stuyfzand, P. J.: Uncertainty estimation of end-member mixing using generalized likelihood uncertainty estimation (GLUE), applied in a lowland catchment: Uncertainty Estimation of End-Member Mixing, Water Resour. Res., 49(8), 4792–4806, doi:10.1002/wrcr.20341, 2013.

Detty, J. M. and McGuire, K. J.: Topographic controls on shallow groundwater dynamics: implications of hydrologic connectivity between hillslopes and riparian zones in a till mantled catchment, Hydrol. Process., 24(16), 2222–2236, doi:10.1002/hyp.7656, 2010.

Efron, B.: Bootstrap Methods: Another Look at the Jackknife, Ann. Stat., 7(1), 1–26, doi:10.1214/aos/1176344552, 1979.

Engel, M., Penna, D., Bertoldi, G., Dell'Agnese, A., Soulsby, C. and Comiti, F.: Identifying run-off contributions during melt-induced run-off events in a glacierized alpine catchment, Hydrol. Process., 30(3), 343–364, doi:10.1002/hyp.10577, 2016.

Erwin, K. L.: Wetlands and global climate change: the role of wetland restoration in a changing world, Wetl. Ecol. Manag., 17(1), 71–84, doi:10.1007/s11273-008-9119-1, 2009.

Evans, C. and Davies, T. D.: Causes of concentration/discharge hysteresis and its potential as a tool for analysis of episode hydrochemistry, Water Resour. Res., 34(1), 129–137, doi:10.1029/97WR01881, 1998.

Favier, V., Coudrain, A., Cadier, E., Francou, B., Ayabaca, E., Maisincho, L., Praderio, E., Villacis, M. and Wagnon, P.: Evidence of groundwater flow on Antizana ice-covered volcano, Ecuador / Mise en évidence d'écoulements souterrains sur le volcan englacé Antizana, Equateur, Hydrol. Sci. J., 53(1), 278–291, doi:10.1623/hysj.53.1.278, 2008.

Fenicia, F., McDonnell, J. J. and Savenije, H. H. G.: Learning from model improvement: On the contribution of complementary data to process understanding, Water Resour. Res., 44(6), W06419, doi:10.1029/2007WR006386, 2008.

Freeze, R. A.: Role of subsurface flow in generating surface runoff: 1. Base flow contributions to channel flow, Water Resour. Res., 8(3), 609–623, doi:10.1029/WR008i003p00609, 1972a.

Freeze, R. A.: Role of subsurface flow in generating surface runoff: 2. Upstream source areas, Water Resour. Res., 8(5), 1272–1283, doi:10.1029/WR008i005p01272, 1972b.

von Freyberg, J., Radny, D., Gall, H. E. and Schirmer, M.: Implications of hydrologic connectivity between hillslopes and riparian zones on streamflow composition, J. Contam. Hydrol., 169, 62–74, doi:10.1016/j.jconhyd.2014.07.005, 2014.

Fröhlich, H. L., Breuer, L., Vaché, K. B. and Frede, H.-G.: Inferring the effect of catchment complexity on mesoscale hydrologic response, Water Resour. Res., 44(9), W09414, doi:10.1029/2007WR006207, 2008.

Genereux, D.: Quantifying uncertainty in tracer-based hydrograph separations, Water Resour. Res., 34(4), 915–919, doi:10.1029/98WR00010, 1998.

Gibbon, A., Silman, M. R., Malhi, Y., Fisher, J. B., Meir, P., Zimmermann, M., Dargie, G. C., Farfan, W. R. and Garcia, K. C.: Ecosystem Carbon Storage Across the Grassland–Forest Transition in the High Andes of Manu National Park, Peru, Ecosystems, 13(7), 1097–1111, doi:10.1007/s10021-010-9376-8, 2010.

Gibson, J. J., Edwards, T. W. D., Birks, S. J., St Amour, N. A., Buhay, W. M., McEachern, P., Wolfe, B. B. and Peters, D. L.: Progress in isotope tracer hydrology in Canada, Hydrol. Process., 19(1), 303–327, doi:10.1002/hyp.5766, 2005.

Guzha, A. C., Nobrega, R. L. B., Kovacs, K., Rebola-Lichtenberg, J., Amorim, R. S. S. and Gerold, G.: Characterizing rainfall-runoff signatures from micro-catchments with contrasting land cover characteristics in southern Amazonia, Hydrol. Process., 29(4), 508–521, doi:10.1002/hyp.10161, 2015.

Harden, C. P.: Human impacts on headwater fluvial systems in the northern and central Andes, Geomorphology, 79(3), 249–263, doi:10.1016/j.geomorph.2006.06.021, 2006.

Harden, C. P., Hartsig, J., Farley, K. A., Lee, J. and Bremer, L. L.: Effects of Land-Use Change on Water in Andean Páramo Grassland Soils, Ann. Assoc. Am. Geogr., 103(2), 375–384, doi:10.1080/00045608.2013.754655, 2013.

Hooper, R. P.: Applying the scientific method to small catchment studies: a review of the Panola Mountain experience, Hydrol. Process., 15(10), 2039–2050, doi:10.1002/hyp.255, 2001.

Hooper, R. P.: Diagnostic tools for mixing models of stream water chemistry, Water Resour. Res., 39(3), 1–13, doi:10.1029/2002WR001528, 2003.

Hugenschmidt, C., Ingwersen, J., Sangchan, W., Sukvanachaikul, Y., Duffner, A., Uhlenbrook, S. and Streck, T.: A three-component hydrograph separation based on geochemical tracers in a tropical mountainous headwater catchment in northern

Thailand, Hydrol. Earth Syst. Sci., 18(2), 525–537, doi:10.5194/hess-18-525-2014, 2014.

Inamdar, S., Dhillon, G., Singh, S., Dutta, S., Levia, D., Scott, D., Mitchell, M., Van Stan, J. and McHale, P.: Temporal variation in end-member chemistry and its influence on runoff mixing patterns in a forested, Piedmont catchment, Water Resour. Res., 49(4), 1828–1844, doi:10.1002/wrcr.20158, 2013.

Inamdar, S. P. and Mitchell, M. J.: Contributions of riparian and hillslope waters to storm runoff across multiple catchments and storm events in a glaciated forested watershed, J. Hydrol., 341(1), 116–130, doi:10.1016/j.jhydrol.2007.05.007, 2007.

IUSS Working Group WRB: World reference base for soil resources 2014, update 2015 international soil classification system for naming soils and creating legends for soil maps., FAO, Rome., 2015.

Iwasaki, K., Katsuyama, M. and Tani, M.: Contributions of bedrock groundwater to the upscaling of storm-runoff generation processes in weathered granitic headwater catchments, Hydrol. Process., 29(6), 1535–1548, doi:10.1002/hyp.10279, 2015.

James, A. L. and Roulet, N. T.: Investigating the applicability of end-member mixing analysis (EMMA) across scale: A study of eight small, nested catchments in a temperate forested watershed, Water Resour. Res., 42, 1–17, doi:10.1029/2005WR004419, 2006.

Jasechko, S., Kirchner, J. W., Welker, J. M. and McDonnell, J. J.: Substantial proportion of global streamflow less than three months old, Nat. Geosci., 9(2), 126–129, doi:10.1038/ngeo2636, 2016.

Jencso, K. G., McGlynn, B. L., Gooseff, M. N., Wondzell, S. M., Bencala, K. E. and Marshall, L. A.: Hydrologic connectivity between landscapes and streams: Transferring reach- and plot-scale understanding to the catchment scale, Water Resour. Res., 45(4), W04428, doi:10.1029/2008WR007225, 2009.

Josse, C., Cuesta, F., Navarro, G., Barrena, V., Cabrera, E., Chacón-Moreno, E., Ferreira, W., Perlavo, M., Saito, J. and Tovar, A.: Atlas de los Andes del Norte y Centro. Bolivia, Colombia, Ecuador, Perú y Venezuela., Secretaría General de la Comunidad Andina, Programa RegionalECOBONA, CONDESAN-Proyecto Páramo Andino, ProgramaBioAndes, EcoCiencia, NatureServe, LTA-UNALM, IAvH, ICAE-ULA, CDC-UNALM, RUMBOL SRL, Lima, Perú. [online] Available from: http://www.condesan.org/ppa/node/3678 (Accessed 21 October 2016), 2009.

Juston, J., Seibert, J. and Johansson, P.-O.: Temporal sampling strategies and uncertainty in calibrating a conceptual hydrological model for a small boreal catchment, Hydrol. Process., 23(21), 3093–3109, doi:10.1002/hyp.7421, 2009.

Kabubi, J., Mutua, F., Willems, P. and Mngodo, R. J.: Low Flow Analysis Using Filter Generated Series For Lake Victoria Basin, pp. 94–95, Friend / Nile, Cairo, Egypt., 2005.

Kampstra, P.: Beanplot: A boxplot alternative for visual comparison of distributions, J. Stat. Softw., 28(1), 1–9, 2008.

Karalis, S., Karymbalis, E., Valkanou, K., Chalkias, C., Katsafados, P., Kalogeropoulos, K., Batzakis, V. and Bofilios, A.: Assessment of the Relationships among Catchments' Morphometric Parameters and Hydrologic Indices, Int. J. Geosci., 5(13), 1571–1583, doi:10.4236/ijg.2014.513128, 2014.

Katsuyama, M., Ohte, N. and Kobashi, S.: A three-component end-member analysis of streamwater hydrochemistry in a small Japanese forested headwater catchment, Hydrol. Process., 15(2), 249–260, 2001.

Katsuyama, M., Kabeya, N. and Ohte, N.: Elucidation of the relationship between geographic and time sources of stream water using a tracer approach in a headwater catchment, Water Resour. Res., 45(6), W06414, doi:10.1029/2008WR007458, 2009.

Kirchner, J. W.: Aggregation in environmental systems – Part 1: Seasonal tracer cycles quantify young water fractions, but not mean transit times, in spatially heterogeneous catchments, Hydrol Earth Syst Sci, 20(1), 279–297, doi:10.5194/hess-20-279-2016, 2016a.

Kirchner, J. W.: Aggregation in environmental systems – Part 2: Catchment mean transit times and young water fractions under hydrologic nonstationarity, Hydrol Earth Syst Sci, 20(1), 299–328, doi:10.5194/hess-20-299-2016, 2016b.

Kirchner, J. W., Tetzlaff, D. and Soulsby, C.: Comparing chloride and water isotopes as hydrological tracers in two Scottish catchments, Hydrol. Process., 24(12), 1631–1645, doi:10.1002/hyp.7676, 2010.

Klaus, J. and McDonnell, J. J.: Hydrograph separation using stable isotopes: Review and evaluation, J. Hydrol., 505, 47–64, doi:10.1016/j.jhydrol.2013.09.006, 2013.

Ladouche, B., Probst, A., Viville, D., Idir, S., Baqué, D., Loubet, M., Probst, J.-L. and Bariac, T.: Hydrograph separation using isotopic, chemical and hydrological approaches (Strengbach catchment, France), J. Hydrol., 242(3–4), 255–274, doi:10.1016/S0022-1694(00)00391-7, 2001.

Lana-Renault, N., Regüés, D., Serrano, P. and Latron, J.: Spatial and temporal variability of groundwater dynamics in a sub-Mediterranean mountain catchment, Hydrol. Process., 28(8), 3288–3299, doi:10.1002/hyp.9892, 2014.

Le Tellier, V., Carrasco, A. and Asquith, N.: Attempts to determine the effects of forest cover on stream flow by direct hydrological measurements in Los Negros, Bolivia, For. Ecol. Manag., 258(9), 1881–1888, doi:10.1016/j.foreco.2009.04.031, 2009.

Lee, E. S. and Krothe, N. C.: A four-component mixing model for water in a karst terrain in south-central Indiana, USA. Using solute concentration and stable isotopes as tracers, Chem. Geol., 179(1–4), 129–143, doi:10.1016/S0009-2541(01)00319-9, 2001.

Levia, D. F., Carlyle-Mosses, D. and Tanaka, T., Eds.: Forest hydrology and biogeochemistry: synthesis of past research and future directions, Springer Science & Business Media. [online] Available from: https://books.google.de/books/about/Forest_Hydrology_and_Biogeochemistry.html?hl=es&id=D5CX7BRx9kQC (Accessed 22 June 2016), 2011.

Liu, F., Williams, M. W. and Caine, N.: Source waters and flow paths in an alpine catchment, Colorado Front Range, United States, Water Resour. Res., 40(9), W09401, doi:10.1029/2004WR003076, 2004.

Lloyd, C. E. M., Freer, J. E., Johnes, P. J. and Collins, A. L.: Using hysteresis analysis of high-resolution water quality monitoring data, including uncertainty, to infer controls on nutrient and sediment transfer in catchments, Sci. Total Environ., 543, 388–404, doi:10.1016/j.scitotenv.2015.11.028, 2016.

Luz, B., Barkan, E., Yam, R. and Shemesh, A.: Fractionation of oxygen and hydrogen isotopes in evaporating water, Geochim. Cosmochim. Acta - GEOCHIM COSMOCHIM ACTA, 73, 6697–6703, doi:10.1016/j.gca.2009.08.008, 2009.

Maloszewski, P. and Zuber, A.: Determining the turnover time of groundwater systems with the aid of environmental tracers 1. Models and their applicability, J. Hydrol., 57, 207–231, doi:10.1016/0022-1694(82)90147-0, 1982.

McCartney, M. P., Neal, C. and Neal, M.: Use of deuterium to understand runoff generation in a headwater catchment containing a dambo, Hydrol Earth Syst Sci, 2(1), 65–76, doi:10.5194/hess-2-65-1998, 1998.

McDonnell, J. J.: Where does water go when it rains? Moving beyond the variable source area concept of rainfall-runoff response, Hydrol. Process., 17(9), 1869–1875, doi:10.1002/hyp.5132, 2003.

McDonnell, J. J. and Beven, K.: Debates—The future of hydrological sciences: A (common) path forward? A call to action aimed at understanding velocities, celerities and residence time distributions of the headwater hydrograph, Water Resour. Res., 50(6), 5342–5350, doi:10.1002/2013WR015141, 2014.

McGlynn, B. L. and McDonnell, J. J.: Quantifying the relative contributions of riparian and hillslope zones to catchment runoff, Water Resour. Res., 39(11), 1310, doi:10.1029/2003WR002091, 2003.

McGuire, K. J. and McDonnell, J. J.: A review and evaluation of catchment transit time modeling, J. Hydrol., 330(3–4), 543–563, doi:10.1016/j.jhydrol.2006.04.020, 2006.

McGuire, K. J. and McDonnell, J. J.: Hydrological connectivity of hillslopes and streams: Characteristic time scales and nonlinearities: HYDROLOGICAL CONNECTIVITY OF HILLSLOPES AND STREAMS, Water Resour. Res., 46(10), W10543, doi:10.1029/2010WR009341, 2010.

McIntyre, N., Lee, H., Wheater, H., Young, A. and Wagener, T.: Ensemble predictions of runoff in ungauged catchments, Water Resour. Res., 41(12), W12434, doi:10.1029/2005WR004289, 2005.

McIntyre, N., Ballard, C., Bruen, M., Bulygina, N., Buytaert, W., Cluckie, I., Dunn, S., Ehret, U., Ewen, J., Gelfan, A., Hess, T., Hughes, D., Jackson, B., Kjeldsen, T. R., Merz, R., Park, J.-S., O'Connell, E., O'Donnell, G., Oudin, L., Todini, E., Wagener, T., Wheater, H. and web-support@bath.ac.uk: Modelling the hydrological impacts of rural land use change, Hydrol. Res., 45(6), 737–754, 2014.

van Meerveld, H. J., Seibert, J. and Peters, N. E.: Hillslope–riparian-stream connectivity and flow directions at the Panola Mountain Research Watershed, Hydrol. Process., 29(16), 3556–3574, doi:10.1002/hyp.10508, 2015.

Mena, P. V. and Hofstede, R.: Los páramos ecuatorianos, Botánica Económica Los Andes Cent., 91–109, 2006.

Moore, R. D.: Introduction to salt dilution gauging for streamflow measurement Part 2: Constant-rate injection., Streamline Watershed Manag. Bull., (8 (1)), 11–15, 2004.

Morel, B., Durand, P., Jaffrezic, A., Gruau, G. and Molenat, J.: Sources of dissolved organic carbon during stormflow in a headwater agricultural catchment, Hydrol. Process., 23(20), 2888–2901, doi:10.1002/hyp.7379, 2009.

Mosley, M. P.: Streamflow generation in a forested watershed, New Zealand, Water Resour. Res., 15(4), 795–806, doi:10.1029/WR015i004p00795, 1979.

Mosquera, G., Lazo, P., Cárdenas, I. and Crespo, P.: Identificación de las principales fuentes de agua que aportan a la generación de escorrentía en zonas Andinas de páramo húmedo: mediante el uso de los isótopos estables deuterio (δ2H) y oxígeno-18 (δ18O), Maskana, 3(2), 87–105, 2012.

Mosquera, G. M., Lazo, P. X., Célleri, R., Wilcox, B. P. and Crespo, P.: Runoff from tropical alpine grasslands increases with areal extent of wetlands, CATENA, 125, 120–128, doi:10.1016/j.catena.2014.10.010, 2015.

Mosquera, G. M., Célleri, R., Lazo, P. X., Vaché, K. B., Perakis, S. S. and Crespo, P.: Combined Use of Isotopic and Hydrometric Data to Conceptualize Ecohydrological Processes in a High-Elevation Tropical Ecosystem, Hydrol. Process., n/a-n/a, doi:10.1002/hyp.10927, 2016a.

Mosquera, G. M., Segura, C., Vaché, K. B., Windhorst, D., Breuer, L. and Crespo, P.: Insights into the water mean transit time in a high-elevation tropical ecosystem, Hydrol. Earth Syst. Sci., 20(7), 2987–3004, doi:10.5194/hess-20-2987-2016, 2016b.

Muñoz-Villers, L. E. and McDonnell, J. J.: Runoff generation in a steep, tropical montane cloud forest catchment on permeable volcanic substrate: STORM RUNOFF IN A MONTANE FOREST, Water Resour. Res., 48(9), W09528, doi:10.1029/2011WR011316, 2012.

Neal, C., Reynolds, B., Neal, M., Pugh, B., Hill, L. and Wickham, H.: Long-term changes in the water quality of rainfall, cloud water and stream water for moorland, forested and clear-felled catchments at Plynlimon, mid-Wales, Hydrol Earth Syst Sci, 5(3), 459–476, doi:10.5194/hess-5-459-2001, 2001.

Neill, C., Chaves, J. E., Biggs, T., Deegan, L. A., Elsenbeer, H., Figueiredo, R. O., Germer, S., Johnson, M. S., Lehmann, J., Markewitz, D. and Piccolo, M. C.: Runoff sources and land cover change in the Amazon: an end-member mixing analysis from small watersheds, Biogeochemistry, 105(1–3), 7, doi:10.1007/s10533-011-9597-8, 2011.

Ochoa-Tocachi, B.: Regionalisation of hydrological indices to assess land-use change impacts in the Tropical Andes., MSc thesis, Imperial College London., 2014.

Ochoa-Tocachi, B. F., Buytaert, W., De Bièvre, B., Célleri, R., Crespo, P., Villacís, M., Llerena, C. A., Acosta, L., Villazón, M., Guallpa, M., Gil-Ríos, J., Fuentes, P., Olaya, D., Viñas, P., Rojas, G. and Arias, S.: Impacts of land use on the hydrological response of tropical Andean catchments, Hydrol. Process., n/a-n/a, doi:10.1002/hyp.10980, 2016.

Olden, J. D. and Poff, N. L.: Redundancy and the choice of hydrologic indices for characterizing streamflow regimes, River Res. Appl., 19(2), 101–121, doi:10.1002/rra.700, 2003.

Padrón, R. S., Wilcox, B. P., Crespo, P. and Célleri, R.: Rainfall in the Andean Páramo: New Insights from High-Resolution Monitoring in Southern Ecuador, J. Hydrometeorol., 16(3), 985–996, doi:10.1175/JHM-D-14-0135.1, 2015.

Penna, D., van Meerveld, H. J., Oliviero, O., Zuecco, G., Assendelft, R. S., Dalla Fontana, G. and Borga, M.: Seasonal changes in runoff generation in a small forested mountain catchment, Hydrol. Process., 29(8), 2027–2042, doi:10.1002/hyp.10347, 2015.

Penna, D., van Meerveld, H. J., Zuecco, G., Dalla Fontana, G. and Borga, M.: Hydrological response of an Alpine catchment to rainfall and snowmelt events, J. Hydrol., 537, 382–397, doi:10.1016/j.jhydrol.2016.03.040, 2016.

Perrin, C., Oudin, L., Andreassian, V., Rojas-Serna, C., Michel, C. and Mathevet, T.: Impact of limited streamflow data on the efficiency and the parameters of rainfall—runoff models, Hydrol. Sci. J., 52(1), 131–151, doi:10.1623/hysj.52.1.131, 2007.

Picarro: ChemCorrectTM - Solving the Problem of Chemical Contaminants in H2 0 Stable Isotope Research, White Pap., 2–4, 2010.

Post, D. A. and Jakeman, A. J.: Predicting the daily streamflow of ungauged catchments in S.E. Australia by regionalising the parameters of a lumped conceptual rainfall-runoff model, Ecol. Model., 123(2–3), 91–104, doi:10.1016/S0304-3800(99)00125-8, 1999.

Pratt, W. T., Figueroa, J. F. and Flores, B. C.: Geology and mineralization of the area between 3 and 48S, Western Cordillera, Ecuador., Br. Geol. Surv. Open File Rep. WCr97r28, 1997.

Quichimbo, P., Tenorio, G., Borja, P., Cárdenas, I., Crespo, P. and Célleri, R.: Efectos sobre las propiedades físicas y químicas de los suelos por el cambio de la cobertura vegetal y uso del suelo: Páramo de Quimsacocha al Sur del Ecuador, Soc. Colomb. Cienc. Suelo, 2(42), 138–153, 2012.

Rice, K. C. and Hornberger, G. M.: Comparison of hydrochemical tracers to estimate source contributions to peak flow in a small, forested, headwater catchment, Water Resour. Res., 34(7), 1755–1766, doi:10.1029/98WR00917, 1998.

Rinderer, M., van Meerveld, H. J. and Seibert, J.: Topographic controls on shallow groundwater levels in a steep, prealpine catchment: When are the TWI assumptions valid?, Water Resour. Res., 50(7), 6067–6080, doi:10.1002/2013WR015009, 2014.

Rinderer, M., van Meerveld, I., Stähli, M. and Seibert, J.: Is groundwater response timing in a pre-alpine catchment controlled more by topography or by rainfall?, Hydrol. Process., 30(7), 1036–1051, doi:10.1002/hyp.10634, 2016.

Roa, C. and Weiler, M.: Integrated response and transit time distributions of watersheds by combining hydrograph separation and long-term transit time modeling, Hydrol. Earth Syst. Sci., 14(8), 1537–1549, doi:10.5194/hess-14-1537-2010, 2010.

Roa-García, M. C., Brown, S., Schreier, H. and Lavkulich, L. M.: The role of land use and soils in regulating water flow in small headwater catchments of the Andes, Water Resour. Res., 47(5), W05510, doi:10.1029/2010WR009582, 2011.

Rodríguez-Blanco, M. L., Taboada-Castro, M. M. and Taboada-Castro, M. T.: Rainfall–runoff response and event-based runoff coefficients in a humid area (northwest Spain), Hydrol. Sci. J., 57(3), 445–459, doi:10.1080/02626667.2012.666351, 2012.

Sajikumar, N. and Remya, R. S.: Impact of land cover and land use change on runoff characteristics, J. Environ. Manage., 161, 460–468, doi:10.1016/j.jenvman.2014.12.041, 2015.

Scanlon, B. R., Jolly, I., Sophocleous, M. and Zhang, L.: Global impacts of conversions from natural to agricultural ecosystems on water resources: Quantity versus quality, Water Resour. Res., 43(3), W03437, doi:10.1029/2006WR005486, 2007.

Seeger, S. and Weiler, M.: Reevaluation of transit time distributions, mean transit times and their relation to catchment topography, Hydrol. Earth Syst. Sci., 18(12), 4751–4771, doi:10.5194/hess-18-4751-2014, 2014.

Sefton, C. E. M. and Howarth, S. M.: Relationships between dynamic response characteristics and physical descriptors of catchments in England and Wales, J. Hydrol., 211(1–4), 1–16, doi:10.1016/S0022-1694(98)00163-2, 1998.

Seibert, J. and Beven, K. J.: Gauging the ungauged basin: how many discharge measurements are needed?, Hydrol. Earth Syst. Sci., 13(6), 883–892, doi:10.5194/hess-13-883-2009, 2009.

Seibert, J. and McDonnell, J. J.: On the dialog between experimentalist and modeler in catchment hydrology: Use of soft data for multicriteria model calibration, Water Resour. Res., 38(11), 1241, doi:10.1029/2001WR000978, 2002.

Seibert, J. and McDonnell, J. J.: Gauging the Ungauged Basin: Relative Value of Soft and Hard Data, J. Hydrol. Eng., 20(1), A4014004, doi:10.1061/(ASCE)HE.1943-5584.0000861, 2015.

Shaw, G. D., Conklin, M. H., Nimz, G. J. and Liu, F.: Groundwater and surface water flow to the Merced River, Yosemite Valley, California: 36Cl and Cl− evidence, Water Resour. Res., 50(3), 1943–1959, doi:10.1002/2013WR014222, 2014.

Soulsby, C., Tetzlaff, D., Rodgers, P., Dunn, S. and Waldron, S.: Runoff processes, stream water residence times and controlling landscape characteristics in a mesoscale catchment: An initial evaluation, J. Hydrol., 325(1–4), 197–221, doi:10.1016/j.jhydrol.2005.10.024, 2006.

Soulsby, C., Birkel, C., Geris, J., Dick, J., Tunaley, C. and Tetzlaff, D.: Stream water age distributions controlled by storage dynamics and nonlinear hydrologic connectivity: Modeling with high-resolution isotope data, Water Resour. Res., 51(9), 7759–7776, doi:10.1002/2015WR017888, 2015.

Strahler, A. N.: Quantitative analysis of watershed geomorphology, Trans. Am. Geophys. Union, 38(6), 913–920, doi:10.1029/TR038i006p00913, 1957.

Tetzlaff, D., Seibert, J., Mcguire, K. J., Burns, D. A., Dunn, S. M. and Soulsby, C.: How does landscape structure influence catchment transit time across geomorphologic provinces ?, Hydrol. Process., 23(January), doi:10.1002/hyp.7240, 2009.

Tetzlaff, D., Birkel, C., Dick, J., Geris, J. and Soulsby, C.: Storage dynamics in hydropedological units control hillslope connectivity, runoff generation, and the evolution of catchment transit time distributions, Water Resour. Res., 50(2), 969–985, doi:10.1002/2013WR014147, 2014.

Timbe, E., Windhorst, D., Crespo, P., Frede, H.-G., Feyen, J. and Breuer, L.: Understanding uncertainties when inferring mean transit times of water trough tracer-based lumped-parameter models in Andean tropical montane cloud forest catchments, Hydrol. Earth Syst. Sci., 18(4), 1503–1523, doi:10.5194/hess-18-1503-2014, 2014.

Tunaley, C., Tetzlaff, D., Lessels, J. and Soulsby, C.: Linking high-frequency DOC dynamics to the age of connected water sources: LINKING DOC TO FLOW PATHS AND WATER AGES, Water Resour. Res., doi:10.1002/2015WR018419, 2016.

Tunaley, C., Tetzlaff, D. and Soulsby, C.: Scaling effects of riparian peatlands on stable isotopes in runoff and DOC mobilisation, J. Hydrol., 549, 220–235, doi:10.1016/j.jhydrol.2017.03.056, 2017.

U. S. DI Bureau of Reclamation: Water Measurement Manual, Washington DC., 2001.

Uchida, T., Miyata, S. and Asano, Y.: Effects of the lateral and vertical expansion of the water flowpath in bedrock on temporal changes in hillslope discharge, Geophys. Res. Lett., 35(15), L15402, doi:10.1029/2008GL034566, 2008.

Vuille, M.: Climate Change and Water Resources in the Tropical Andes, Technical Notes, Inter-American Development Bank. [online] Available from: http://publications.iadb.org/handle/11319/5827 (Accessed 13 September 2017), 2013.

Vuille, M., Bradley, R. S. and Keimig, F.: Interannual climate variability in the Central Andes and its relation to tropical Pacific and Atlantic forcing, J. Geophys. Res. Atmospheres, 105(D10), 12447–12460, doi:10.1029/2000JD900134, 2000.

Wagener, T. and Montanari, A.: Convergence of approaches toward reducing uncertainty in predictions in ungauged basins, Water Resour. Res., 47, doi:10.1029/2010WR009469, 2011.

Wagener, T., McIntyre, N., Lees, M. J., Wheater, H. S. and Gupta, H. V.: Towards reduced uncertainty in conceptual rainfall-runoff modelling: dynamic identifiability analysis, Hydrol. Process., 17(2), 455–476, doi:10.1002/hyp.1135, 2003.

Weiler, M., McGlynn, B. L., McGuire, K. J. and McDonnell, J. J.: How does rainfall become runoff? A combined tracer and runoff transfer function approach: TRACER AND RUNOFF TRANSFER FUNCTION, Water Resour. Res., 39(11), doi:10.1029/2003WR002331, 2003.

Wenninger, J., Uhlenbrook, S., Tilch, N. and Leibundgut, C.: Experimental evidence of fast groundwater responses in a hillslope/floodplain area in the Black Forest Mountains, Germany, Hydrol. Process., 18, 3305–3322, doi:10.1002/hyp.5686, 2004.

Willems, P.: Parsimonious rainfall–runoff model construction supported by time series processing and validation of hydrological extremes – Part 1: Step-wise model-structure identification and calibration approach, J. Hydrol., 510, 578–590, doi:10.1016/j.jhydrol.2014.01.017, 2014.

Windhorst, D., Waltz, T., Timbe, E., Frede, H.-G. and Breuer, L.: Impact of elevation and weather patterns on the isotopic composition of precipitation in a tropical montane rainforest, Hydrol. Earth Syst. Sci., 17(1), 409–419, doi:10.5194/hess-17-409-2013, 2013.

Wolock, D. M., Fan, J. and Lawrence, G. B.: Effects of basin size on low-flow stream chemistry and subsurface contact time in the Neversink River watershed, New York, Hydrol. Process., 11(9), 1273–1286, 1997.

Wood, E. F., Sivapalan, M., Beven, K. and Band, L.: Effects of spatial variability and scale with implications to hydrologic modeling, J. Hydrol., 102(1), 29–47, doi:10.1016/0022-1694(88)90090-X, 1988.

Yadav, M., Wagener, T. and Gupta, H.: Regionalization of constraints on expected watershed response behavior for improved predictions in ungauged basins, Adv. Water Resour., 30(8), 1756–1774, doi:10.1016/j.advwatres.2007.01.005, 2007.

6 ACKNOWLEDGEMENTS

This research project was generously funded by the National Secretariat for Higher Education, Science, Technology, and Innovation of Ecuador (SENESCYT), the German Science Foundation (DFG), and the Central Research Office of the University of Cuenca (DIUC). I am very grateful for this opportunity and also want to thank to institutions and companies for access to data and facilities: IDRHICA of the University of Cuenca, NRI of Aberdeen University, and NVMETALS S.A.

This dissertation is a group effort and would not have been possible without the help and support of many people which I would now like to thank.

I would like to express my special appreciation and thanks to my advisor Prof. Dr. Lutz Breuer you have been a tremendous mentor for me, thanks for the continuous support, motivation, immense knowledge and for allowing me to grow as a research scientist. I am deeply grateful as well to Dr. David Windhorst for his patience and guidance with my multitude of questions, many innovative suggestions and for always being ready to provide feedback. Thanks David for your invaluable help and friendship.

My deepest gratitude also goes to my co-advisors in Ecuador, respectively Dr. Patricio Crespo, Dr. Rolando Célleri, and Prof. Dr. Jan Feyen. You coached me during my first steps on the path of research, a path that finally led to the public defense of my doctoral thesis. Many thanks for the helpful ideas during the field research and the constructive support in the preparation and revision of articles. Special thanks to Prof. Dr. Jan Feyen for your constant enthusiasm and encouragement.

I deeply appreciate Prof. Dr. Doerthe Tetzlaff (Aberdeen University) generous hospitality during my visit to her research group and thank her for fruitful discussions and her inspiration in the scientific and personal way. Thanks Doerthe for inspire me and many other women to stay in science.

Further thanks for all the people who support my field work in Ecuador, especially to Ryan Padrón, Patricio Lazo and Camila Silva for their energy and friendly faces during many weeks living in tents trying to “catch” storm events for sampling.

I thank my colleagues for the stimulating discussions and for all the fun we have had in the last years. Thank to you I have developed a lot, both professionally and personally, improving my research skills as well as learning from different cultures and life experience in Germany.

Last but not least, I would like to thank my parents, Magdalena and Jaime, who are my biggest fans and endlessly support and encourage me with everything that I do. Thanks to my siblings: Cecilia, Thomas, Diego, Tatiana; nieces and nephews: Soledad, Maria Paz, Tamya, Diego and Jaime and my family at this side of the world: Marta, Carla and Björn, this work is for you!

DECLARATION

I declare that I have completed this dissertation single-handedly without the unauthorized help of a second party and only with the assistance acknowledged therein. I have appropriately acknowledged and cited all text passages that are derived verbatim from or are based on the content of published work of others, and all information relating to verbal communications. I consent to the use of an anti-plagiarism software to check my thesis. I have abided by the principles of good scientific conduct laid down in the charter of the Justus Liebig University Giessen „Satzung der Justus-Liebig-Universität Gießen zur Sicherung guter wissenschaftlicher Praxis“ in carrying out the investigations described in the dissertation.”

Giessen, 16th October 2017

_____

Alicia Beatriz Correa Barahona